Addis Ababa University

Addis Ababa Institute of Technology

School of Mechanical and Industrial Engineering

Design, Simulation and Performance Evaluation of “teff" Separating and Cleaning machine

By

Eyob Hailu Taye

Feb-2023

Addis Ababa, Ethiopia

Addis Ababa University

Addis Ababa Institute of Technology

School of Mechanical and Industrial Engineering

Design, simulation, and performance evaluation of the "teff" cleaning and separating machine

---

By

Eyob Hailu Taye

A Thesis Submitted to the post graduate office of AAU for the Partial Fulfillment of Degree of Masters of Science in Mechanical Engineering (Mechanical Design),

Advisor

Dr. - Daneil Tilahun

Co-Advisor

Dr. Zenebe Mengiste

Feb-2023

Addis Ababa, Ethiopia

Letter of Certification

Addis Ababa University

Addis Ababa Institute of Technology

School of Graduate Studies

This is to certify that the thesis prepared by Eyob Hailu Taye entitled “Design, simulation, and performance evaluation of the "teff" cleaning and separating machine” in partial fulfillment of the requirements for the degree of Masters of Science in Mechanical Engineering (Design Engineering) compiles with the regulation of Addis Ababa University and meets the accepted standards concerning originality and quality.

Board of Examining Committee:

Daneil Tilahun (Asst. Professor)	Signature: ……	Date: …….
Advisors:		
Haileleul Sahle (PhD)	Signature: ……	Date: ……
External examiner:		
Hairedin Ismael (PhD)	Signature: ……	Date: …….
Internal examiner:		
Araya Abera (PhD) School of Mechanical And Industrial Dean	Signature: ……	Date: …….

Declaration

I, the undersigned, declare that this thesis is the result of my work and that all sources or materials used for this thesis have been dually acknowledged. This work is submitted in partial fulfillment of the requirements for a Master's Degree in Mechanical engineering (Mechanical Design) at Addis Ababa University, Addis Ababa Institute of Technology, School of Mechanical and Industrial Engineering. I certainly declare that this thesis has not been submitted to any other institution anywhere for the award of any academic degree, diploma, and/or certificate.

Eyob Hailu Taye ……

This is to certify that the above declaration made by the candidate is correct to the best of my knowledge.

Dr.-Daneil Tilahun ……

Acknowledgment

Glory is to the Father, and to the Son, and to the Holy Spirit, one God; for his immeasurable love and guidance in what had seemed like an insurmountable journey, Amen! My veneration and gratitude to the Holy Virgin Saint Merry, for lifting me up in every bit of this journey and for making the path brighter

I would like to acknowledge and give my warmest thanks to my supervisor Dr. Daniel Tilahun who made this work possible. His guidance and advice carried me through all the stages of writing my project. I am grateful to Dr. Zenebe Mengiste for his advice and guidance in writing this thesis, as well as for your wonderful comments and suggestions.

I am also grateful to EIAR (Ethiopian Institute of Agricultural Research) MELKKASA agricultural engineering directorate staff member for their unlimited support to accomplish this paper.

No words could adequately express my gratitude to my mother, Gudaye Tarekegn Endeshaw, for her unceasing support in all facets of my life, for having faith in me, and for passing on the discipline and meticulousness. I adore you so much and pray that God gives you a long life and good health. Thank you to my father, Hailu Taye Yigletu, for his encouragement, counsel, and strength. My sincere gratitude also extends to my brothers and sisters.

I want to express my gratitude to my friends for all of the ways they have encouraged me all along path.

Abstract

Teff is a staple food in Ethiopia. It is the most important crop in terms of cultivation area and production value. While the majority of farmers still thresh their crops by hand, significant efforts have recently been made to change the traditional method of threshing and cleaning teff. However, due to flaws in these machines, such as the capacity of the thresher and the cleaning mechanism used to clean the teff grain, the farmer's needs are not met. The major goal of the thesis is to design, and simulate a 3.5 Quintal/hr. teff thresher with a cleaning mechanism in Autodesk Inventor Pro 2016 is used to model the product and ANSYS 2018 was used to calculate the static analysis of the threshing drum, display the modal response, and perform computational simulation of the cyclone separator. For the simulation of cleaning the teff grain with the chaff and other pollutants in the cyclone, three alternative particle sizes and speeds were used, and the separation effectiveness was assessed. The results of the demonstration show that the average grain to straw ratio, threshing drum rotational speed (rpm), and feed rate (kg/hr.) were 0.4875, 1044.5, and 820.6, respectively. These data were used to design the newly improved teff thresher. Three cases with constant inlet velocity were chosen for the cleaning mechanism. Because the particle diameter of teff grain varies with moisture content, three different moisture contents were used: 6%, 12%, and 30%, with particle sizes of 0.7114, 0.7735, and 0.871 mm, respectively. The properties of the grains in the cyclone have been investigated and presented. The cleaning efficiency of the cyclone increases as particle size increases, and as particle size decreases, the cleaning mechanism also decreases.The design and analysis of a teff thresher with a cyclone separator and a capacity of 3.5 quintal/hr were explained in this research paper. As a result, the thresher's capacity was increased. Furthermore, a new type of cleaning mechanism is introduced, which has a good cleaning performance and is a nearly non-maintainable machine component due to the lack of moving part. Adoption of teff and mechanization technologies will benefit small households by lowering grain losses and increasing income due to improved handling methods and market prices. The research will allow for the generation of a wide range of benefits in terms of research knowledge and capacity. Policymakers, local manufacturers, researchers, and agricultural extension workers all benefit from the research knowledge.

Key words: Threshing, cleaning efficiency, teff, threshing drum, computational simulation

List of Abbreviations

EIAR	Ethiopian Institute of Agricultural Analysis
MARC	MEKASSA Agricultural Research Center
ANOVA	Analysis of variance
FDRE	Federal Democratic Republic of Ethiopia
FEA	Finite Element Analysis
FEM	Finite Element Method
CFD	Computational fluid dynamics
MOG	Mixture of grain and material other than grains
DZARC	DEBREZEIT Agricultural Research center

Nomenclatures

k_T = threshing constant

V_b = peripheral Velocity of beaters

δ_d = crop bulk density (dry basis)

D = cylinder diameter

β =moisture content of wet crop (decimal)

Fr = feed rate

N = Speed of the threshing cylinder (rpm)

N = power factor

U_F = Factor depending on power to overcome the friction

M_c = Mass of the threshing cylinder

r = effective radius

L= drum length

q= feed rate (Kg/s)

q_o = permissible feed rate(Kg/s)

D_c = Diameter of the cylinder

V_c =peripheral speed of threshing cylinder

N_c =rotational speed of the threshing cylinder

z = Grain to straw ratio

Q_g =Quantity of the grain

Q_s =Quantity of the straw

N = number of turns inside the device (no units)

H = height of inlet duct (m or ft.)

L_b = length of cyclone body (m or ft.)

L_c = length (vertical) of cyclone cone (m or ft.).

Δt = time spent by gas during spiraling descent (sec)

D=cyclone body diameter

Q=Volumetric in flow (m^3/s or ft^3/s) = Q/WH

H= Height of in let (m or ft.)

W= width of inlet (m or ft.)

L_c = Length of threshing cylinder, (m)

q=Material feed rate; (kg/s),

Δ= Thickness of the plant mass layer at the entrance in meter (equal to the concave clearance at the entrance)

η= Coefficient of cylinder length utilization

ρ= Bulk density of plant mass entering;

u_1 = Velocity of plant mass entering

Table of Contents

List of Figure

List of table

Chapter 1 Introduction

1.1 Background of the Study

Teff [Eragrostis teff (Zuca) Trotter] is the most important dietary staple food crop in Ethiopia hence it is a critical commodity for income, food, and nutritional security. It is a major source of carbohydrates and fiber, has a high content of calcium, phosphorus, iron, potassium, and thiamine, and contains no gluten. More than 6.5 million households are engaged in teff production. [1].

Teff accounted for approximately 24% of total grain-cultivated area in 2017, and nearly half of smallholder farmers grew it between 2004 and 2014 [2]. Teff provides two-thirds of the daily protein intake and 11% of the per capital caloric intake in the country [3].

Teff is commercialized crop in the cereal industry, with an estimated 30% of production being sold [4]. Teff's commercial surplus, or the portion of production that is sold, was valued at 750 million USD in 2013/14, or 50 percent of the cereal industry's overall commercial surplus. This is equivalent to the country's total annual commercial surplus of all other grains. However, when comparing the monetary value collected by farmers from the sales of teff with the income earned from the sale of coffee and sesame, two of the largest export commodities, revenue from teff is 34% more than that from sesame sales, while income from coffee is 32% higher. Thus, teff is by far the most significant cash crop in the nation [1].

The harvest season traditionally lasts from the beginning of October to the end of January, depending on the region, rainfall, altitude, and other local features. The average growing season of teff is 17 weeks. Farmers harvest teff by mowing with sickles after the crops are matured and dried in the field. The crops are piled in the field and then transported to the threshing area. [5]

Traditional methods of production and technical inefficiency have the biggest impact on the ability to produce teff. Teff production is technically inefficient, with a 0.4 ton/ha grain yield difference between the projected maximum potential and the actual teff grain yield. The country's Teff grain yield gap is anticipated to be roughly 1.1 million tons due to technical inefficiencies [6]. Teff is typically contaminated with stones, sticks, chaff, mud, and dust when it is handled using standard postharvest handling techniques. Because the presence of long

straws, chaff, tiny pieces of spikes, leaves, dust, dirt, and other foreign materials will speed up deterioration and result in poor physical condition with traditional threshing and cleaning techniques, teff grain cannot be stored, used for consumption, or used as planting material during or after threshing.

Teff dries for an average of 40 days between harvesting and threshing. Traditionally, farmers prepare the threshing area by coating it with a layer of cattle dung. This specific flat area is called "awudima". Once the teff has been brought to the area, the teff is threshed by oxen trampling the teff. Further separation of seeds and cleaning is done by hand with traditional tools. winnowing, or the removal of undesired materials, is done manually by throwing the grain into the air and letting the wind remove the lightest impurities, leaves, and significant amounts of detritus with a specific amount of grains. In recent years, researchers have worked to overcome these obstacles by creating multi-crop threshers, particularly tef threshers. In the private sector, companies like Hayle Engineering and Amiyo Engineering have developed teff thresher machines without cleaning mechanisms. Abayineh Awgchew[1] has developed a motor-derived tef grain cleaning and separating machine in the Assela Research Center. Melkassa Agricultural Research center also customized multi crop thresher to teff Thresher. Merga Worku[2] and Geta Kidanemariam[3] have developed teff thresher machines with sieve cleaning types in the Bako Research Center and AAIT.

1.2 Statement of the problem

Ethiopia, one of the world's oldest civilizations, has a more than 2500-year-old agricultural culture [7]. After 25 centuries, the sector's performance is quite poor; the majority of the labor force, or 85%, is still involved in agriculture, and the farmers continue to use antiquated agricultural practices that are comparable to those of their ancestors.

Ethiopian agricultural productions, in general, and the cereal sector, in particular, suffer significant difficulties. The most frequent problems are a lack of better varieties, better technology, production inputs, better management techniques, managing soil fertility, and controlling weeds and pests [8].

Mechanization has received little attention in Ethiopia, where Teff research has primarily focused on breeding and improving agronomic practices [2]. Teff is traditionally threshed on flat ground known as "Obdi," which is typically covered in cow dung. The harvested Teff is spread out across the "Obdi" and trampled by cattle or pack animals to separate the grain from the straw. In other ways, humans thresh grain by hitting harvested Teff with such a stick. Nonetheless, this technique results in significant yield losses. Furthermore, because the threshing is done on the ground and the Teff grain may mix with the soil, the grain's quality is affected by sand and other unnatural substances. Teff becomes contaminated by foreign matter, particularly tiny soil and sand grains that are difficult to clean, which has a significant impact on the market value of Teff [8].

Here in Ethiopia, labor is used to separate agricultural grain goods including teff, wheat, and sorghum from undesirable products and other grains of dust. Winnowing is an ancient technique that has been used to separate the grain from the chaff. This process is laborious and necessitates a large workforce as well as additional time. Apparently, the amount of grain lost during the teff threshing process was requested from the farmers [9]. It should be emphasized that teff is threshed almost solely utilizing traditional techniques in Ethiopia, just like the majority of cereal crops reported losses during this process. According to [9] 57 percent of the farmers reported having lost harvest during the threshing process. Of those that reported losses, this amounted to 0.25 quintals on average (and a median of 15 kg). When we compare this to the total quantity that was harvested for those farmers that reported losses (12.3 quintals on average), this amounts to a loss of 3.1 percent of the total harvest. If we take into account the large number of farmers

that did not report any losses, the estimated amount of loss during the threshing process equates to 1.8 percent of the total teff harvest.

The majority of farmers continue to thresh their crops by hand, but recently some works have been done to change the traditional method of threshing and cleaning of teff. However, due to flaws in these machines, such as ***low capacities***, the acceptance from the end user was observed by the researcher while promoting the MELKASSA-made teff thresher. Not only the capacity but also portability and hugeness of the machine were also a major problem. So we need to come up with a remedy for the aforementioned issues as well as the fact that some threshers don't have a mechanism to clean and those that do have many falling parts. As a result, the thresher's capacity must be increased in order to balance a cleaning mechanism, and it must be easily transportable and maintainable. Thus, the goal of this research is to create a technique for cleaning and separating teff seed from the chaff with increased capacity, having a good cleaning mechanism, and making the thresher Portable.

1.3 Objective of the Study

1.3.1 General Objectives

The general objective of the study is: To Design, analyze and Simulate increased capacity Teff Threshing Machine with a cleaning mechanism.

1.3.2 Specific objectives

Specific objective

(1) To design teff separating and cleaning the machine with Autodesk and ANSYS.
(2) To increase the capacity of the teff thresher and to evaluate the effectiveness of the machine on cleaning efficiency based on the three different particle sizes and speeds on the cyclone separator.

1.4 Scope of the Research

With the main goal of improving the thresher machine with increased capacity, this study aims to investigate improving the design and analysis of the teff thresher. It also examines the effectiveness of the design on cleaning in terms of cleaning efficiency, and cleaning loss based on the pressure difference on the cyclone separator. This study excludes the experimental evaluation in favor of a machine simulation using ANSYS2018.

1.5 Significance of the Study

Here in Ethiopia Agricultural grains like “teff” are threshed and cleaned in Traditional ways that contribute to the post-harvest loss and decrease in the quality of “teff” production. This could be minimized by utilizing modern technology; however, most Ethiopian farmers are in subsistence farming and have no opportunity to use modern technology. The new threshing and cleaning unit would solve the existing technical problem and will increase in quantity and quality by saving Time, Manpower and will result in a great competitive machine.

1.6 Limitation of the Research

Teff aerodynamic properties were taken from recent literature due to a lack of laboratory equipment and given the variety of teff grown in Ethiopia, the research did not include the

production of an improved model of a teff threshing machine [12]. The DebreZeit Agricultural Research Center's "Dagim" teff variety was utilized in the study, and due to the market's high rate of inflation, it was challenging to obtain the supplies required to build the machine in our workshop.

1.7 Organization of the Thesis

The study organized into five chapters:

Chapter One: presented the background information on the topic of the cultural aspects of teff threshing in Ethiopia and how important teff is as a crop in our nation. It also discussed the techniques currently being employed by farmers and described post-harvest losses brought on by inappropriate handling. Following that, it is discussed what the problem statement, the overall objective, the three particular objectives, the study's scope, its importance, and its limitations.

Chapter Two: Theoretical and conceptual literature was discussed in relation to the following topics: threshing unit; threshing parameters; threshing drum, feed rate, and output capacity; physical and aerodynamics properties of teff; cleaning system; Effective spins per revolution, cut point diameter, pressure drop, and cyclone effectiveness. The topic of threshing using ergonomic criteria is covered last.

Chapter Three: In this section, the methodology use to do the research were well explained on the design of the threshing drum and how to do the modal analysis and the stress analysis of the rotating drum and also the design methodology for the cyclone separator was discussed.

Chapter Four: In this chapter, the simulation results are presented and discussed concerning different models under different parameters. The parametric study to analyze the Modal response of the threshing cylinder, and analysis of the cleaning and separation efficiency of the cyclone separator at three different speeds and particle sizes were discussed.

Chapter Five: Finally, conclusions are presented based on the result of the study and possible courses of action for research areas point out for future recommendations.

Chapter 2 Literature Review

2. Introduction

Threshing is a method for separating kernels from ears or pods and involves rubbing and impacting motions [4]. Four different threshing principles exist: impact, rubbing, pre-cut combine, grinding, and others [5]. Since the first grain harvester was created more than 200 years ago, grain threshing technology has advanced.

2.1 Threshing Unit

According to different mounting positions of threshing components, there are three primary threshing technologies including cross, longitudinal and vertical harvester respectively [6].When threshing components are installed perpendicularly to straw flow, it is called cross-direction harvester. In the same way, when parallel to straw flow, it is called longitudinal-direction harvester. And when vertical to straw flow, it is called vertical-direction harvester.

The structure of the threshing component, which is frequently used to assess the effectiveness of grain threshing, is strongly related to the second kind of classification of grain threshing technology. That is, the grain flow might be divided into axial-flow and tangential-flow depending on its orientation in relation to the axis of the threshing unit.[5] Over 200 years ago, these two types of harvesters were granted patents. By combining the aforementioned three categories, there are four typical forms of grain threshing, including cross-tangential flow (Figure 2.1), longitudinal-axial flow (Figure 2.3), vertical-axial flow (Figure 2.4), and pre-cut combing threshing harvesters (Figure 2.2).

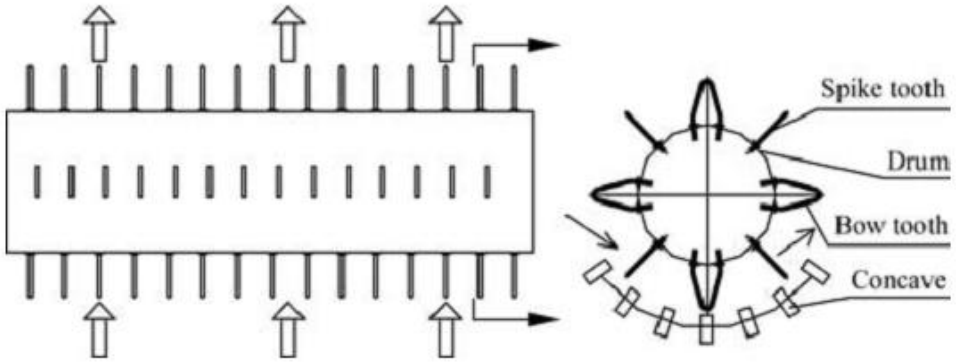

Figure 2-1 Cross-Tangential Threshing Cylinder [6]

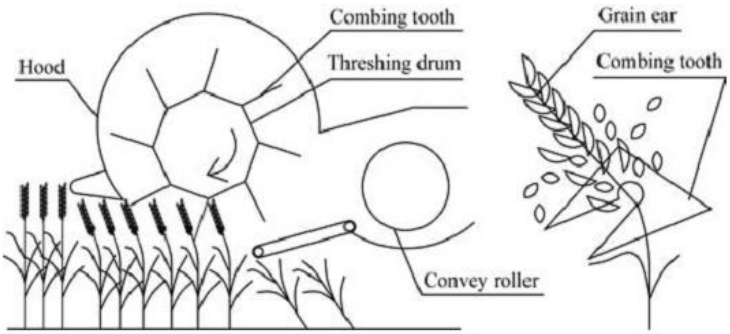

Figure 2-2- Pre-cut combing threshing harvester [6]

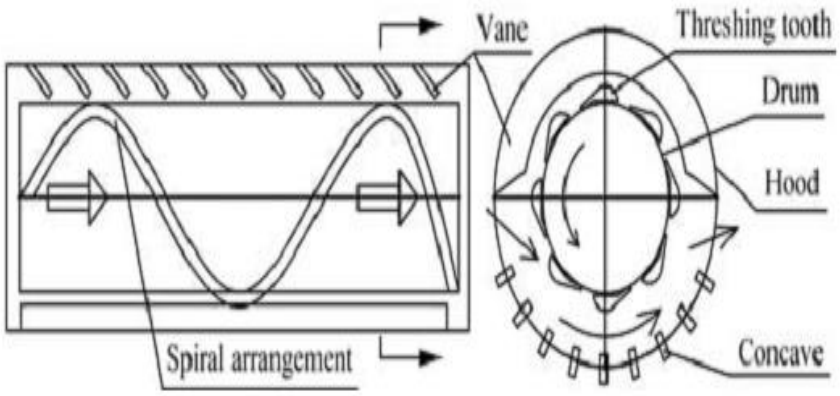

Figure 2-3 - Longitudinal-axial threshing cylinder [6]

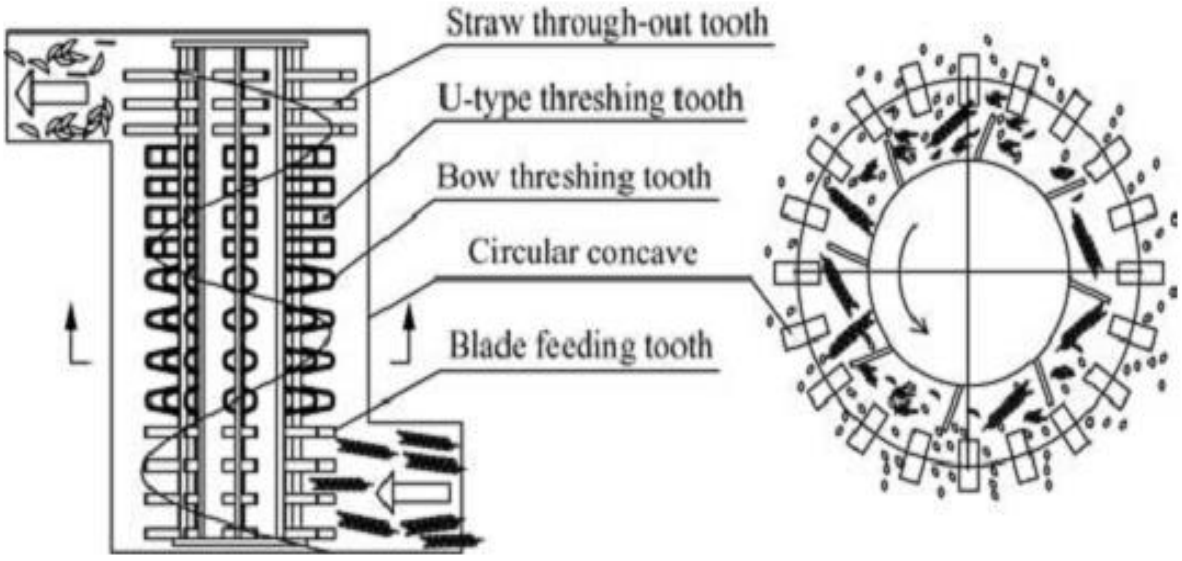

Figure 2-4 - Vertical-axial threshing cylinder [6]

The following factors make up the majority of the performance criteria for threshing devices: throughput, threshing losses, grain separation, grain damage, MOG-separation, and power needs. Threshing loss is calculated as the weighted percentage of whole grains that are not detached from the ears, the weighted percentage of separated grains at the concave, and the weighted percentage of damaged grains in the sample relative to the total weight of 0 grains entering the threshing unit [7]. On the operating quality of a 19 rotary threshing machine, [8] demonstrated the effects of MOG-throughput, peripheral speed, MOG moisture content, and amount of green material. In these trials, this threshing unit was contrasted with a tangential threshing method that utilized walkers. Higher MOG-separation, lower grain damage rates, higher throughput within a given machine envelope, and higher power requirements were all characteristics of this kind of axial threshing unit. In general, rotary threshing machines have an edge over tangential units when it comes to threshing rice, corn, and soy, but they are less versatile overall. Compared to tangential threshers, rotary threshing units are more sensitive to crop moisture levels. Ground surface roughness has no effect on axial threshing units (slopes). The axial type threshing unit with tangential feeding is therefore preferred for stationary threshers in order to have a higher separation rate with limited length/or space of concave.

2.2 Governing Parameters influencing the threshing process

The majority of the performance criteria for threshing devices are as follows: throughput, threshing losses, grain separation, grain damage, MOG-separation, and power requirements.[4]which are dependent on the drum diameter, concave clearance, the spike tooth number and orientation and the peripheral speed of the threshing drum.

2.2.1 Power needed for the teff threshing Unit

According to [9] the energy required to detach grain from the panicle is presented as follows;

$$E_d = \frac{K_e V_s^{1/2} fr^{3/2}}{\rho w^2} \qquad (2.1)$$

Where K_e =is constant (Grain size characteristics)

F_r = feed rate (Kg/hr.)

E_d =Energy required to detach the grain

V_s =Peripheral velocity (m/s)

ρ = density of the grain

w = Angular velocity (rad/sec)

The power required to detach the grain from the panicle is obtained in equation (2.2).

$$P_d = K_s \left[\frac{K_e V_s^{1/2} fr^{3/2}}{\rho w^2} \right] \frac{V_T}{L_c} \qquad (2.2)$$

Where;

K_r=K_s K_e; K_r is a constant that is influenced by the resistance of the crop material to the machine component.

L_c =concave length

Relating the power output from the cylinder in terms of the detached grain and the power input through the impact from the beater bars, the power to detach grain crop is

$$P_d = \frac{3K_e}{2} \left[\frac{V_s^{1/2} fr^{3/2}}{\rho w^2 L_c} \right] \qquad (2.3)$$

$$\rho_w, V_g, hr/day, \frac{3600}{1200}$$

The power required to overcome the frictional force during threshing operation is

$$P_f = \frac{2}{3} Nf \left[\frac{\sigma_{\max}}{c} \right]^n .\pi D L_c \qquad (2.4)$$

The power required to turn the unloaded cylinder is

$$p_u = \frac{2\pi NrM_c}{60 \times 75} \left[g + \frac{V_T^{\,2}}{r} \right] \qquad (2.5)$$

The total power required for threshing operation is

$$P = \frac{3K_e}{2} \left[\frac{V_s^{1/2} fr^{3/2}}{\rho w^2 L_c} \right] + \frac{2}{3} Uf \left[\frac{\sigma_{\max}}{c} \right]^n .\pi D L_c + \frac{2\pi NrM_c}{60 \times 75} \left[g + \frac{V_T^{\,2}}{r} \right] \qquad (2.6)$$

Where: N = Speed of the threshing cylinder (rpm)

n = power factor

U_F = Factor depending on power to overcome the friction

M_c = Mass of the threshing cylinder

r = effective radius

2.2.2 Threshing drum

Threshing systems can use up to 55–85% of the available energy, so they need to be well investigated [10]. According to [11], a cylinder with a big diameter required less power than one with a greater feed rate. Many studies have found that the threshing percent rises with rising cylinder peripheral speed and falls with rising moisture content. [12] Suggests a speed for spike teeth cylinders of 800-950 m/min.

Long concave are possible with large cylinder diameters; however as cylinder diameter increases, the centrifugal forces required for good separation diminish. A 600 mm diameter is typical. Most manufacturers have switched to multiple cylinder threshing systems in order to enhance threshing and grain separation using the traditional design for big capacity combines [13]. Numerous studies have found that the main machine factors that can affect threshing performance are variations in cylinder peripheral speed, effective concave clearance, and fan speed[12].Drum length, diameter, beater count, and drum speed are the four main threshing drum parameters [14]. The drum's length was measured using [15]

$$Q = q_0.L.M \qquad (2.7)$$

Where; L= drum length

q= feed rate (Kg/s)

q_o = permissible feed rate (Kg/s)

- Diameter of cylinder

$$D_c = \left(\frac{V_c * 60}{\pi N_c} \right) \qquad (2.8)$$

Where

D_c = Diameter of the cylinder

V_c =peripheral speed of threshing cylinder

N_c =rotational speed of the threshing cylinder

- Length of threshing cylinder:

Length of cylinder can be determined by the model given [9].

$$L_c = q / \Delta \times \eta \times \rho \times u_1 \qquad (2.9)$$

Where,

L_c =Length of threshing cylinder, (m)

q=Material feed rate; (kg/s),

Δ= Thickness of the plant mass layer at the entrance in meter (equal to the concave clearance at the entrance)

η=Coefficient of cylinder length utilization (0.7-0.8),

ρ=Bulk density of plant mass entering; (20-40 kg/m3 [16] and [17].

u_1 = Velocity of plant mass entering (3-5m/s)[16]

2.2.3 Feed rate

According to [18], increasing the feed rate will have a negative effect on how clean the crop is. In their trial, they found that the cleaning loss was 10% at a feed rate of 0.49 tons per hour and decreased to 54% at a feed rate of 0.68 tons per hour.[19] Came to the same result after looking into the inverse relationships that were suggested between feed rate and cleanliness. Due to the rising load on the screen, which impeded the free movement of grains and undesirable debris, the negative relationship between cleanliness and feed rate was evident. When fed at a rate of 0.12 tons per hour, the cleanliness was 40.13%, but when fed at a rate of 0.6 tons per hour, it fell to 36.83%. The effectiveness of the pneumatic separation method in separating almond seeds from their fractured shells was examined by [20]. Their findings showed that when feed rate and mixture supply angle increased, separation efficiency dropped. While the lowest amount was recorded at an airflow velocity 6.5 m/s, the best cleanliness was reported at 9.5 m/s.

Feed rate is affected by the following parameters

- ✓ The threshing space between the threshing drum and the threshing concave.
- ✓ Grain weight
- ✓ Feeding Velocity
- ✓ Concave clearance
- ✓ Threshing drum width and speed.

To calculate the feed rate first we have to determine the grain to straw ratio

$$z = \frac{Q_g}{Q_s} \quad \text{..... (2.10)}$$

Where z = Grain to straw ratio

Q_g =Quantity of the grain

Q_s =Quantity of the straw

For a specified grain to straw ratio we can have a relation

$$Q_g = \delta \times Q_s$$

The total feed rate is obtained by adding the grain and straw quantities after determining the planned output capacity of the thresher, which is the quantity of the grain. The entire feed rate input can therefore be represented as

$$F_r = Q_g + Q_s \quad \text{..... (2.11)}$$

2.2.4 Output capacity

The output capacity, or quantity of grain threshed in an hour, is a significant factor in assessing the effectiveness of a grain thresher. The output capacity is frequently influenced by the threshing technique. Crops are traditionally threshed by being beaten with a pestle stick and trodden under a bullock [21].

Utilizing Buckingham's pi theory and dimensional analysis, the thresher output capacity model was created [22]. The output capacity of a thresher (C_T) is determined using a dimensional analysis by assuming key variables such as feed rate (F_r), grain to straw ratio (z), and separation efficiency (Se), which is the percentage of threshed grain recovered through concave opening by

concave configuration. In his model, moisture content is included as a key variable, and foreign materials like weed and grass are ignored.

$$C_T = f(F_r, z, S_e)$$

Threshing efficiency is the percentage of the threshed grains calculated on the basis of the total grain entering the threshing mechanism. It grows asymptotically with concave length until a certain point is reached. Extending the concave length beyond the maximum point has no effect on threshing efficiency and may even reduce it under certain conditions. However, [15] experiments show that under easy threshing conditions there is little advantage of increasing the concave length beyond 33 cm. Threshing losses increase at a rate of about 0.9% for every 7.5 cm increase in diameter of the conventional threshing cylinder. The number of rasp bars and their spacing do not seem to have any effect on the threshing efficiency. Cylinder speed is one of the most important variables affecting threshing losses. For hard-to thresh crops and/or conditions, threshing losses can be significantly reduced by increasing the cylinder speed. According to [23] one set of experiments increasing the speed from 23 to 33 m/s reduced losses from 8% to 4%. The cylinder-concave gap affects threshing losses adversely. An increase of 1/8 in. increased the un threshed loss from 0.6% to 2.0%. Changing the concave clearance ratio (the ratio of the gap at the front to that at the rear of the cylinder) is done to facilitate crop feeding into the cylinder, but the effect of this variable on the threshing efficiency is not consistent [23]. Threshing losses increase as the material feed rate increases, which is usually expressed in tons/h of material other than grain (MOG). Grain feed rate and total feed rate are two other ways to express material feed rate. Threshing losses also increase with the MOG-to-grain ratio. Moisture content also affects threshing efficiency. Generally, the crop becomes hard to thresh at higher moisture content and as a result the threshing losses become higher. Furthermore, if the crop is not fully mature and contains a lot of green material, threshing becomes difficult and losses increase.

2.2.5 Concave clearances

When studying the impact of concave clearances on total threshing losses, it was discovered that differences in losses were significant at concave clearances of 10 mm and 15 mm but negligible at 20 mm. However, as concave-clearance was raised, there was a modest rise in overall threshing losses.

2.2.6 Drum speed

In some research [21] results, it was shown that the capacity has positive correlation with the drum speed. The speed of threshing unit (drum) could not influencing the power consumption of the thresher as some studies showed the speed of the drum has no significant effect on the process power[4] showed that the output capacity rapidly increased with an increase in drum speed for all feed rates and grain moisture content.[4] Take the initial speed 900 rpm the output were good, on the 1000 and 1200rpm the capacity decline. This could be because of the teff stem properties which had high tensile strength and could be rolled with the drum bars of the SG-2000 thresher. In newly developed threshing unit, after 1000 rpm, again the capacity shows increments and this could happened under the closed type drum and concave where the material got opportunity to contact more than one times for rubbing and cut the teff stem in a better way. The optimum rpm of the threshing process could be 1000rpm.

2.3 Aerodynamic and physical property of teff

2.3.1 Physical property of teff

When designing equipment and analyzing how a product behaves during agricultural process operations like handling, planting, harvesting, threshing, washing, sorting, and drying, physical and engineering qualities are crucial [24].

Teff is a tiny grain, with an equivalent diameter that ranges from 0.71 to 0.87 mm and a thousand grain mass that ranges from 0.257 to 0.421 g [25]. Here is a list of all of teff characteristics. [25] Derived the following teff seed derivable properties:

- ✓ The equivalent sphere diameter was determined as given in equation (2.12).

$$D_e = \left(\frac{6m_s}{\pi\rho_t}\right)^{\frac{1}{3}} \text{..... (2.12)}$$

Where: m_s in kg and ρ_t in kg/m^3 are the mass and density of seed, respectively.

- ✓ The Sphericity ϕ was determined using the following relationship in equation (2.13).

$$\phi = \frac{D_e}{D_c} \text{..... (2.13)}$$

Where: De and Dc are diameter of the equivalent sphere and diameter of smallest circumscribing circle in mm, respectively

- ✓ The porosity of teff seed was calculated from the following relationship in equation (2.14).

$$\varepsilon = \left(1 - \frac{\rho_b}{\rho_t}\right) * 100 \ldots\ldots\ldots\ldots\ldots (2.14)$$

Where: ε is the porosity in %; ρ_b is the bulk density in kg/m^3; and ρ_t is the true density kg/m^3.

✓ Seed size

With a rise in moisture content from 5.6% to 29.6%, the length, width, and equivalent-sphere diameter of seeds increased from 1.01 to 1.27 mm, 0.59 to 0.68 mm, and 0.71 to 0.87 mm, respectively. It was discovered that there is a linear relationship between length, width, equivalent sphere diameter, and moisture content. [25]

$$L = 0.0062Mc + 1.11 \ldots\ldots\ldots\ldots\ldots\ldots\ldots\ldots\ldots (2.15)$$

$$W = 0.0032Mc + 0.75 \ldots\ldots\ldots\ldots\ldots\ldots\ldots\ldots\ldots (2.16)$$

$$D_e = 0.0069Mc + 0.67 \ldots\ldots\ldots\ldots\ldots\ldots\ldots\ldots\ldots (2.17)$$

Where: Mc is moisture content in %.

✓ Sphericity

The Sphericity decreased from 0.70 to 0.63 and then increased to 0.69 when the moisture content increasing from 5.6% to 21.43% and then again to 29.6%. It has been established that Sphericity and moisture content are linked. [25]

$$\phi = 0.005Mc^2 - 0.0185Mc + 0.7858 \ldots\ldots\ldots\ldots\ldots\ldots\ldots\ldots (2.18)$$

✓ Bulk and true density

Samples' true and bulk densities dropped as moisture content rose. The bulk and actual densities were found to drop from 840 to 696 and 1361 to 1207 Kg/m3, respectively, in the moisture content range of 5.6-29.6% wet base less weight gain as a result of the increased moisture could explain the relative decrease in densities at high moisture content. The dependency of true and bulk densities on moisture is depicted here as a linear relationship. [25]

$$\rho_t = -6.093Mc + 1420.8\ Kg/m^3 \ldots\ldots\ldots\ldots\ldots\ldots\ldots\ldots\ldots (2.19)$$

$$\rho_b = -6.1196Mc + 895.31\ Kg/m^3 \ldots\ldots\ldots\ldots\ldots\ldots\ldots\ldots\ldots (2.20)$$

With values for $R^{2\ 0f}$ 0.83 and 0.90, respectively

✓ Porosity

Porosity was found to be a linear function of moisture content as shown in equation (2.21).

$$\varepsilon = 0.1912Mc + 36.738 \ldots\ldots\ldots\ldots\ldots\ldots\ldots\ldots\ldots (2.21)$$

The shear stress, modulus of elasticity, and flexural stiffness of teff were all determined by experiment analysis by [4] . The shear stress was found to be a linear function of the stem's

moisture content, diameter, and thickness. The following are the linear equations for each segment: [4]

$$\tau = 31.143 + 0.41X_1 - 5.78X_2 - 12.43X_3 \ldots\ldots\ldots\ldots \text{upper segment}$$

$$\tau = 43.64 + 0.15X_1 - 3.82X_2 - 15.56X_3 \ldots\ldots\ldots\ldots \text{middle segment}$$

$$\tau = 47.16 + 0.144X_1 - 8.13X_2 - 9.29X_3 \ldots\ldots\ldots\ldots \text{lower segment}$$

Where:

τ- Shear stress, (MPa)

X_1- moisture content, (%) (Wet base)

X_2- diameter of the stem, (mm) X3-thickness of the stem, (mm)

An elastic modulus is a measurement of an object's or substance's resistance to elastic deformation. The elasticity modulus of teff stems was a linear function of stem moisture content, diameter, and thickness. Here are the linear equations for all segments: [4]

$$E = -1.117 + 0.904X_1 + 0.940X_2 - 0.007X_3 \ldots\ldots\ldots\ldots \text{upper segment}$$

$$E = 0.142 + 0.256X_1 + 1.820X_2 - 0.012X_3 \ldots\ldots\ldots\ldots \text{middle segment}$$

$$E = -0.468 + 0.337X_1 + 2.49X_2 - 0.0004X_3 \ldots\ldots\ldots\ldots \text{lower segment}$$

With R^2 value 0.64, 0.73, 0.67 respectively

Where:

E - modulus of elasticity, (GPa)

X_1- diameter of the stem, (mm)

X_2 - thickness of the stem, (mm)

X_3 - moisture content, (%)

Flexural rigidity is defined as the force couple required bending a fixed non-rigid structure by one unit of curvature, or as the resistance offered by a structure while undergoing bending. The flexural rigidity of teff stems (EXI) was a linear function of stem moisture content, diameter, and thickness. The following are the multi linear equations for all segments[4]

$$Fr = ExI = -10.343 + 3.363X_1 + 20.946X_2 + 0.0091X_3 \ldots\ldots \text{Upper segment}$$

$$Fr = ExI = -13.721 + 10.511X_1 + 11.712X_2 + 0.219X_3 \ldots\ldots \text{middle segment}$$

$$Fr = ExI = -4.88 + 2.495X_1 + 8.439X_2 + 0.02X_3 \ldots\ldots\ldots\ldots \text{lower segment}$$

Where:

E-modulus of elasticity, (*GPa*)

I-moment of inertia, (mm^4)

X_1- diameter of the stem, (mm)

X_2- thickness of the stem, (mm)

X_3- moisture content, (%) (Wet base)

2.3.2 Aerodynamic property of teff

In the process of cleaning and separating grains, aerodynamic forces are crucial. Since the drag force produced by the air stream is proportional to the second power of the air velocity, air velocity has a significant impact on cleaning effectiveness. Numerous writers have investigated how air velocity affects how effectively grains are separated and cleaned [28]. On the other hand, it has been discovered that another significant factor determining cleaning effectiveness is the direction of the air stream introduced to the substance [29]. This study of adding a pre-cleaner to the combine cleaning system is therefore interested in how the interaction of these two parameters impacts separation and cleaning efficiency.

The air density, viscosity, elastic modulus, and relative velocity between the air and the particle are all factors that affect the aerodynamic drag force F_d that acts upon a particle travelling through air.

$$F_d = f(A_p, p_a, \mu, E, V_r) \quad \text{.....2.22}$$

The general form of F_d determined with the Buckingham π theorem is:

$$F_d = \frac{1}{2} * C_d * A_p * \mathrm{p}_a * {V_r}^2 \quad \text{.....2.23}$$

Where C_d is a dimensionless quantity related to Reynolds number and is called the drag coefficient [25], calculated the drag coefficient and terminal velocity of teff as follows:

Both terminal velocity and drag coefficient were linearly related to moisture content as shown in Eqns.

$$V_t = 0.0363Mc + 2.8858 \quad \text{.....2.24}$$

$$C_d = -0.0074Mc + 0.8627 \quad \text{.....2.25}$$

Where:

V_t = is terminal velocity in ms^{-1},

C_d = drag coefficient and *Mc* is moisture content %.

Terminal velocity of teff grain increased linearly from 3.08 to 3.96 ms^{-1} with increase in moisture content from 6.5 to 30.1% wet base [25].

2.4 Cleaning system

Despite its high efficiency in separation, the sieve mechanism is the most widely used cleaning system in threshers. Their weight is high due to their design, and the sieve device's shaking drive is correspondingly strained. This causes unwanted vibration, which can spread throughout the machine. Furthermore, heavy wear affects the suspension. As a result, the sieve wears out after a few harvesting cycles and must be replaced. Furthermore, the fabrication of such fin sieves is complicated and costly.

According to [30], the cyclone is a device with no moving parts and thus requires no maintenance. It allows micrometer-sized particles to be separated from an air stream at about 15m/s without excessive pressure drop. The typical cyclone efficiency is 70-80% solids separation, but if the stream contains a large amount of solids, the separation efficiency exceeds 99%. [31]

2.5 Threshers based on Ergonomics design criterion

Wheat and rice are threshed using power-driven machines called threshers during the harvest season. These devices are powered by diesel or electric motors or tractor power takes off. At the opening of the threshing drum, the conventional thresher is equipped with a feeding chute with a slope of 10-15 degree.

According to a study from Pakistan, threshers were responsible for 16% of injuries [31]. According to their analysis, the three primary causes of thresher injuries were belt entanglement, electric shock, and feeding crop without safety; 17% of accidents were caused by mechanical problems. In a survey from India, [24] recorded 30 thresher injuries out of 50, although the study provided no information on the injury's kind or mechanism. In a different study from Punjab, India, 73% of the incidents of thresher injuries were linked to human factors. These included being inattentive, dressing loosely, working too hard, and being physically incapable, among other things [32]. These observations, however, were not supported by any thorough examinations. No study has assessed design advancements or any safety features.

According to [31], 16% of human injuries in Pakistan occurred as a result of improper thresher operating in 1989. It was imperative to develop a mechanical crop feeding conveyor for minimizing accidents and vibrational impacts in order to prevent such human injuries and machine vibrations.

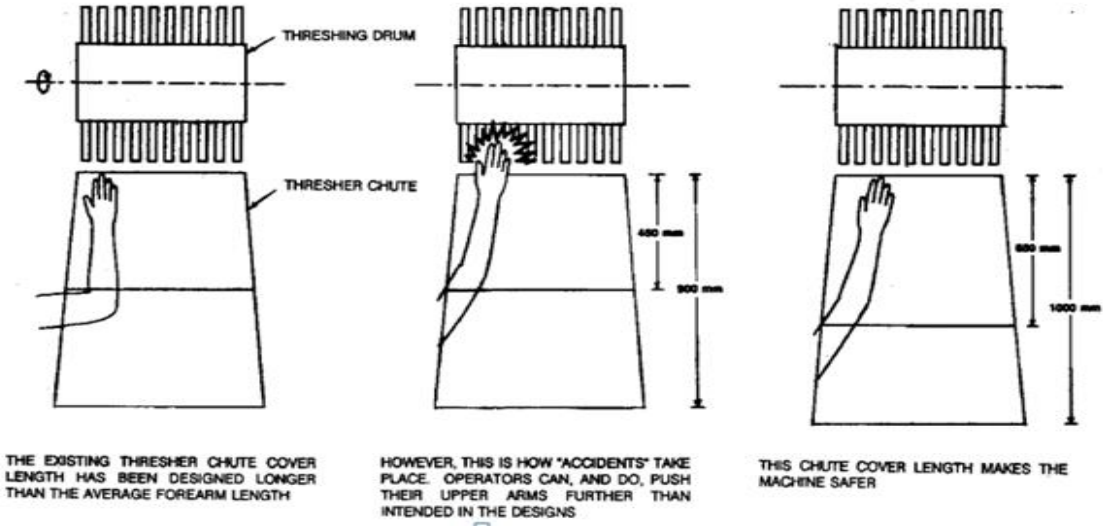

Figure 2-5 Top View of thresher indicating injury mechanism [32]

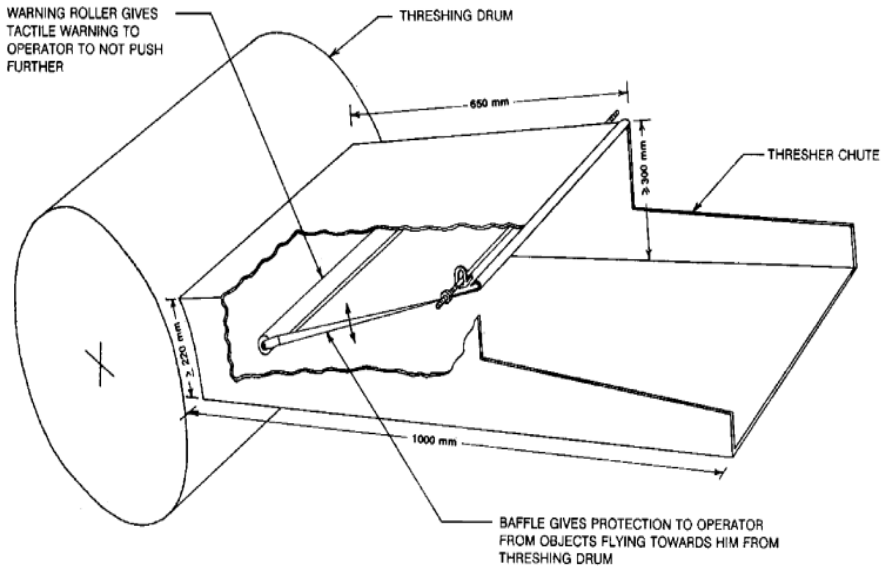

Figure 2-6 - Proper safer chute for thresh [32]

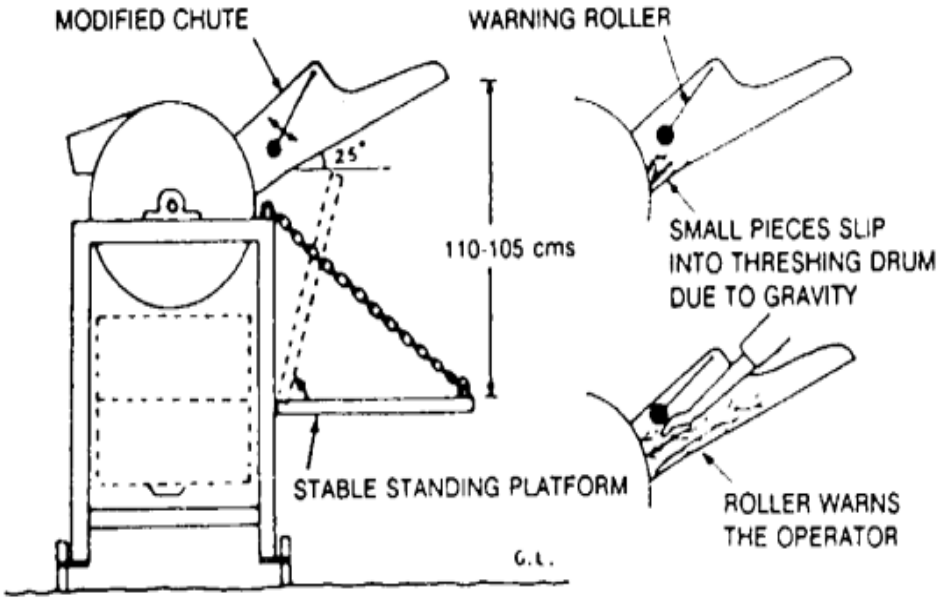

Figure 2-7 -Safe threshing Operation [32]

2.6 Summary of Literature

In order to have high capacity a cylinder with a big diameter required less power than one with a high feed rate. Many studies have found that the threshing % rises with rising cylinder peripheral speed and falls with rising moisture content. [12] Suggests a speed for spike teeth cylinders of 800-950 m/min. long concave are possible with large cylinder diameters; however as cylinder diameter increases, the centrifugal forces required for good separation diminish. A 600 mm diameter is typical. Most manufacturers have switched to multiple cylinder threshing systems in order to enhance threshing and grain separation using the traditional design for big capacity combines [13]. Numerous studies have found that the main machine factors that can affect threshing performance are variations in cylinder peripheral speed.

According to [18], increasing the feed rate will have a negative effect on how clean the crop is. In their trial, they found that the cleaning loss was 10% at a feed rate of 0.49 tons per hour and decreased to 54% at a feed rate of 0.68 tons per hour.[19] Came to the same result after looking into the inverse relationships that were suggested between feed rate and cleanliness.

Utilizing Buckingham's pi theory and dimensional analysis, the thresher output capacity model was created [22]. The output capacity of a thresher (C_T) is determined using a dimensional

analysis by assuming key variables such as feed rate (F_r), grain to straw ratio (z), and separation efficiency (Se), Despite its high efficiency in separation, the sieve mechanism is the most widely used cleaning system in threshers. Their weight is high due to their design, and the sieve device's shaking drive is correspondingly strained. This causes unwanted vibration, which can spread throughout the machine. Furthermore, heavy wear affects the suspension. As a result, the sieve wears out after a few harvesting cycles and must be replaced. Furthermore, the fabrication of such fin sieves is complicated and costly.

2.6.1 Summary of Teff threshing technology done in Ethiopia

1. Theoretical and Experimental Investigation of Threshing Mechanism for Teff (Eragrostistef (Zucc.) Trotter) on the Basis of its Engineering (Physical and Mechanical) Properties *by Geta Kidanemariam Gelaw was done in 2020*. The research project's goal was to look into theoretical and practical threshing mechanisms in order to design a teff threshing unit based on its mechanical and physical characteristics. The diameter, length, elastic modulus, shear strength, and flexural stiffness of teff, together with other physical and mechanical characteristics, were identified. Sickles were used to cut the test variety at a minimum height of 1-1.5 cm from the ground. The stem was cut into three equal lengths, and the panicles were detached from the stem. The physical dimensions of the segments were measured and coded. They were measured for their mechanical characteristics using a texture analyzer and a universal testing machine. Moisture content, stem diameter, and stem thickness were taken into account. Analysis of variance (ANOVA) linear modeling coupled with multi-linear modeling was used to analyze experimental data. In R i386.3.0.1 program, the results showed that the Kora and Guduru kinds of teff had moduli of elasticity with minimum and maximum values of 1.03 and 3.88 Gpa at moisture levels of 5.5% and 19.70% in the top and lower positions, respectively. The shear strength of the teff stem's and maximum elasticity modulus were used to calculate the power needs of the threshing unit. The threshing units were then designed and made in accordance with accepted design practices. The design impact of the SG-2000 model and the newly designed (closed type concave and drum) threshing units were assessed after manufacturing the newly developed threshing unit and setting up the test stands. The three factors include threshing capacity, cleaning effectiveness, and separation effectiveness on feed rate and drum speed with three levels of 275, 325, and 400 kg/hr. and 900, 1000, and 1200 rpm, respectively. Analysis of

variance (ANOVA), non-linear modeling, correlation with polynomial modeling, and spearman methods were all used to analyses the experimental data. The means were compared using various range tests, and graphs were constructed and analyzed using the software packages R i386.3.0.1, ANSYS 2015, and MATLAB 2014a. The test results showed that the newly created (cylindrical type concave) significantly. The highest threshing capacity for newly built and SG-2000 V threshing units, respectively, were found to be 70.88 and 52.11 kg.hr-1.

Figure 2-8 Teff thresher developed by Geta Kidanemariam Gelaw [3]

2. Development and Evaluation of Teff Threshing Machine Merga Workesa Dula in 2020.

Teff crop threshing was made possible by the development and testing of the teff threshing machine. The study's observational data for analysis the initial phase involved gathering the essential data regarding the difficulties associated with traditional teff threshing, which results in significant grain and quality losses. Further discussions with the relevant parties were then held. Teff threshing technology availability was surveyed to kick off the job. The two multi crop thresher, Asella model and IITA type multi crop thresher were found to be threshing teff as well. Thus, the optimum design that satisfies the requirements for teff threshing is identified. The designs for all sections were created after thoroughly analyzing all components required for threshing teff. Maximum total grain losses of 4.536% were recorded at drum speed of 700 rpm at feeding rate of 28 kg/min, while minimum total grain losses of 2.706% were obtained at feed rate of 23 kg/min at drum speed of 750 rpm. While the cleaning and threshing efficiencies of 99.250

and 97.529%, respectively, were attained at a constant drum speed of 750 rpm and a feeding rate of 23 kg/min. At a constant drum speed of 700 rpm, the maximum drum loss was measured to be 1.564, 1.992, and 2.501% at feeding rates of 23, 25, and 28 kg/min, respectively. The machine's threshing efficiency is good at 750 rpm with feeding rates ranging from 23 kg/min to 25 kg/min, with values of 99.250 and 99.058%, respectively. The machine's cleaning efficiency is similarly good at the given feeding rate, with values of 99.028 and 98.035%. As a suggestion, the presence of the step sieves, which occupy a lot of space and give the machine the appearance of being extremely large, leaves room for improvement or modification to reduce the size of the machine. When the moisture content of the biomass being threshed is higher than the ideal moisture content for teff threshing, the machine's capacity and efficiency are reduced, requiring a high energy input from the engine and even the possibility of engine shutdown.

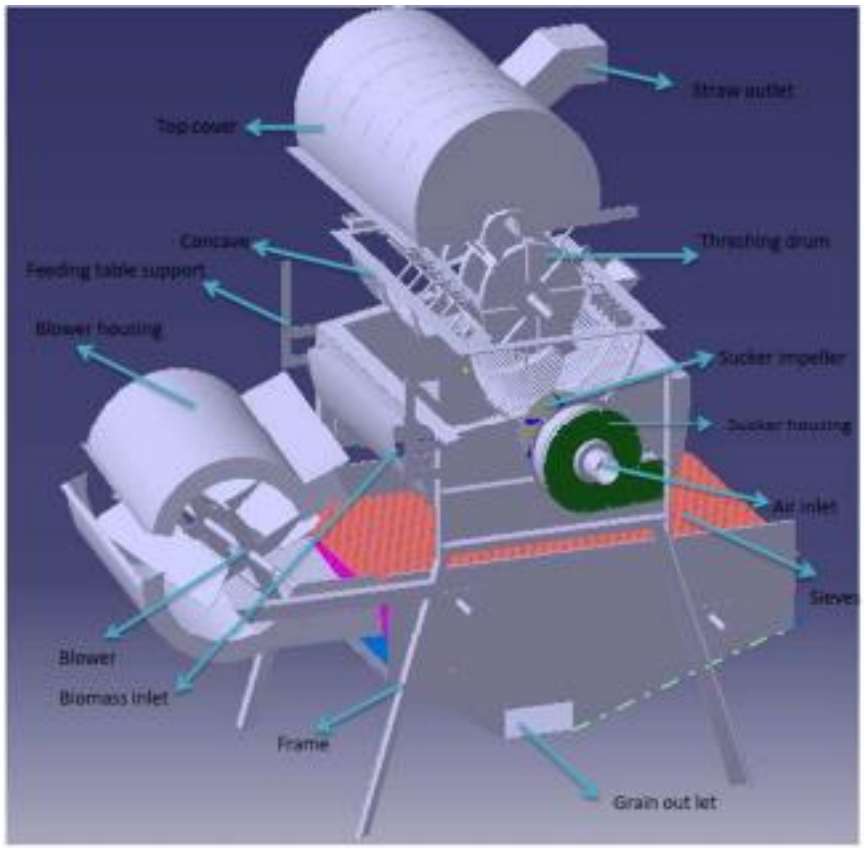

Figure 2-9 Teff Thresher developed Merga Workesa [2]

Chapter 3 Methodology

3.1 Seed size

With a rise in moisture content from 5.6% to 29.6%, the length, width, and equivalent-sphere diameter of seeds increased from 1.01 to 1.27 mm, 0.59 to 0.68 mm, and 0.71 to 0.87 mm, respectively. It was discovered that there is a linear relationship between length, width, equivalent sphere diameter, and moisture content. [34]

$$L = 0.0062M + 1.11$$

$$W = 0.0032M + 0.75$$

$$D_e = 0.0069M + 0.67$$

Where: M is moisture content in % wet base with values for the coefficient of determination, R^2 of 0.82, 0.74, and 0.89, respectively

Take the moisture content to be 12 percent L***=1.111 mm, W=0.751 mm, D=0.671mm***

3.2 Design of the threshing cylinder drum

This section introduces the method employed for the study and details of numerical expressions of the overall modeling of threshing drum, the screw conveyor and the cyclone separator to achieve the research objective mentioned above. Figure 3.1 show the schematic diagram of the conceptual framework of the applied methodologies to design the threshing drum.

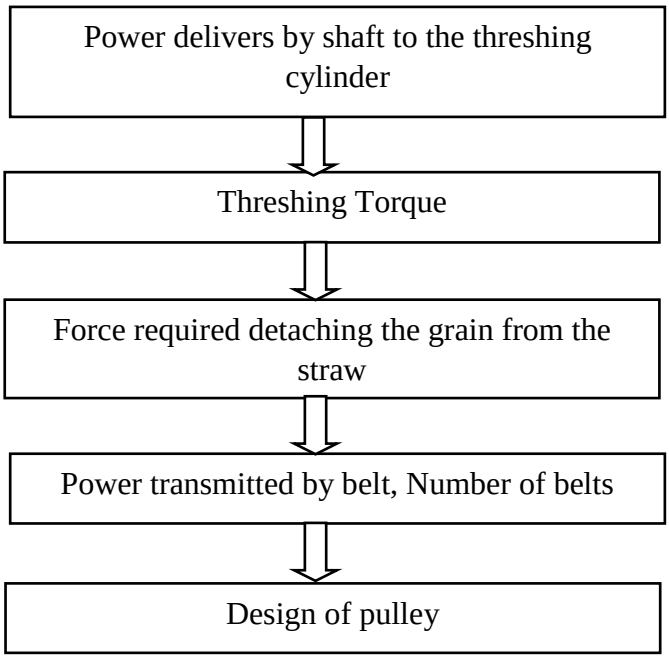

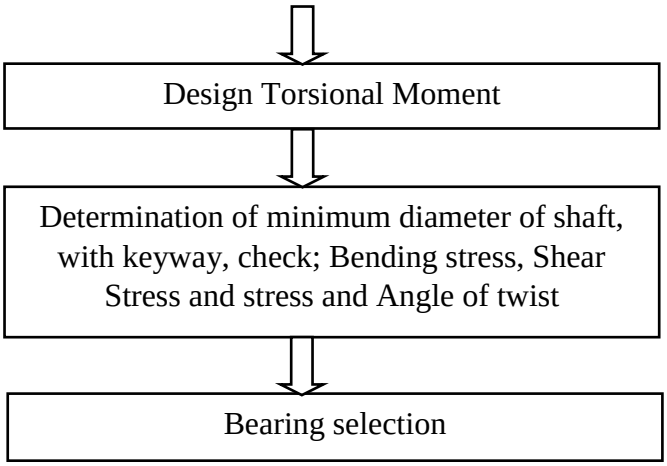

Figure 3-1 Design flow diagram of the threshing cylinder drum

On the design of the threshing drum, we will analyses it using both theoretical methods by using normal calculations and numerical methods by using Autodesk inventor simulation and eventually comparing the results found.

3.3 Modal Analysis

Because of its massive size and rapid speed, the Tangential flow threshing cylinder shakes violently throughout the threshing process. The periodic centrifugal force induced by vibration produces local deformation of the cylinder, increasing the rate of grain breakage and loss. The vibration radiation transmission on the bearing frame becomes the primary excitation source of the combined vibration, which has a significant impact on the stability of the working parts and the overall machine reliability [5].

3.3.1. Modal Analysis and Test of Threshing Cylinder

The finite element free modal analysis can obtain the vibration characteristics of the threshing drum in the unconstrained state, that is, the inherent characteristics in the ideal state, and can solve the vibration characteristics of the threshing cylinder [29]. The natural frequencies and modal morphologies of a threshing cylinder in the Free State can be successfully solved by the development of the threshing cylinder finite element model and simulation analysis in ANSYS Workbench.

3.3.1.1 Free Modal Analysis of Finite Elements

Prior to performing a free modal analysis, the finite element model must first be established. Due to the numerous components and intricate shapes of a threshing cylinder, as well as the interference of the mesh number, element type, mesh quality, and other factors [30], it is required to take the model's simplification into account in order to produce an accurate finite element model. Therefore, local features that were much smaller than the mesh size, such as bolt holes, fillets, and chamfers, were disregarded. It was decided not to consider the welding flanging, which has little bearing on the structure and changes in material properties brought on by the welding joint. The structure was condensed into a model with rigid connections.

The elastic modulus E = 205 GPa, Poisson's ratio u = 0.29, density = 7870 kg/m3, and yield strength s = 208 Mpa of the material were used to identify it as AISI 1018 Carbon Steel structural steel. The finite element analysis program ANSYS Workbench received the three-dimensional solid model of the threshing cylinder in the STP format. The ANSYS mesh module was used to do the meshing, and the sizing command was used to manage the grid quality.

3.4 Cyclone

The physical properties of the teff seed and grain that are useful to do the analysis in the cyclone separator are presented below.

Table 3-1 Physical property of teff grain

Moisture content (wet basis)	Thousands grain mass mass(TGM)(grain)	Grain density(Kg/m^3)	Average diameter (mm)	Terminal velocity(m/s)	Drag coefficient(c_d)
11.94 %	0.292	1361.8	0.74	3.24	0.76
15.1%	0.320	1358.2	0.76	-	-
21.1%	0.361	1314.9	0.86	-	-
24.2%	0.392	1283.7	0.87	-	-
27.1%	0.421	1252.9	0.88	4.04	0.66

Table 3-2 Physical property of teff chaff

Straw length (mm)	Node free		Middle node		End node	
	Mass(gram)	Diameter (mm)	Mass(gram)	Diameter(mm)	Mass(gram)	Diameter(mm)
6	0.029	1.630	0.032	1.760	0.032	1.810
8	0.034	1.870	0.060	1.712	0.061	1.720
10	0.058	1.670	0.064	1.880	0.063	1.830

- To design the cyclone separator the following design procedure was used.

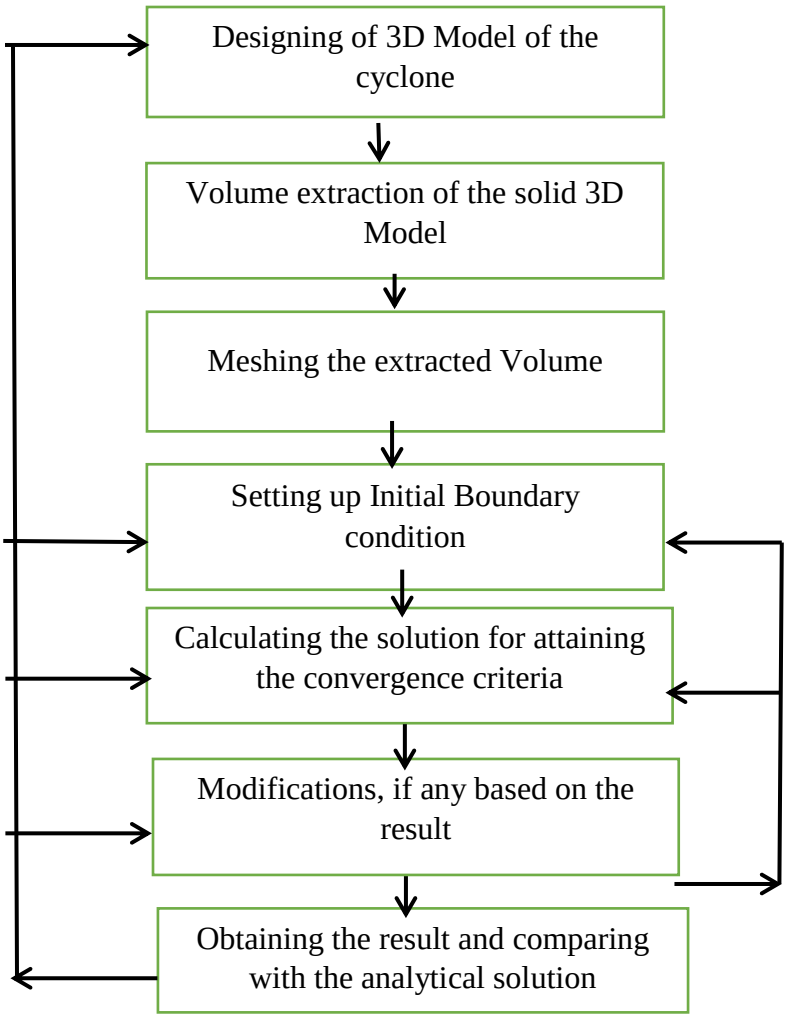

Figure 3-2 - Methodology to design the cyclone Separator

Chapter 4 Result and discussion

4.1 Threshing Drum Design

The threshing unit which consists of a rotating drum and concave jointly thresh the grains from the straws. The threshing teeth are welded tangentially on the flat bar on the drum. In the separation unit, threshed grains falls through the lower concave openings and fall in to the screw conveyor Then after the fan hits the chaff and the teff seed in to the cyclone separator and the cleaning will done on the cyclone separator, the teff seed will come out from the bottom of the cyclone while the chaff and other impurities will goes out in the top.

Rpm=1200 rpm, Radius = 600 mm (from literature summary)

$Q = 1250 kg/hr = 0.34 kg/s$ (Feed rate)

g/s =0.49 (Grain to straw)

Length of threshing cylinder $L = q * \eta * \rho * u_1$

$$\underline{\underline{L}} = 0.8925 \text{ m} \approx \underline{\underline{0.9 \text{ m}}}$$

4.1.1 Spike tooth Design

Design of threshing element:

The following Assumptions where taken in account to design the spike tooth

- The cross sections of the peg tooth and spike tooth types of threshing elements are, respectively, circular and rectangular.
- Only bending stress, provided by the crop during threshing, is applied to the threshing element.
- The bending force is applied 80 mm above the cylinder bar (height of element, he)
- [7] Reported a width to thickness ratio of 3:1 for a peg teeth type threshing element (t = 0.33b).
- A mild steel threshing part with a yield stress of 175 MPa is manufactured.

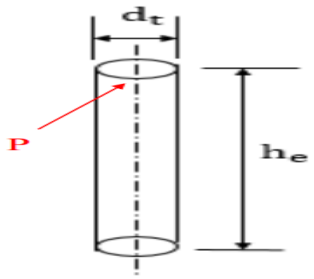

(a)-Spike Tooth (Circular cross section)

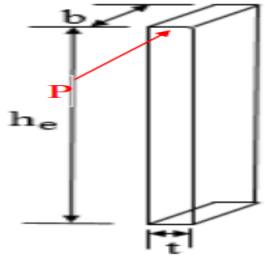

(b)-Peg Tooth (Rectangular cross section)

Figure 4-1- spike tooth and peg tooth geometry

Taking the physical properties of a mild steel as follows [33]

$\sigma_p = 350mpa$ (Mild steel)

$h_e = 80mm$ (Assumed spike tooth)

σ_b =Working bending stress of mild steel (yield stress/factor of safety=250/2.5=125 mpa)

Where

$$y = \frac{d_t}{2}$$

$$I = \frac{4\pi}{16.d_t}$$

$$M = p * h_e$$

Where $p = p_1 + p_2$ =tangential force acting on the element during threshing

$$p = \frac{m'.V_p}{1 - f}$$

Where m' =Mass flow rate

V_p =peripheral speed

f = rubbing friction =0.9

p =8.5 KN from this

d_t =8 mm

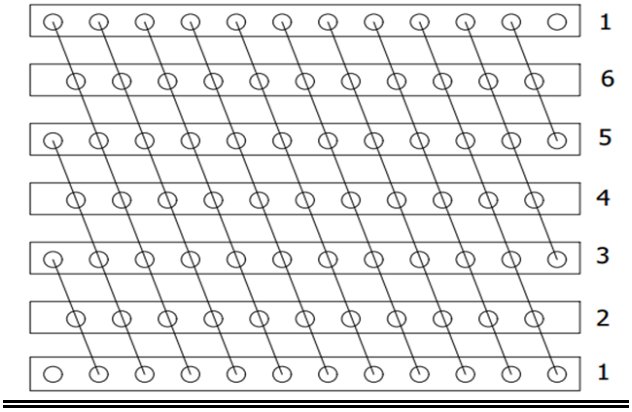

Figure 4-2 Orientation of the pegs Around the cylinder bar

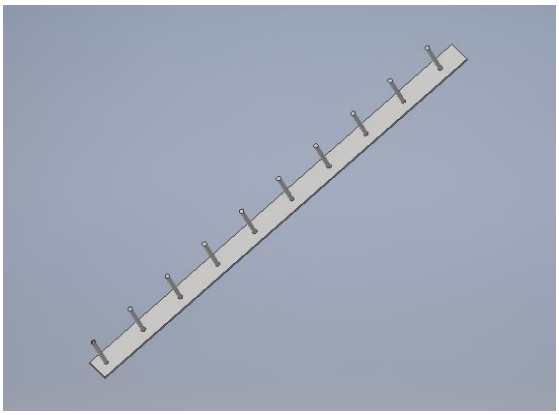

Figure 4-3 Spike tooth physical model

4.1.2 Design of shaft

In this paper, it includes of three main parts, which are; Design Consideration of Threshing Drum, Theoretical Analysis of Threshing Drum, Numerical Analysis of Threshing Drum

(A) Design Consideration of Threshing Drum

(1). Total weight of threshing drum:

Total weight of threshing drum,

$$W_{Toatal} = W_{discs} + W_{bars} + W_{support} + W_{teeth} + W_{blades} + W_{hubs} \text{ (All Dimensions are in N)}$$

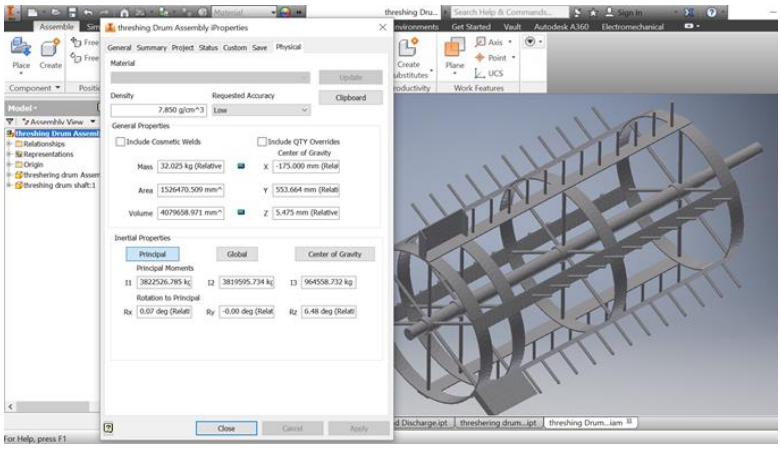

Figure 4-4 Mass of the threshing drum from Autodesk Inventor 2016

From figure 4-4 the mass of the threshing is to be 32.025 kg (=314.16525 N)

(B) Theoretical Analysis of Threshing Drum Structural behavior (von-Misses stress, effective strain) of threshing drum is calculated by theoretical approach. The threshing drum is made of AISI 1018 Carbon Steel (UNS G10180).

Material property	**Values**	**Units**
Density	7.87	*g / cc*
Ultimate strength	347	*Mpa*
Yield Strength	208	*Mpa*
Modulus of Elasticity	205	*Gpa*
Poisson's ratio	0.29	-
Shear modulus	80	*Gpa*

Table 4-1 Material Properties of AISI 1018 Carbon Steel (UNS G10180)[34]

(1) Bending stress for threshing drum:

The bending moment on the threshing drum by the weight of the threshing drum, weight of the pulley and the pulley tensions is calculated

$$M = (8kgx9.81x0.125m) + (510x0.125m) = 73.66Nm$$

- The bending stress will be

$$\sigma_b = \frac{Mxy}{I} = \frac{32xM}{\pi x d^3} = 34.7534 \ Mpa$$

- The equivalent stress can be calculated

$$\sigma_e = \frac{1}{2}\sqrt{\sigma_b{}^2 + 4.\tau^2} = \frac{16}{\pi d^3}\sqrt{M^2 + T^2} = 81.994 \ Mpa$$

When shaft is subjected to fluctuating load then the equivalent stress is given by the equation solving for the diameter by replacing all the values

- $\sigma_e = \frac{16}{\pi d^3}\sqrt{(k_b M)^2 + (K_t T)^2}$ =43mm.

(2)Shear stress for threshing drum:

$$\tau = \frac{T \times r}{j} = \frac{Tx(\frac{d}{2})}{(\frac{\pi}{2})d^4} = \frac{16xT}{\pi x d^3} = \frac{16x52.54N.m}{\pi x 0.6^3} = 3.358\,Mpa\,.$$

using radius of the shaft not the cylinder

Table 4-2 shows the calculated Bending and shear stress threshing drum design used in Teff Thresher

Parameter	Value	Unit
Total weight of threshing drum	314.16525	N
Angular Velocity	125.6	*rad* / sec
Threshing Power	6.6	kW
Threshing Torque	52.54	N-m
Centrifugal force	175.13	k-N
Radius	0.3	M
Bending Stress	34.75	Mpa
Shear Stress	3.358	Mpa

(C) ***Numerical Analysis of Threshing Drum:*** The shear diagram, bending moment diagrams are generated by Inventor pro 2016.by applying the required forces and Moments. By applying the bending moment resulted from the rotating drum pegs and the concentrated loads and also the tension force from the pulley were applied and compared the results with the theoretical ones.

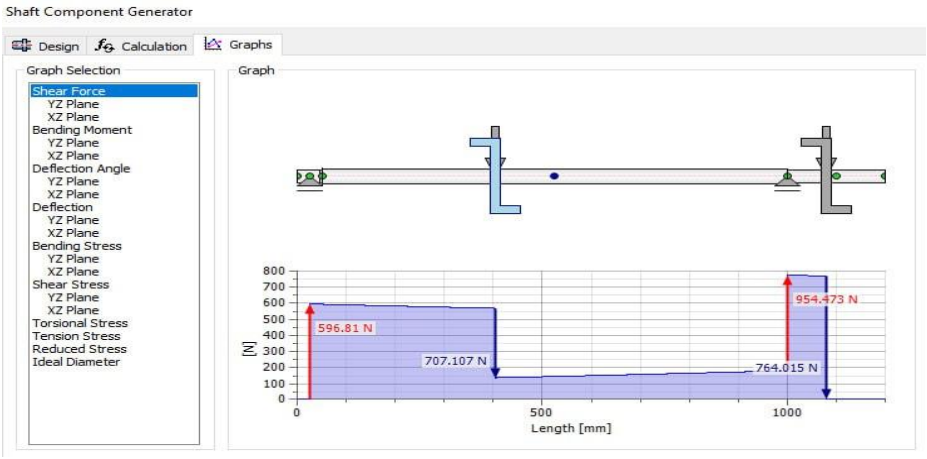

Figure 4-5 shear force diagram of the shaft

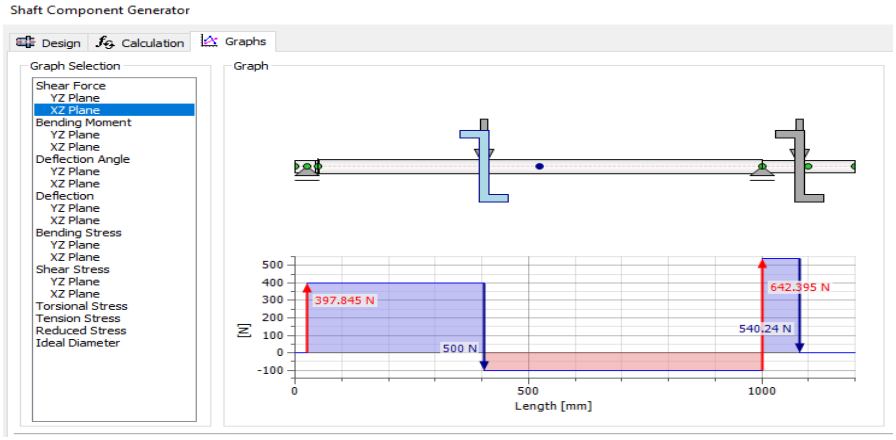

Figure 4-6 Bending moment

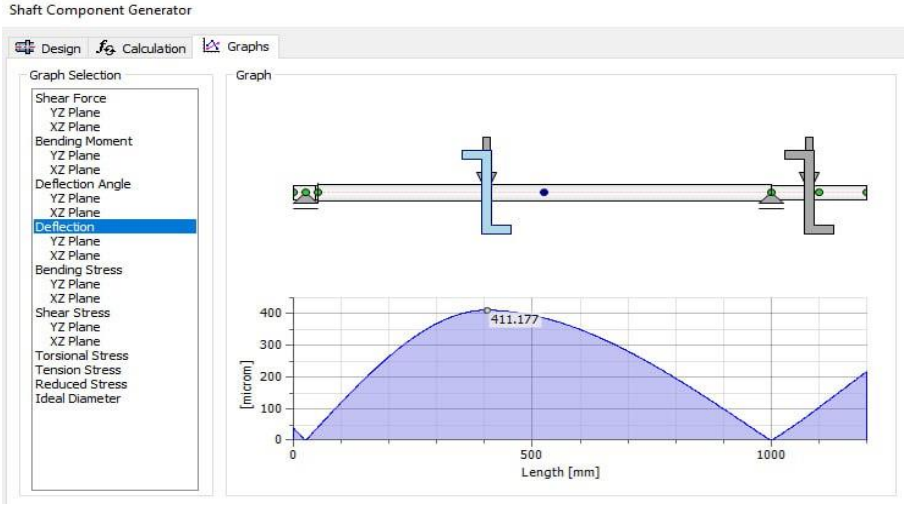

Figure 4-7 Deflection

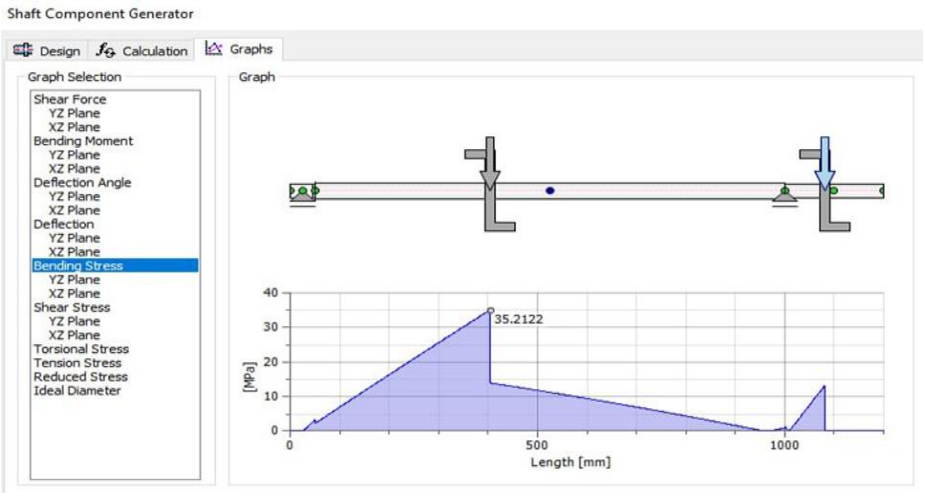

Figure 4-8 Bending stress

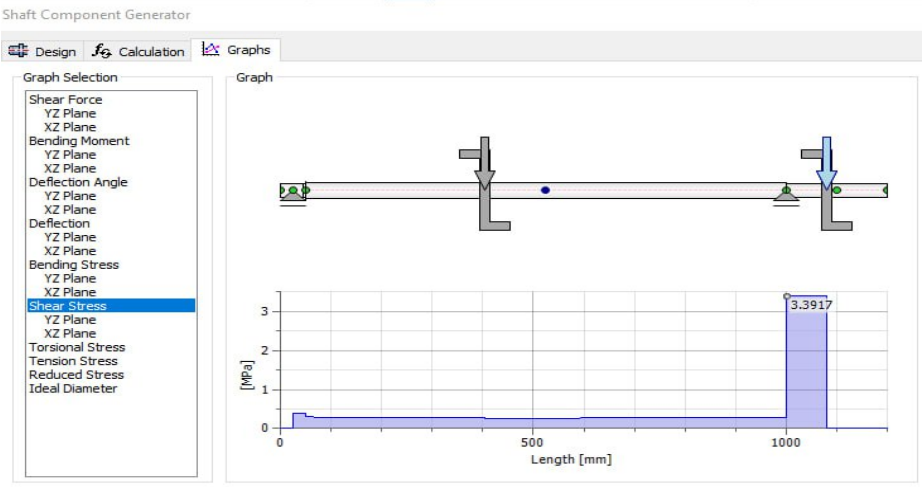

Figure 4-9 Shear stress

Table 4-3 comparison of results from the theoretical and Numerical

No.		Autodesk Inventor Result	Manually calculated	Error
1.	Bending Stress	35.2122 Mpa	34.7534 Mpa	1.3 %
2.	Shear Stress	3.3917 Mpa	3.358 Mpa	1%
3.	Ideal Diameter	44.3 mm	43 mm	3%
4.	Deflection	411.7microns	-	

From the analysis using the Autodesk Inventor the results are discussed below

- *From the result we can see that the analytical results are greater than the theoretical results .we observe not that much significant difference we will take the results from the numerical Approach.*

4.1.3 Bearing Selection

Since the reaction forces are tangential and radial force we can select roller bearing as follow:

The dimensional less load factor

$$XD = \frac{LD}{L10} = \frac{60x\ LDxnD}{L10} = \frac{60x900x1200}{10^6} = 720$$

From the Weibull parameter take application factor of 1.2 and a=10/3 for the roller bearing

$$C_{10} = affd[\frac{Xd}{Xo + (\theta - Xo)(1 - Rd)^{1/b}}]^{1/a}$$

$$C_{10} = 1.2x954.473[\frac{720}{0.02 + (4.439)(1 - 0.99)^{1/1.483}}]^{3/10}$$

$$C_{10} = 13.03KN$$

- ✓ Using C10 value we can select 02serious cylindrical roller bearing with dimensional value of:

Selected bearing dimensions:-

- ✓ Outside diameter=72 mm
- ✓ Bore =35 mm
- ✓ Width=17 mm
- ✓ Load rating=25.5 kN

4.1.4 Selection of the drive system

4.1.4.1 Belt Selection

In general ,belt drives are applied where the rotational speed are relatively high, as the first stage of the speed reduction from an electric motor of engine .the linear speed of a belt is usually 2500-6500 ft./min. A speed of 4000 ft. /min is generally ideal.

Many types of belts are available like flat belts, Grooved or cogged belt, standard v-belt, double angle v-belt and others. But among the above stated types of belts the widely used type of belt particularly in industrial drives and vehicles applications is the v-belt drive. The shape causes the belt to wedge tightly into the groove increasing friction and allowing high torque to be transmitted before slipping occur.

Initial data for selecting the belt drive the total power required is 6kw based on that the available engine is 6.6kw at 3600 rpm.

- Power of the engine (Torque) =6.6kw=8hp
- Speed of the engine =3600 rpm.

From [33] table 7-1-taking the assumption of working 6-15 hr/day the V-belt service factors will be 2.

- ✓ Step- 1 –calculate the design power

Then the design power is 8hp (2) =16 hp.

- ✓ Step -2 – Compute the nominal ratio

To find out the nominal ratio we have stated the rpm of the drum shaft to be 1200 rpm.

Nominal ratio= $\frac{3600}{1200}$ =3.

- ✓ Compute the driving sheave size that would produce at the belt speed of 4000 ft. /min.

Belt speed = $V_b = \frac{\pi D_1 n_1}{12}$ $ft/\min$

$$D_1 = \frac{12v_b}{\pi n_1} = 4.24 \text{ in } (107 \text{ mm})$$

Min pulley diameter =12cm

- ✓ Specify a trail center distance

$$D_2 \le C \le 3(D_2 + D_1)$$

$$48 < C < 180$$

In the interest of considering the space and geometrical modeling let us take 80cm.

$$L = 2C + 1.57(D_2 + D_1) + \frac{(D_2 - D_1)}{4c}$$

Replacing the values

L=258.25 cm next standard belt length is 2582=100 in

$$C = 0.25\left\{L_p.\frac{\pi(D+d)}{2} + \sqrt{L_P.\frac{\pi(D+d)^2}{2} - 2(D-d)^2}\right\}$$

C=77.818 cm

- ✓ Compute the angle wrap of the belt on the small sheave

$$\theta_1 = 180^0 - 2\sin^{-1}\left[\frac{D_2 - D_1}{2C}\right]$$

$$\theta_1 = 154^0$$

- ✓ Determine the correction factor for $\theta_1 = 154^0$

$\theta_1 = 154^0 \Rightarrow C_\theta = 0.93$
$L = 100in \Rightarrow C_L = 0.96$

- ✓ Correction power $= C_\theta . C_L . {}^{p} = 0.93*0.96*8\ {}^{hp} = 7.1424\ {}^{hp}$
  - ➢ The pulley diameters are D_1=12cm and D_2=48cm.

4.1.4.2 Design of pulley

V- Belt drives look like similar to chain drive system but there is one important difference in which both sides of the v-belt are in tension.

$$F_N = F_1 - F_2$$
$$T = F_N * r$$
$$T = \frac{60 * power(kw)}{2\pi * speed(rpm)}$$

T=Replacing the values p=6.6 kW and rpm=1200

T=52.54 Nm.

Since the torque drive is transmitted by a belt drive

$$F_N = T / r = 52.54*10^3 \text{ N mm}/240 \text{ mm} = 218.9 \text{ N}$$

The tension ratio of $F_1 \& F_2 = 2.5$ meaning $\frac{F_1}{F_2} = 2.5$, $F_1 = 2.5F_2 =$

$F_1 = 145.9\text{N}$ and $F_2 = 364.91$ N

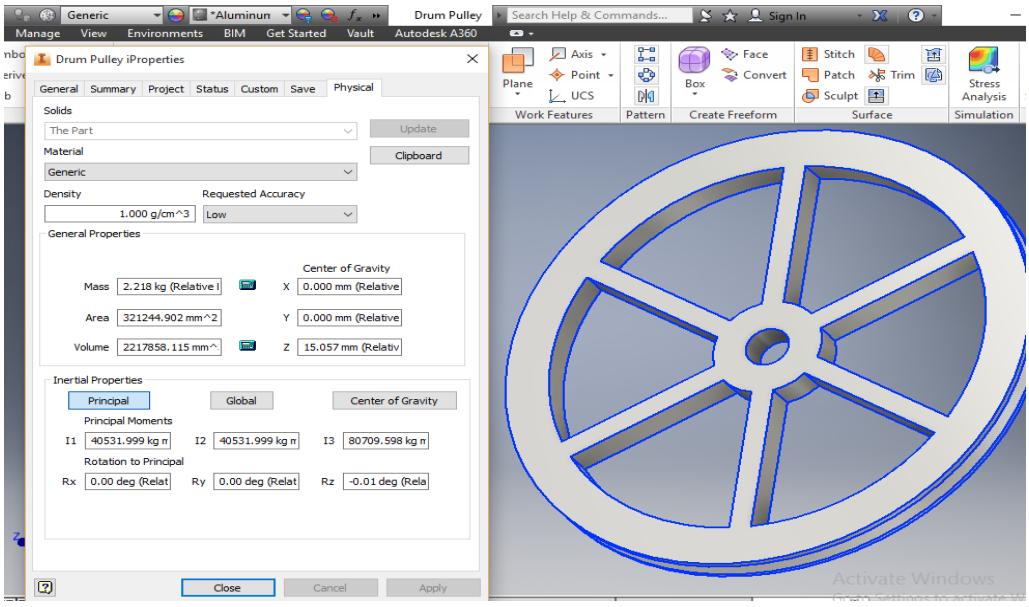

Figure 4-10 Physical Property of the pulley collected from Autodesk Inventor 2016.

- Total weight of the pulley is 3 kg=29.43N. Then the total load applied is

$$F_{@\,pulley} = 29.43+364.91+145.9 = 540.24 \text{ N}.$$

$$F_{@\,pulley} = F_1 + F_2 + W = 540.24\text{N}$$

Design Summary

- Input Diesel engine =8 *hp*
- Service Factor – 2
- Design Power= 16 *hp*
- Belt -3V cross section 100 in length, 2belts.
- Actual Output = 1200 rpm
- Center Distance= 77.7 cm

Total cylinder weight, threshing power, threshing speed, threshing torque, and moment were all calculated in the threshing cylinder design. Power transmission shaft design calculations are performed under the assumption that the shafts are only in torsion and bending. The necessary belt type and number of belts were computed in the V-belt drive calculation. The suitable bearing numbers for each bearing were calculated during bearing design and selection. After reviewing the results, it was discovered that existing theories and computed results are strongly similar.

4.2. Determination of power required threshing

Source of power – There are various power sources used to operate agricultural machinery, such as manual operation, animal powered, engine motor (Diesel or Benzene), tractor (small to large size), and recently solar powers, which are especially useful in irrigation fields. Because we intend to create a high capacity teff thresher, we have omitted manual and animal-driven operations because they are employed for lower capacities. Our design requirements are focused on land holding capacity and technology affordability ease of operation for most farmers, and higher quality of work. As a result, there are several options:

• Motor (diesel or Benzene)

• Electrical Motor

• Tractor PTO

Selection criteria are:

1. Low cost
2. Easy for operation

3. Availability of electric source

4. Appropriate for small scale farmers and small land holding

Table 4-4 Evaluation criteria for selecting power source

Selection Criteria	(Reference) Manually operated	Motor (diesel or Benzene)	Electrical Motor	Tractor PTO
1. Low cost(Affordability)	0	-	-	-
2. Easy for operation	0	-	0	-
3. Availability of power source	0	0	-	0
4. Appropriate for small scale farmers and small land holding	0	1	1	0
5. High power and torque	0	1	1	1
6.Availablity in remote and farming areas	0	0	-	0
Sum +s	0	2	2	1
Sum –s	0	2	2	3
Sum 0s	6	2	2	2
Net Score	0	2	2	1
Rank	4	1	1	2
Continue?	No	Yes	Yes	Yes

The concept-screening matrix we have rated the concepts against the reference concept using a simple code (+ for “better than,” 0 for “same as,” − for “worse than”).

Table 4-5 Weighted evaluation criteria for selecting power source. (Dieter and Schmidt, 2013)

Selection Criteria	Weight	Motor (diesel or Benzene)		Electrical Motor		Tractor PTO	
		Rating	Weighted score	Rating	Weighted score	Rating	Weighted score
1. Low cost(Affordability)	20 %	5	1	5	1	3	0.6
2. Easy for operation	10%	4	0.4	5	0.5	3	0.3
3. Availability of power source	15%	5	0.75	3	0.45	5	0.75
4. Appropriate for small scale farmers and small land holding	15%	5	0.75	4	0.6	4	0.6
5. High power and torque	20%	4	0.8	4	0.8	5	1
6.Availablity in remote and farming areas	20%	5	1	3	0.6	5	1
Net Score			4.7		3.95		4.25
		use					

- Based on the selection criteria Motor (Diesel/Benzene) is selected.

4.2.1 Force required threshing the grain

In the process of static analysis, when the threshing cylinder works and rotates, it is mainly affected by the

I. ***Torque M transmitted by the engine*** to the threshing cylinder,
II. ***The force F exerted by crops*** on the Spike teeth,
III. G***ravity G of the threshing drum***, and
IV. S***upporting force FN at both ends*** of the bearing (ignoring the effect of air resistance and bearing friction)

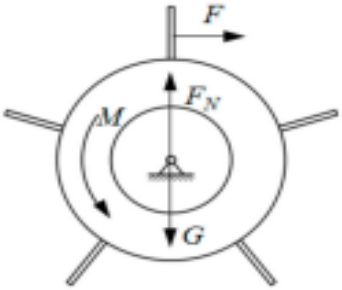

Figure 4-11 Static force of a threshing cylinder

- To thresh teff crop a force 'F' is needed, which is a function of cylinder linear speed as well as the friction coefficients between the crop-crop and crop-metal.

$$F = F_C + F_r$$

F = the force needed for threshing crop (N)

F_c = Impact for the cylinder (N)

F_r = Friction force (N)

The impact force F_c

$$F_c = Q(V_2 - V_1)$$

$$V_2 = \alpha V$$

$$V = \frac{R * 2\pi * N}{60}$$

$$F_r = f * F$$

R=threshing cylinder radius (m)

N=cylinder (rpm)

f =the coefficient f, for spike tooth equal to 0.7-0.8.

V=30.159 m/s

Q =0.3472 kg / s

$V_1 = 12 m/s$ (Assuming the inlet velocity)

Fc=6.3 n and F_r =5.04

F=11.3N (Force required to thresh the teff Grain)

4.2.2 Required Force for teff Thresher: The threshing bars, discs, teeth and other parts which are attached to the contained in the threshing drum, rotate with the shaft due to centrifugal force.

Centrifugal force at threshing drum: F = m×ω2×r

Angular velocity of threshing drum:

$$\omega = \frac{2\pi \times N_{drum}}{60} = 125.6\, rad/\sec$$

Where,

F - Centrifugal force (N)

m - Mass of threshing Drum (kg)

ω - Angular velocity (rad/sec)

r - Radius of threshing Drum (m)

N - Speed of the drum (rpm)

F=303.1KN (Centrifugal force at threshing drum)

4.2.3 Power required turning the unloaded cylinder

N =rpm of the drum=1200 rpm

R=radius of the drum=0.3m

M_c =Mass of the cylinder=20 kg (from inventor software)

g = gravitational Acceleration = 9.81 m/s^2

V_T=Peripheral Velocity= $V = \frac{\pi DN}{60} = 37.7\ m/s$

$$p_u = 5{,}962.784 \; w = 5.963 \; kw$$

- ***Power required detaching the grain***

$$P_d = \frac{3K_e}{2}\left[\frac{V_s^{1/2} fr^{3/2}}{\rho w^2 L_c}\right]$$

fr = feed rate

L_c =length of the cylinder

ρ_w = Bulk density

V_g = Velocity of the grain

K_r= k_s, k_e, k_r is a constant that is influenced by the resistance of the crop material to the machine component.

$$P_d = 30.863w$$

$$P = \frac{3K_e}{2}\left[\frac{V_s^{1/2} fr^{3/2}}{\rho w^2 L_c}\right] + \frac{2}{3} Nf \left[\frac{\sigma_{\max}}{c}\right]^n .\pi D L_c + \frac{2\pi NrM_c}{60 \times 75}\left[g + \frac{V_T^{\,2}}{r}\right]$$

P =5.9kw+30.863=5.9 kW = **8hp**

4.3. Feeding table

A folding feeding table was designed for the specific teff thresher so that in idle cases it can be folded down to diminish the overall size of the thresher. The dimension were selected from ergonomic and safety precautions. Length 0.9m, width 1m, Height 0.22 m

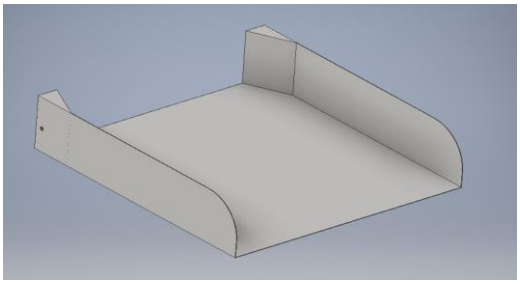

Figure 4-12 - Feeding table for the threshing drum

4.4 Concave

The concave performs two functions. It must support the threshed material in order to maintain the rubbing or impact action. The concave must allow the maximum possible amount of threshed material or mixture with grains. [15] Reported that, increasing concave length increased concave separation, for unit increase in concave length the proportion of grain separated is equal to 1- e -k, where e is the natural logarithms and k is the rate of constant. With crops that are easily threshed a longer concave produced little increase in threshing efficiency, however crops which were difficult to thresh the increase was not that much. The amount of grain damage increased with concave length since the grain which was not separated through the concave was subjected to a greater number of impacts before leaving the threshing crescent. For the case of very small grains like teff it is not much suspicious for damage and the length of concave is not affecting, rather the length of concave may affect the separation rate of teff threshing. 42 There were comparison studies in regard of concave openness, the two concave types, open and closed type was studied on wheat crop and they come up with the result that there were four times as many damaged kernels in the samples produced using closed concaves. For small grains where the grain damage is not series problem, It is possible to use both types. The concaves area is critical for separation because the increase in the area is directly proportional to the separation rate. Based on the results of all tests and assumptions, the closed type concave will be one option for the teff threshing unit.

With the moisture content to be 12 percent the teff seed grain dimension are L=1.111 mm, W=0.751 mm, D=0.671mm.Based on the above dimension and to prevent clogging hole diameter of the concave is 3mm.

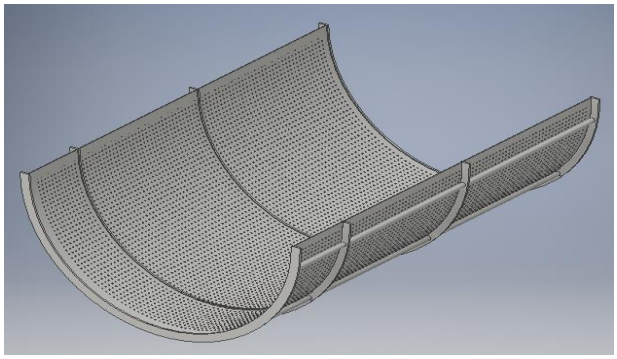

Figure 4-13- concave

4.5 Screw conveyor

A screw conveyor is made up of a circular or U-shaped tube that is rotated by a helix. The helix pushes grain along the tube's bottom, causing the tube to not completely fill. Screw conveyors are commonly used to transport and/or elevate particulates at controlled and consistent rates. They are used in a variety of bulk material handling applications, such as agriculture (moving grain from storage bins to transport vehicles, mixing grain in storage, and moving grain in a bin to a central unloading point), chemicals, pigments, and food processing.

They are very effective conveying devices for free flowing or relatively free flowing bulk solids, providing good throughput control and environmentally clean solutions to process handling problems due to their simple structure, high efficiency, low cost, and low maintenance requirements. They are impractical for high capacity or long transport distances due to the high power requirements. Screw conveyors have diameters ranging from 75 to 400 mm and lengths ranging from less than 1 m to more than 30 m. [38]

The physical properties of the material to be handled should be considered before selecting an appropriate conveying device. Moisture content, average weight per unit volume, angle of repose, and particle size are all important properties for agricultural products. Grain flow rate, distance, incline available space, environment, and economics all have an impact on conveyor design and operation. The strength and size of the conveyor components were calculated and chosen using essential design calculations. This was accomplished using the results of the design analysis and established formulae.

4.5.1 The shaft

The shaft's design was based on determining its diameter in order to ensure adequate strength and rigidity when the shaft is transmitting power during operation and under loading conditions.

Design procedure of a screw conveyor

- Define the required capacity
- Based on the material to be conveyed read the material characteristics from the catalogue
- Based on the though loading from the characteristics table take screw and pipe diameter

- based on the given capacity at 1 rpm calculate your rpm to attain the required volumetric capacity
- If the resulted rpm is greater than the max. Rpm go back select new screw diameter
- If not choose the resulted rpm
- Calculate your power to drive the screw conveyor

The capacity of a screw conveyor with a standard screw flight can be estimated following

$$Q = \left(D_s^{\,2} - D_p^{\,2}\right) * p * K * N * CF$$

Q =screw capacity in kg / hr .

D_s =Screw diameter in m.

D_p =pipe diameter in m.

p =Screw Pitch in m

N=Screw speed in rpm

K=through loading factor (%)

CF=correction factor

- Step – 1

Define the requirement capacity=3.5 =3500 kg / hr .

From equation (2.30) bulk density of teff is @12 % moisture content is 821.56 kg / m^3. The volumetric capacity required will be 4.26 m^3 / hr .

- Step-2

Among different components of screw conveyor the pitch and the diameter are the essential one. The screw flight can take different shape and pitch according to the application in which it is used.

- **Standard flight:** constant pitch = 1 diameter; suitable for the majority of applications - short pitch: used for inclined screws, but can also be used for fluid materials.

- **Enlarging pitch:** For feeders below a hopper, a smaller pitch at the beginning of the screw can be used to provide a constant feed.
- **Shortening pitch:** Large pitch at the beginning and shorter pitch at the end will cause compression; this is not a common design and can result in a lot of thrust on the screw, a lot of power required, and possibly mechanical damage. If the screw is properly designed, the screw flights can be used as feeding devices for a pressure system, because the compressed powder at the end of the screw acts as a plug, preventing gas from leaking towards the screw.
- **Ribbon :** used mainly for sticky materials

Pitch	Pitch length S
Standard	S=d
Short	S=2/3*D
Half	S=D/2
Long	D=1.5*D

Table 4-6- Standard pitch length

Based on the application let us take standard flights. Where the pitch and the screw diameters are equal the through loading factor (%) is 45%.

- Take the screw diameter to be 6 in. =152.4 mm

Pipe size=2 in. = 50.8

The rpm of the screw conveyor can be calculated

$$N = \frac{C_v(req)}{C_{v@1rpm}}$$ From the table $C_{v@1rpm}$ =2.23

N=150.44/2.23= 67.46 rpm

Power required for the screw conveyor

$$H_{Ptotal} = \frac{(H_{Pf} + H_{Pm})\phi}{e}$$

Where

H_{Ptotal} =total power required

H_{Pf} =power required to rotate unloaded screw conveyor (friction power)

H_{Pm} =power required to convey the material

ϕ =overload factor

e =drive efficiency (0.85 for belt drive)

$$H_{Pf} = \frac{L.N.F_d.F_b}{1,000,000}$$

Where

L=length of the conveyor, N=rpm, F_d = diameter factor, F_b =bearing factor

$$H_{Pm} = (C_v(req))(\rho)(L)(F_m)$$

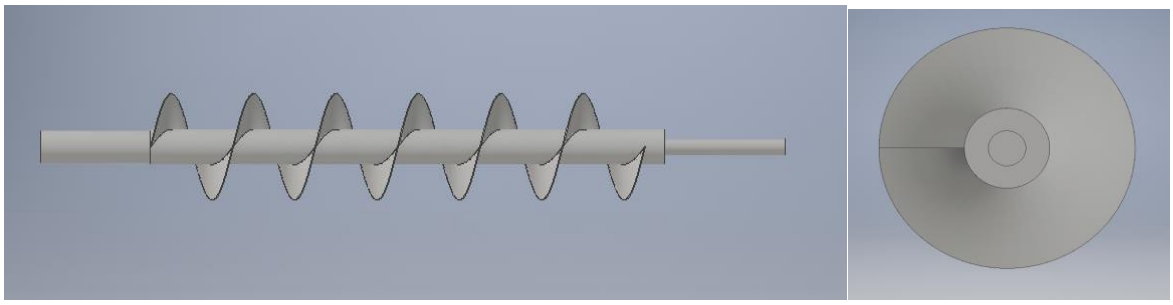

Figure 4-14-3D Model Screw Conveyor

4.5.2 Manufacturing the screw conveyor

P=pitch=150 mm

D=Outer Diameter=150 mm

d = Inside Diameter=50 mm

Step-1

$$l = \sqrt{(d*\pi)^2 + (p)^2}$$

$$D'(<0) = \frac{L}{\left(\frac{D\pi}{360^0}\right)} \quad , \quad d'(<0) = \frac{l}{\left(\frac{D\pi}{360^0}\right)}$$

l =217 mm

$$L = \sqrt{(D*\pi)^2 + (p)^2}$$

L=494.3 mm

$$d' = \frac{D-d}{\left(\frac{L}{l}-l\right)}$$

=78.5 mm

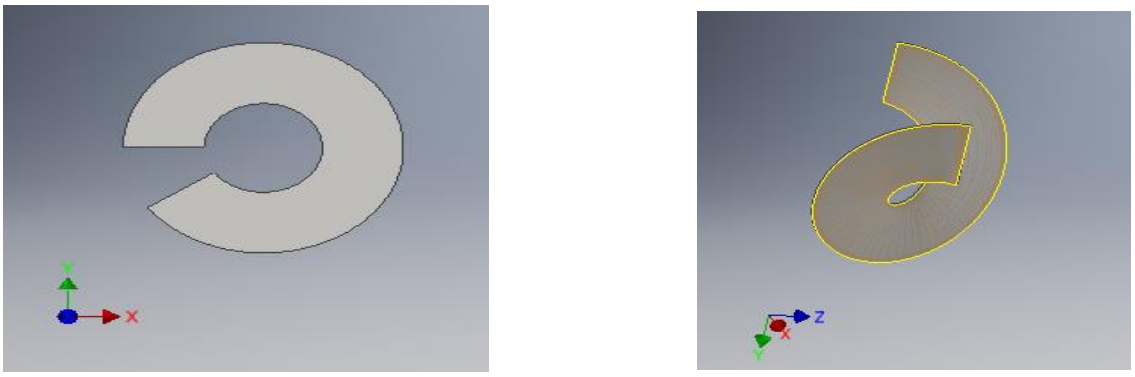

Figure 4-15- Screw manufacturing drawing

4.6 Cyclone separator

The increasing air velocity in the outer vortex exerts a centrifugal force on the particles, causing them to separate from the air stream. When the air reaches the bottom of the cone, it begins to flow radially inwards and out the top as clean air/gas, while particulates fall into the dust collection chamber attached to the cyclone's bottom.

4.6.1 Different Cyclone Model

The most commonly used abatement devices for particulate matter control in the agricultural processing industry are 2D2D (Shepherd and Lapple, 1939) and 1D3D (Parnell and Davis, 1979) cyclone designs. The Ds in the 2D2D designations refer to the cyclone's barrel diameter. The numbers following the Ds indicate the length of the barrel and cone sections, respectively. The barrel and cone lengths of a 2D2D cyclone are two times the barrel diameter, whereas the barrel and cone lengths of a 1D3D cyclone are equal to the barrel diameter and three times the barrel diameter. Figure 3-15 depicts the configurations of these two cyclone designs. Previous research

(Wang, 2000) found that 1D3D and 2D2D cyclones are the most efficient fine dust collectors when compared to other cyclone designs (particle diameters less than 100). When the PM in the inlet air stream contained lint fiber, [39] observed "cycling lint" near the trash exit for the 1D3D and 2D2D cyclone designs. [39] The exit PM concentration for these high efficiency cyclone designs increased significantly, which was attributed to small balls of lint fiber "cycling" near the trash exit, causing fine PM that would normally be collected to be diverted to the clean air exit stream. Simpson and Parnell (1995) developed a new low-pressure cyclone for the cotton ginning industry called the 1D2D cyclones to solve the cycling-lint problem. When compared to 1D3D and 2D2D cyclones, 1D2D cyclones are a better design for high-lint content trash [39]. Figure 3 depicts the 1D2D cyclone design configuration.

4.6.2 Design consideration of cyclone separator.

- Select either the high efficiency or high throughput design, depending on the performance required
- Obtain an estimate of the particle size distribution of the solids in the stream to be treated.
- Calculate the number of cyclone needed in parallel.
- Estimate the cyclone diameter for an inlet velocity of say 15 m/s. Then obtain the other cyclone dimensions from the graphs [35] Then estimate the scale up factor for the transposition of the figure. [35]
- Estimate the cyclone performance and overall efficiency, if the results are not satisfactory try small diameter.
- Calculate the cyclone pressure drop and check if it is within the limit or else redesign.
- Estimate the cost of the system and optimize to make the best use of the pressure drop available [35]

Standard cyclone Dimension (Lapple Dimension)

Conventional Dimensions

Cyclone Separator Dimension		
Dimension	Ratio	Value(m)

Diameter od cyclone Body (Barrel)	D	D	0.3048
Length of the Body	L_b	2D	0.6090
Length of the Cone	L_c	2D	0.6090
Height of the inlet	H	$D/2$	0.1524
Width of the inlet	W	$D/4$	0.0762
Diameter of inlet Pipe	d	$A=\pi r^2$	0.1180
Diameter of Gas Exit	D_e	$D/2$	0.1524
Diameter of Dust Outlet	D_d	$D/4$	0.0762
Length of Vortex Finder	S	0.625	0.1905
Length of S_c	S_c	$D/8$	0.0381
Total Length of cyclone	$L_b + L_c$	4D	1.2192

Table 4-7-Standard Cyclone Dimension (L apple Dimension)

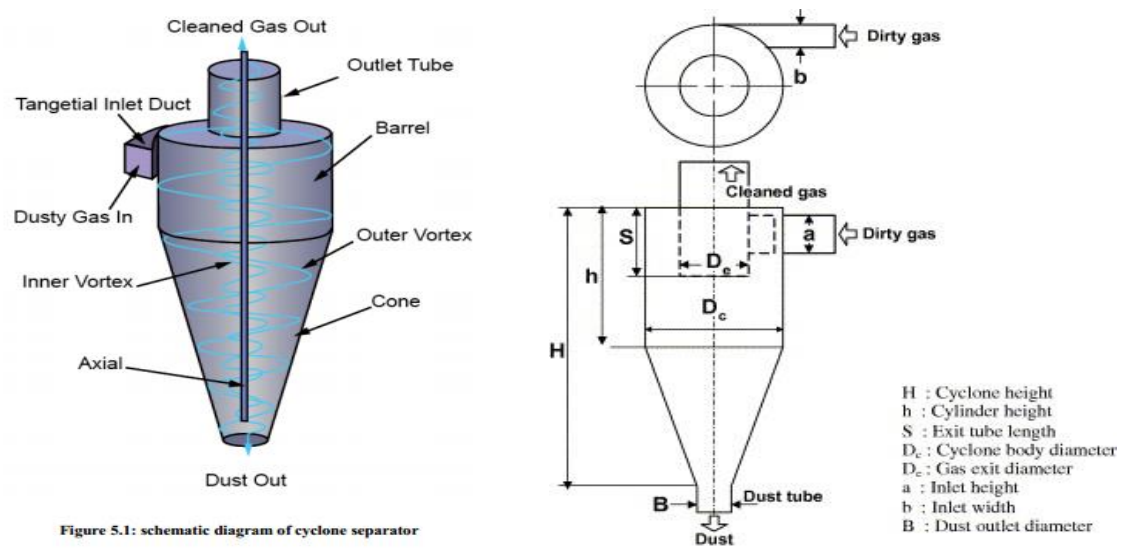

Figure 4-16-Schematic Diagram of Cyclone

- **Blower calculation:-Volumetric flow rate of the blower is 0.0277** m^3/s (given that 0.34 kg/s feed rate)

- **Velocity of air inlet duct**, $V_i = Q/WH$ =0.0277/ (0.0762*0.1524) = 2.97 m/s
- **Dynamic Pressure** $= 1/2\rho V^2$ =0.5*1.22*2.387^2=3478.3 Pa

Number of effective Turn= $N = \frac{1}{H}\left(L_b + \frac{L_c}{2}\right)$

N=4.92 (Values of N can vary from 1 to 10, with typical values in the 4-5 range.)

- **Gas residence time** $\frac{\Delta t = pathlength/speed = \pi DN/V_i}{V_t}$

Δt = 3.14*0.3*4.922/2.387=1.94 second.

- **Particle drift Velocity** $= V_t = W/\Delta t$ =0.0762/1.94=0.0392
- **Terminal drift transverse velocity**= $V_t = (\rho_p - \rho_a) d_p{}^2 . V_i^2 / 9\mu D$

= (821-1.22) (0.0007528)^2. (2.387)^2/9(0.0000183) (0.3)

V_t =52.56

- **Cut point diameter**

The cyclone's cut diameter is defined as the size of the particle collected with a collection efficiency of 50%. It indicates the particle size range that can be collected. It is a useful way of defining because it provides information on the efficacy of a particle size range. A common expression for cut off diameter is

$d_{pc} = \left[\frac{9\mu W}{2\pi N_e V_i (\rho_p - \rho_g)}\right]^{1/2}$ = 1.54x10^{-5} =15.4 μm (minimum diameter of teff seed is 0.71 mm)

- **Pressure drop**

The cyclone pressure drop is determined by the dimensions of the cyclone separator and its operating parameters. The pressure drop over a cyclone is caused by changes in area, wall friction, flow direction change, and vortex finder dissipation (outlet tube). In general, the term

"pressure drop" refers to a decrease in total pressure, which includes both static and dynamic pressure. In other words, the pressure loss between the inlet and outlet of the flow.

$$\Delta P = \frac{1}{2}\rho_g V_i^2 H_v = 1.26\text{pa}$$

- Power requirement $W_f = Q\Delta P$ = 3.5 j/sec
- Outlet Velocity= $V_0 = Q/\pi r_i^2$ =1.52 m/s

- Collection efficiency will be done in Numerical Analysis.

4.7. Modeling and simulation of threshing cylinder

Tangential flows drum as the research Design. Firstly, a three-dimensional solid model of the horizontal axial flow cylinder was established using AUTODESK INVENTOR PRO 2016 software, and the model imported into ANSYS Workbench 18 software. For element division, the setting of boundary conditions and the determination of modal solutions. To improve simulation efficiency, the structural features of the Tangential cylinder were simplified during the modeling process:

(1) Structural features such as rounded corners, threads and small-sized holes, which would have almost no effect on the simulation results but would greatly reduce simulation speed, were removed;

(2) Small size parts such as bolts and nuts were also removed for the same reason. An image of the three-dimensional solid model established in AUTODESK INVENTOR PRO 2016 is shown in fig (26).

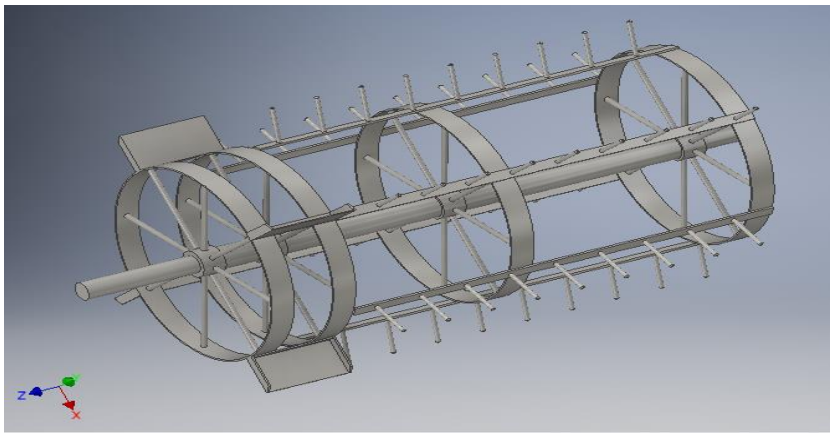

Figure 4-17-AUTODESK INVENTOR 3D Model

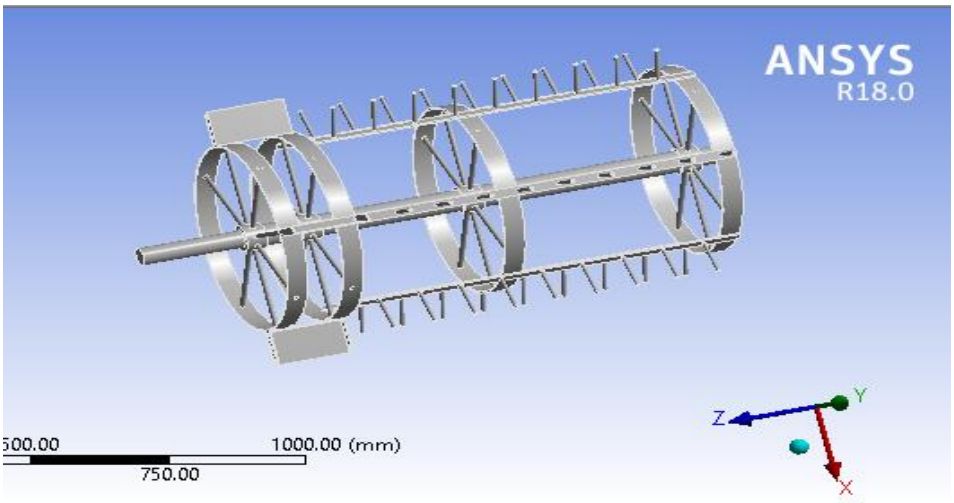

Figure 4-18-ANSYS Imported model

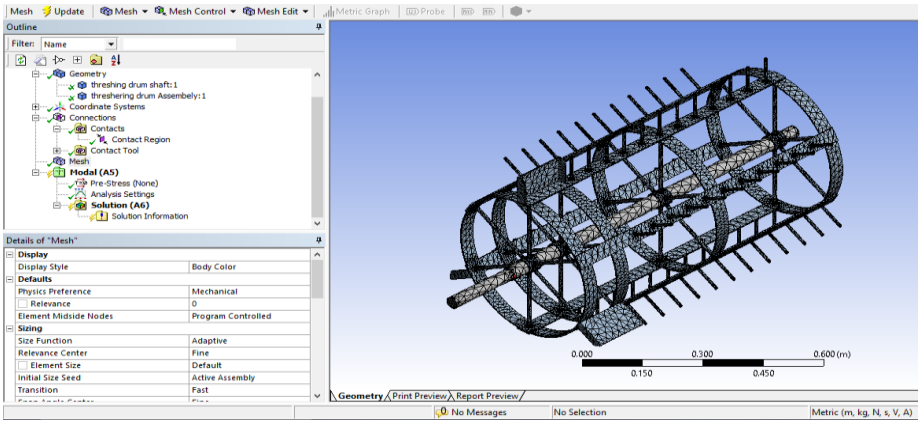

Figure 4-19- Mesh Generated Model

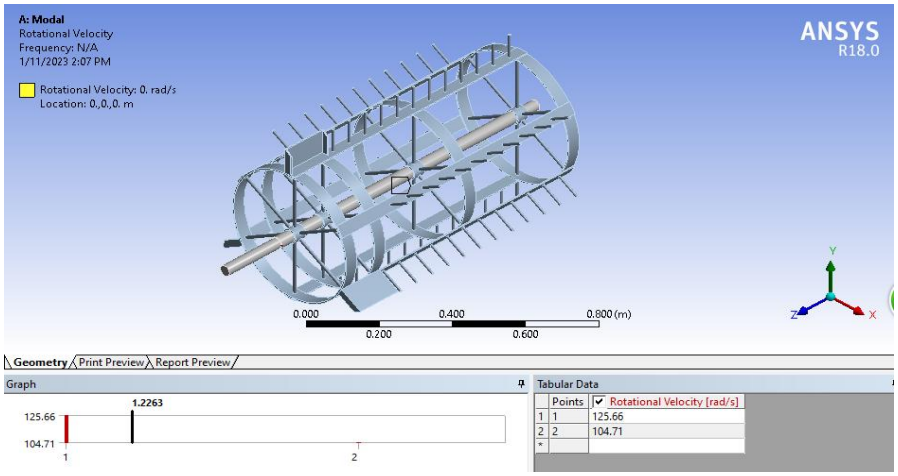

Figure 4-20- Rotational velocity of the threshing drum

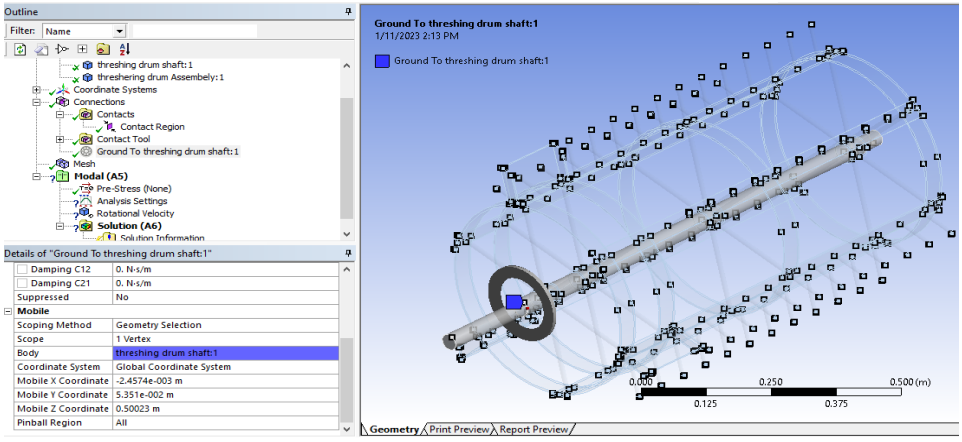

Figure 4-21-Boundary Conditions

As can be seen in fig (4.17), the X axis in the figures represents lateral direction of the threshing cylinder; the Z axis represents the longitudinal or axial direction of the threshing cylinder; and the Y axis represents the vertical direction of the threshing cylinder. The imported model in ANSYS is shown in Fig (4.18). The manufacturing material of the Tangential flow cylinder was selected as mild steel of AISI 1018 Carbon Steel which is typical in manufacture. The relevant material properties were an elastic modulus of 210 *Gpa*, a Poisson's ratio of 0.3, a density of 7850 kg m−3, and a yield stiffness of 235 *mpa*. Automatic grid division was adopted and the element size was set to 2 mm. The number of grids generated by the automatic division is 21,841 and the number of nodes was 48,519.

A static analysis of the horizontal Tangential flow cylinder was carried out. When the Tangential flow cylinder is running, the cylinder is mainly subjected to the torque transmitted by the engine, the tangential force of the cylinder, the supporting force of the bearings at both ends of the cylinder, gravity, air resistance and bearing friction. According to the working conditions, the influence of factors such as cylinder rotation friction, bearing friction and air resistance could be ignored. The boundary condition of the Tangential flow cylinder is shown in Fig (4-21).

As an inherent attribute and characteristic of the horizontal axial flow cylinder, the static mode is different to the material feeding state. Firstly, a modal analysis of the cylinder under no load conditions was carried out. In working conditions, the horizontal axial flow cylinder is solely constrained by the cylindrical surface of the bearing seats located at both ends of the central shaft in the no-load state. Due to the above constraints, the horizontal axis flow roller cannot move or

rotate along the Z-axis and X-axis directions shown in the coordinate system in the figure and can only rotate around its transmission axis (the Z axis).

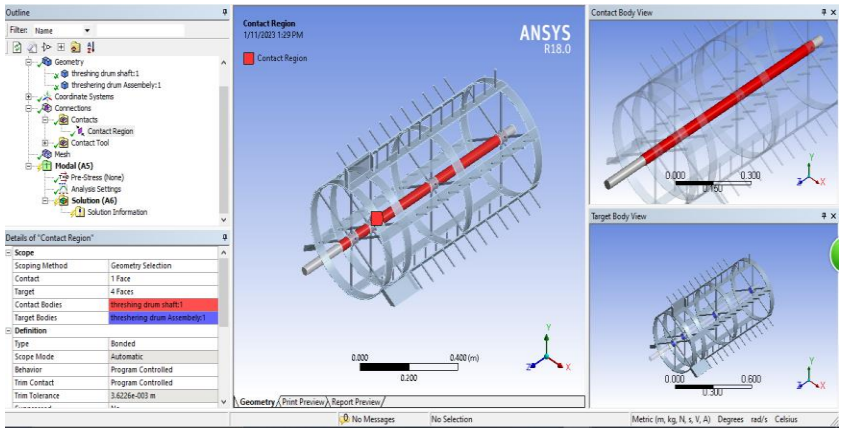

Figure 4-22 - contact type between the shaft and the rotating drum

4.8. Modal response of threshing cylinder

The best threshers preserve the shape and quality of the grain while performing complete threshing with the most crop input, the best grain separation, and the least amount of grain loss. [15] The design, operation, and failure of a threshing drum depend on a number of factors, including the distance between the drum and the concave and the rotational speed. Vibration in the threshing drum causes the distance between the concave and the drum to fluctuate, increasing the risk of threshing drum failure.

Eccentricity induces a centrifugal force deflection in a rotating shaft, which the shaft's flexural stiffness E I opposes. No harm is done as long as deflections are minor. Critical speeds, on the other hand, are another potential issue since they cause the shaft to become unstable and cause deflections to rise without limit. Fortunately, utilizing a static deflection curve provides an accurate estimate of the lowest critical speed even while the dynamic deflection shape is unknown. With zero moment and deflection at both bearings, such a curve satisfies the boundary condition of the differential equation, thus the shaft energy is not overly sensitive to the precise shape of the deflection curve. First critical speeds at least twice the operating speed are what designers aim for. The shaft has a critical speed because of its own mass. The critical speed of an ensemble of attachments to a shaft is also substantially lower than the intrinsic critical speed of the shaft. [34]

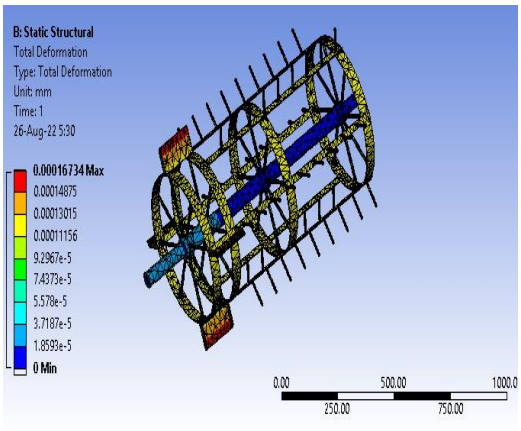

Figure 4-23 (a) -Deformation of threshing drum

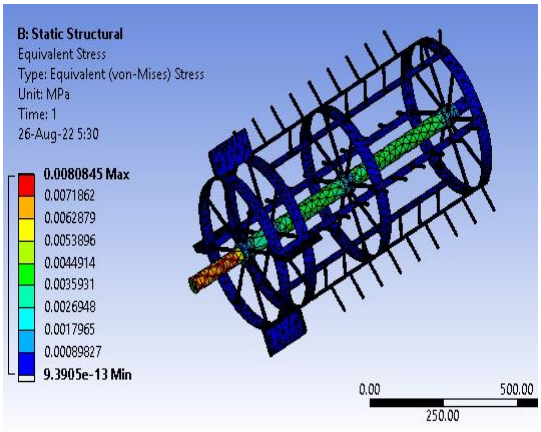

Figure 4-23 (b) – Stress of threshing drum

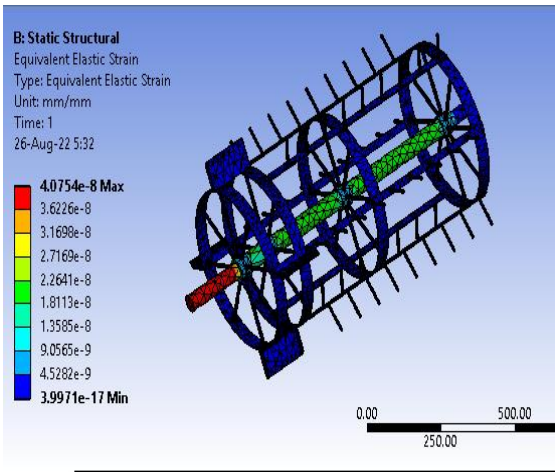

Figure 4-23(c) – Strain of threshing drum drum

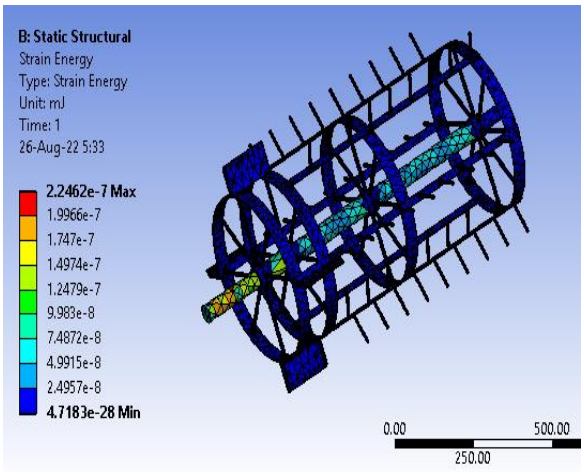

Figure 4-23 (d) - Strain Energy of threshing

Figure 4-23- Modal response of the threshing cylinder

The static analysis results of the horizontal axial flow cylinder, the deformation distribution cloud diagram and stress distribution cloud diagram of the cylinder are shown in Fig. 23 (a-d) The maximum deformation of the horizontal axial flow cylinder under extreme conditions was 0.001673 mm, which is in the range of preferred range of deflection for deep grove ball bearing stated on [34], Appendix table 7-2. That is between 0.001 to 0.003. The maximum stress of the horizontal axial flow cylinder was 19.3 *mpa* , which is within the yield strength range of the AISI 1018 Carbon Steel material.

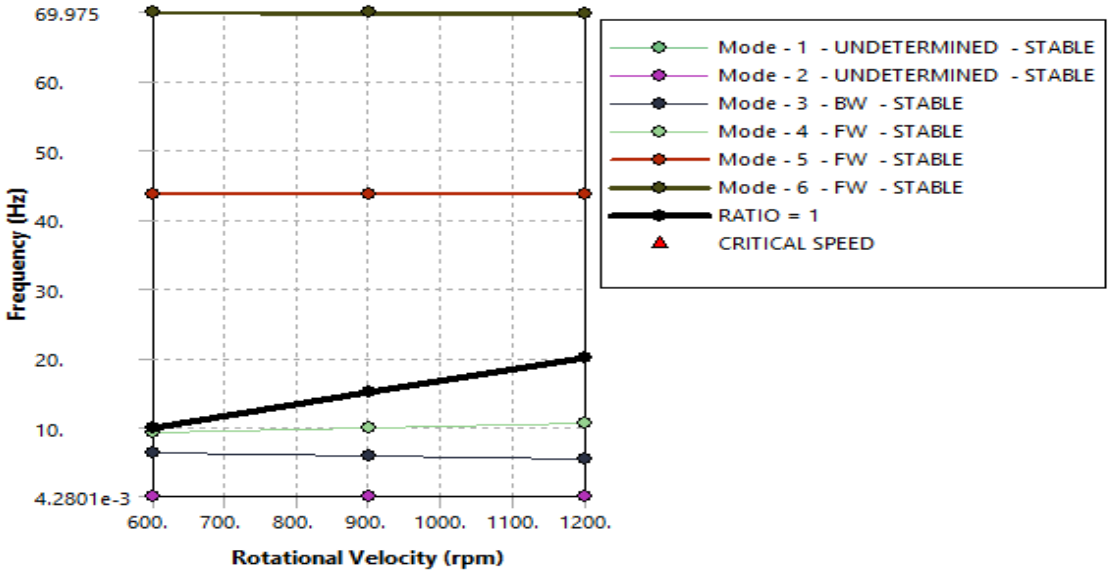

Figure 4-24 Campbell Diagram

Mode	Whirl Direction	Mode Stability	Critical Speed	600 rpm	900 rpm	1200 rpm
1.	BW	STABLE	377.178	6.2863 Hz	5.8412 Hz	5.4172 Hz
2.	FW	STABLE	547.902	9.1317 Hz	9.8186 Hz	10.573 Hz
3.	FW	STABLE	2622.24	43.704 Hz	43.704 Hz	43.704 Hz
4.	FW	STABLE	3198.5	69.975 Hz	69.887 Hz	69.765 Hz

Table 4-8 critical speed for threshing cylinder

The rear whirl direction, or the vibration of the threshing cylinder in the direction opposite to the input rotational speed, is expressed by BW and FW. For example, if the rotation is done in the clockwise direction, the vibration mode will be done in the anticlockwise direction. This vibration mode is known as the back whirl. We have presented the respected critical speed and mode shape for three distinct rotational speeds and four various mode shade shapes to analyze the vibration characteristics of the threshing cylinder. For each of the four mode shapes, we determine four different critical speeds. The critical speed must be larger than three times the operating speed in order for the shaft to exhibit vibrational behavior. [34] All the first critical are less than three times the operating speed so that the threshing drum doesn't exhibit vibrational behavior that influence the operation.

4.9. CFD Analysis of cyclone separator

The cleaning efficiency of a cyclone separator basically depends on the speed at which the particle enters the separation chamber and the weight of the particle.

The purpose of the project is to investigate the impact of gas flow velocity (discrete and continuous phase) and particulate diameter size on the effectiveness of the cyclone separator. ANSYS FLUENT is used for numerical analysis, and CFD-post is used for post-processing. Initially the geometry cleanup is conducted to reduce the inclusion of superfluous (unwanted) features into the meshing and solution platform. The cleaned geometry is imported in ANSYS Meshing and Cartesian mesh is utilized to mesh the geometry. As the flow direction is aligned with the Cartesian mesh, CFD solvers will undoubtedly produce results that are more accurate and have better convergence. Finally, the mesh is loaded into the FLUENT module for numerical analysis using the Discrete Phase Model (DPM). Post-processing is done to the results, and they are then discussed appropriately.

Case studies:

From the analytic analysis we have calculated the inlet velocity to be 3 m/s. then taking the same velocity and varying the particle diameter with the moisture content at 6%, 15%and 30 % the characteristic of the teff grain in the cyclone separator was simulated.

Table 4-9 - Case study One: Varying particle diameter with same inlet Velocity:

cases	Particle diameter (mm)	Particle (Discrete) and continuous fluid velocity (m/sec)
Case 1a	0.7114(@6%moisture content)	3
Case 1b	0.7735(@15%moisture content)	3
Case 1c	0.871(@30%moisture content)	3

I. Pre-Processing

A) Geometry

1. Solid Geometry

The cyclone separator geometry is imported in ANSYS Design Modeler and extra features such as (extra small edges) are removed. This prevents unexpected meshing of the extra features in the domain.

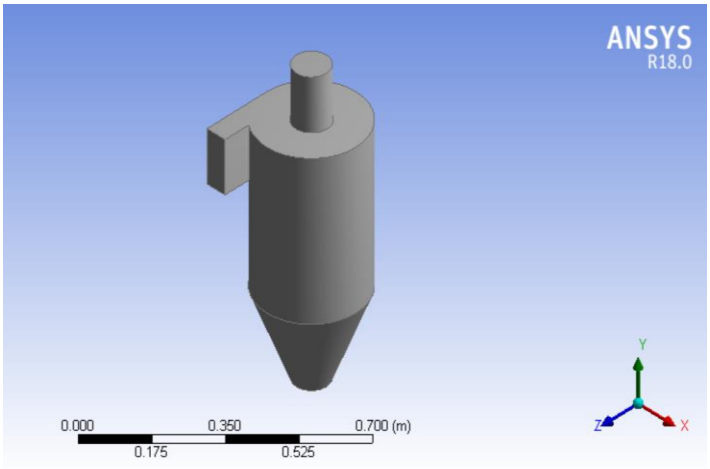

Figure 4-25 - Cyclone Geometry

The following geometry represents cyclone separator with one inlet and two outlets (at the top and the bottom

B) Named selection

The patches colored in red represent the faces which are subjected to subsequent boundary conditions in FLUENT solver. It helps to identify cell face zones and assignment of respective boundary conditions to it.

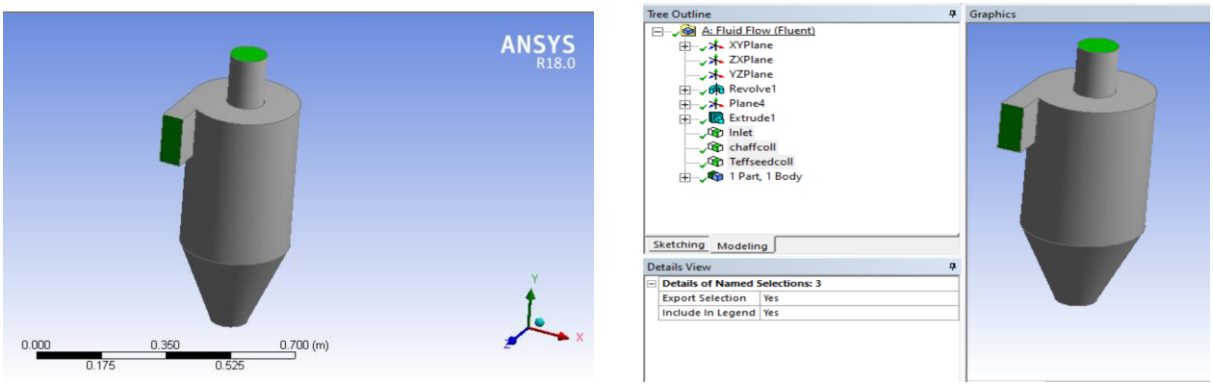

Figure 4-26 - Named selection

C) Mesh Detail

Assembly meshing method	Tetrahedrons mesh
Maximum element size	0.002048
Minimum element size	0.0000005
Body fitted Cartesian mesh	As per global settings
Face sizing	As per local settings
Local face mesh element size	4.7 mm
Total number of nodes	15299
Total number of elements	83048

Table 4-10 - Mesh Detail

Note: Same mesh is used for all case studies to expect consistent and mesh independent results. The mesh settings are selected under different trials to achieve accurate results.

1. Mesh:

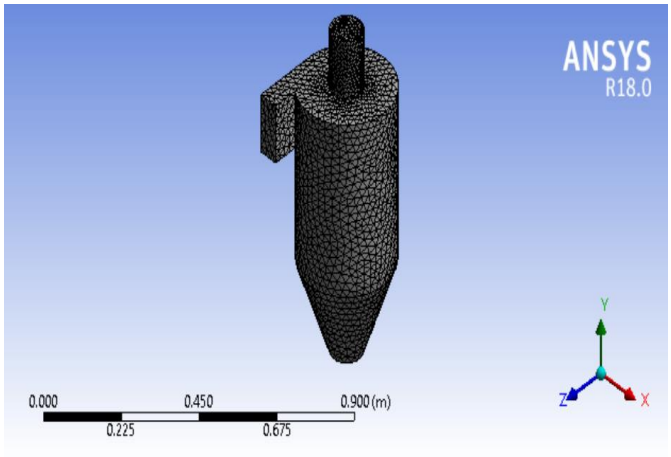

Figure 4-27 – Mesh

D) Mesh Quality

1. Element quality

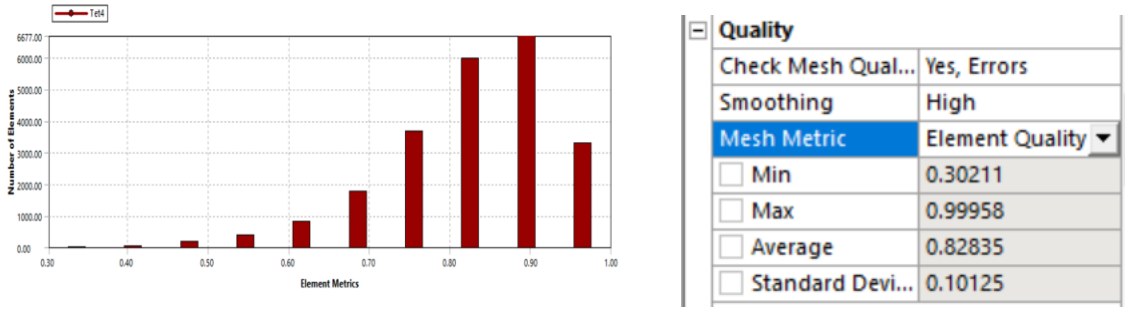

Figure 4-28 - Element quality

2. Skew ness:

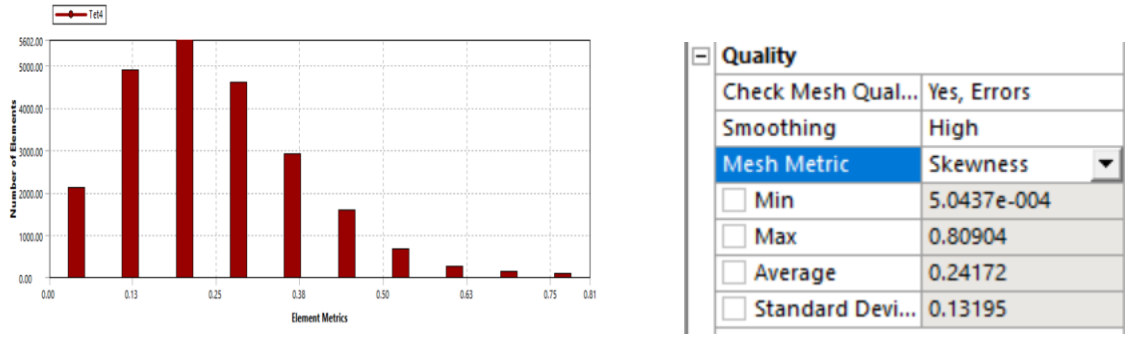

Figure 4-29 – Skew ness of the mesh

3. Orthogonal quality:

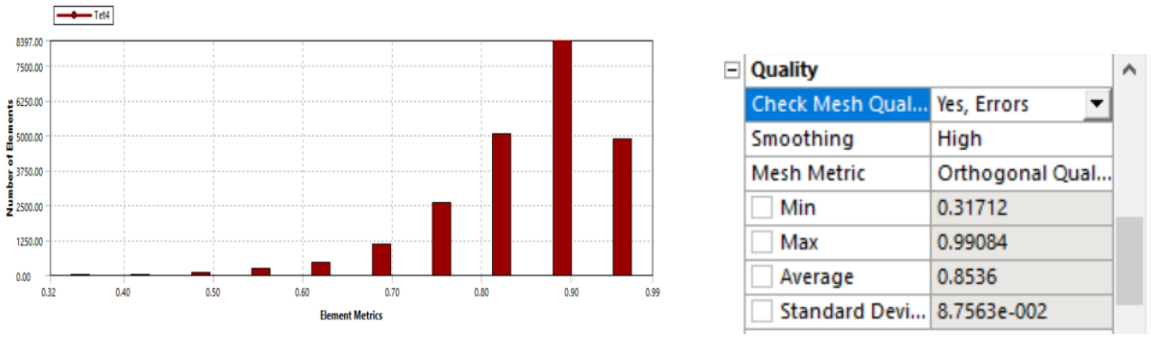

Figure 4-30 - Orthogonal Quality of the mesh

II. Processing

- Initially, the imported Cartesian mesh is verified in the FLUENT solver using "Check Mesh" option.

- Steady state simulation is selected.
- Gravity is enabled in negative Y-direction.
- Viscous model: K-epsilon (RNG) by enabling Swirl Dominated Flow. In this simulation, K-epsilon with RNG and Swirl dominant flow is selected which gives best results in this situation.
- Discrete Phase Model is selected. Following is the snapshot of the Discrete Phase Model (DPM) settings.

1. Turning on interaction with continuous phase and updating DPM sources every 10 iteration interval. Remaining settings are kept to be as default.

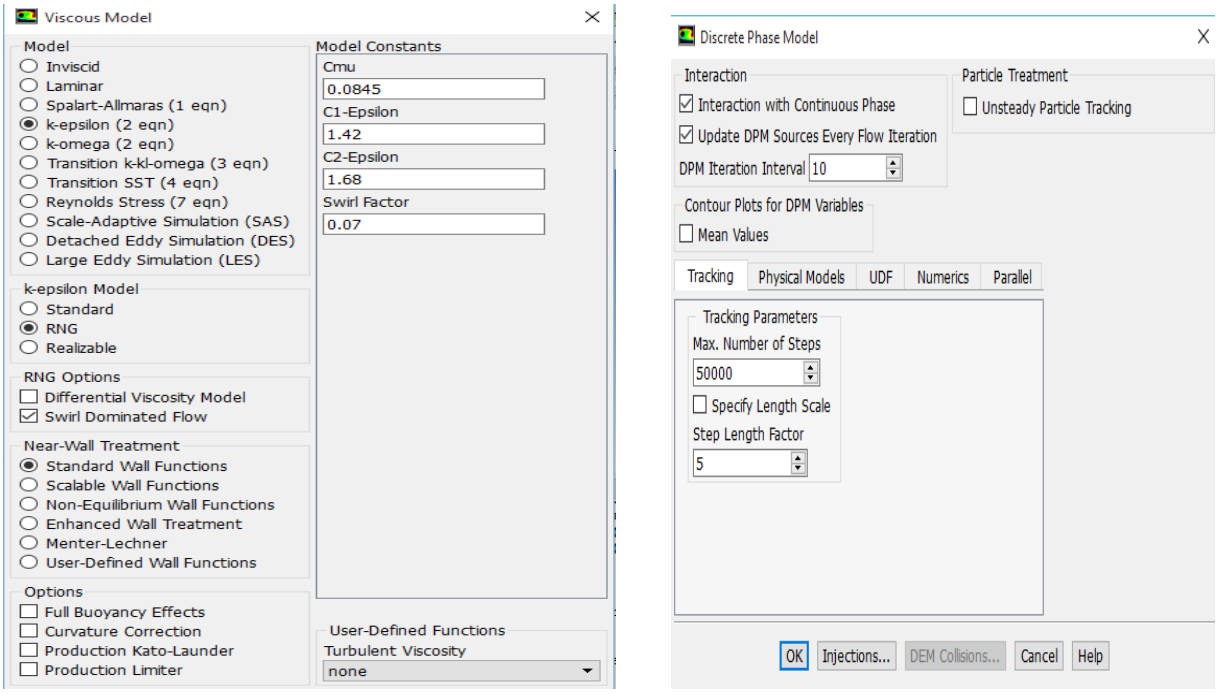

Figure 4-31 - DPM iteration

2. Creating particle injection and Setting injection properties and injecting the flow in normal direction through the face.

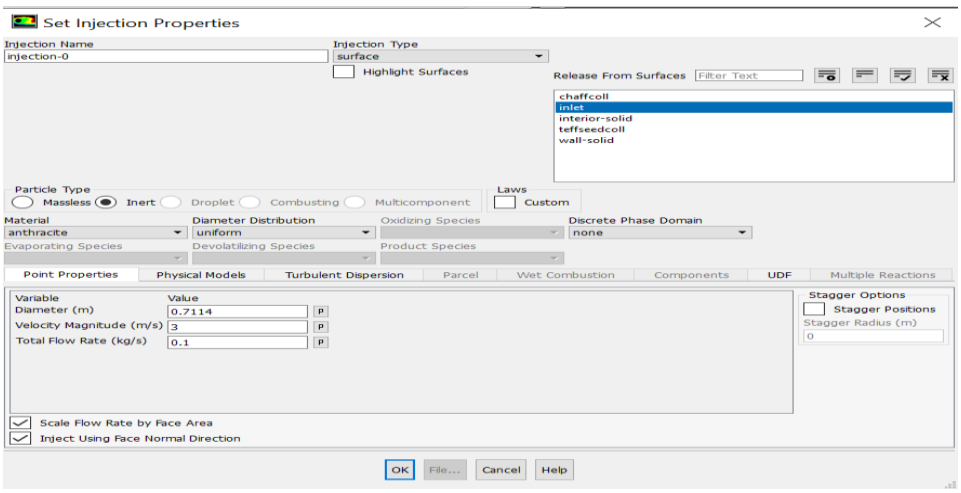

Figure 4-32 - Particle Injection in to the cyclone separator

Properties of the air-solid Phases

Phase	**Material**	$\left(\frac{Kg}{m^3}\right)\rho$	$\left({}^{o}k\right)T$
Fluid	chaff	1.225	298
Solid	Teff seed grain	821	298

Table 4-11 - Properties of the air-solid Phases

Note: Particle diameter and velocity magnitude may vary according to the case studies.

- Setting boundary conditions to be as follows,
  - Inlet: Velocity inlet = "Respective velocity as per each case set-up (m/s)"
  - DPM: Reflect (Here particle rebounds off the boundary with change in momentum. However the coefficient of restitution in normal and tangential direction is by default set to one. Due to this in case the particle rebounds to the inlet boundary there is no change in momentum after reflection)
  - Top outlet: Pressure outlet = 0 gauge pressure (i.e. atmospheric pressure)
  - DPM: Escape (The particle is allowed to leave the outlet boundary with discontinuation of the trajectory calculations and particle fate is reported as "Escape")
  - Bottom outlet: Pressure outlet = 0 gauge pressure (i.e. atmospheric pressure)
  - DPM: Trap (The particle gets caught at the boundary face with termination of the trajectory calculations and particle fate is reported as "Trapped")

- Pressure-velocity coupling solution method is set to SIMPLE and discretization scheme for Turbulent Kinetic Energy (TKE) and Turbulent Dissipation Rate (TDR) is changed to Second Order Upwind. This is done to resolve TKE and TDR more accurately in the flow calculations.
- Solution Initialization: Standard Initialization is performed by computing the flow variables from the inlet patch boundary.
- The numerical solution is time marched up to 500 iterations to achieve steady state solution.

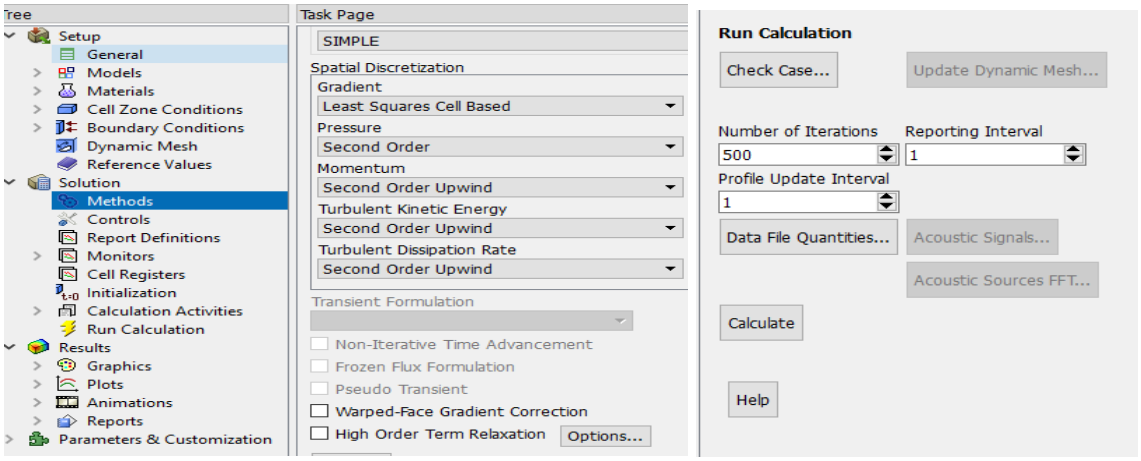

Figure 4-33 – Solution with second order

III] Post-processing:

Case Study One: Varying particle diameter with same inlet velocity (3ms) (0.7114 mm).

1. Scaled residuals:

Case 1a.

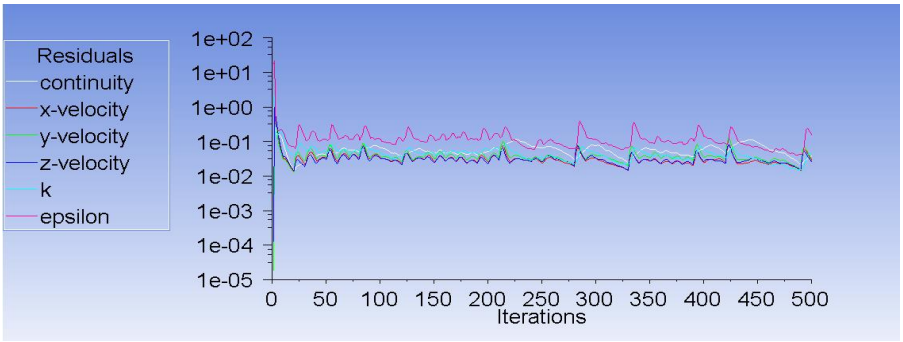

Figure 4-34- Scaled residual for Case 1a.

Case 1b.

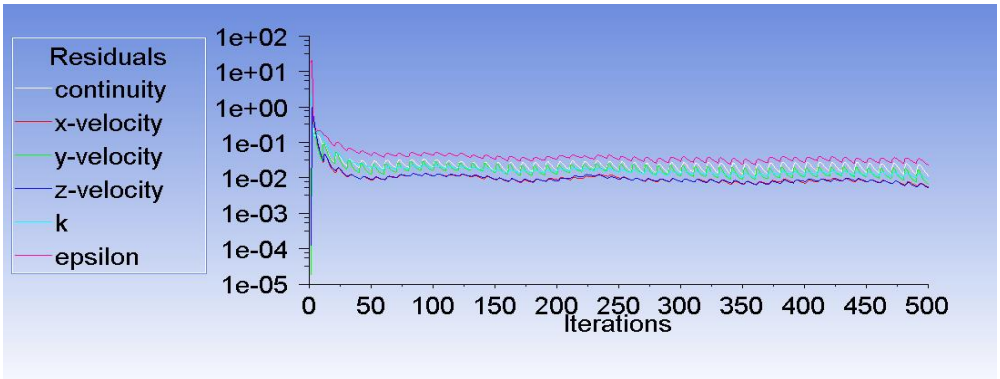

Figure 4-35 - Scaled residual for Case 1b

Case 1c.

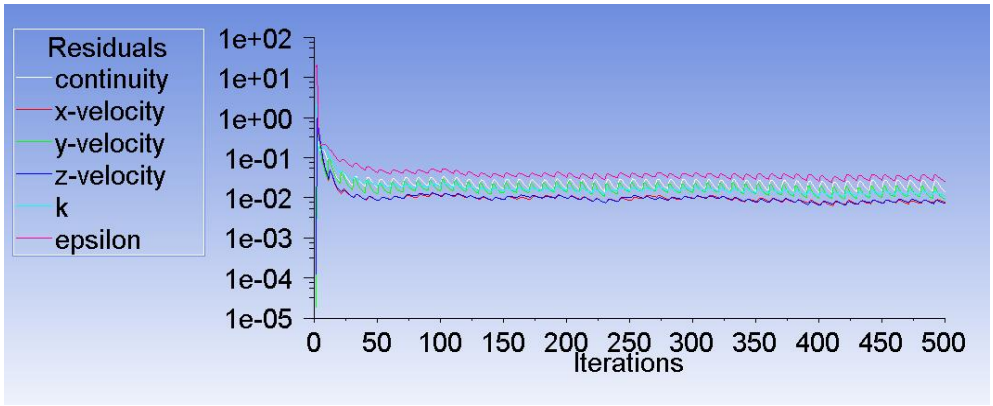

Figure 4-36 - Scaled residual for Case 1c

2. DPM Report:

Case 1a.

```
Calculation complete.
number tracked = 51, escaped = 2, aborted = 0, trapped = 49, evaporated = 0, incomplete = 0
number tracked = 51, escaped = 2, aborted = 0, trapped = 49, evaporated = 0, incomplete = 0
number tracked = 51, escaped = 2, aborted = 0, trapped = 49, evaporated = 0, incomplete = 0

 Fate                  Number          Elapsed Time (s)                      Injection, Index
                                    Min        Max        Avg    Std Dev                  Min                    Max
 ----                  ------  ---------- ---------- ---------- ---------- -------------------- --------------------
 Escaped - Zone 7           2   1.723e+00  1.032e+01  6.020e+00  4.298e+00     injection-0    7     injection-0   44
 Trapped - Zone 8          49   4.279e-01  1.980e+01  6.009e+00  5.543e+00     injection-0   36     injection-0   24

                (*)- Mass Transfer Summary -(*)

 Fate                      Mass Flow (kg/s)
                         Initial      Final     Change
 ----                  ---------- ---------- ----------
 Escaped - Zone 7       3.333e-03  3.333e-03  0.000e+00
 Trapped - Zone 8       9.667e-02  9.667e-02  0.000e+00
 ----                  ---------- ---------- ----------
 Net                    1.000e-01  1.000e-01  0.000e+00
```

Figure 4-37-DPM report; Case 1c.

Case 1b.

```
Calculation complete.
number tracked = 51, escaped = 3, aborted = 0, trapped = 31, evaporated = 0, incomplete = 17
number tracked = 51, escaped = 3, aborted = 0, trapped = 31, evaporated = 0, incomplete = 17
```

Figure 4-38 - DPM report; Case 1b.

Case 1c.

```
Calculation complete.
number tracked = 51, escaped = 5, aborted = 0, trapped = 33, evaporated = 0, incomplete = 13
number tracked = 51, escaped = 5, aborted = 0, trapped = 33, evaporated = 0, incomplete = 13
```

Figure 4-39 - DPM report; Case 1c.

3. Area Average Pressure Report:

Case 1a.

Area-Weighted Average Static Pressure	(pascal)
inlet	38.330922
chaffcoll	42.973224
teffseedcoll	2.1563171
Net	28.578228

Figure 4-40- Area Average Pressure Report: Case 1a

Case 1b.

Area-Weighted Average Static Pressure	(pascal)
inlet	49.818335
chaffcoll	55.384615
teffseedcoll	3.6543819
Net	37.257968

Figure 4-41 - Area Average Pressure Report: Case 1b

Case 1c.

```
Calculation complete.
```

Area-Weighted Average Static Pressure	(pascal)
inlet	52.106321
chaffcoll	57.206717
teffseedcoll	3.1292369
Net	38.522943

Figure 4-42 - Area Average Pressure Report: Case 1c

4. **Pressure Contour:**

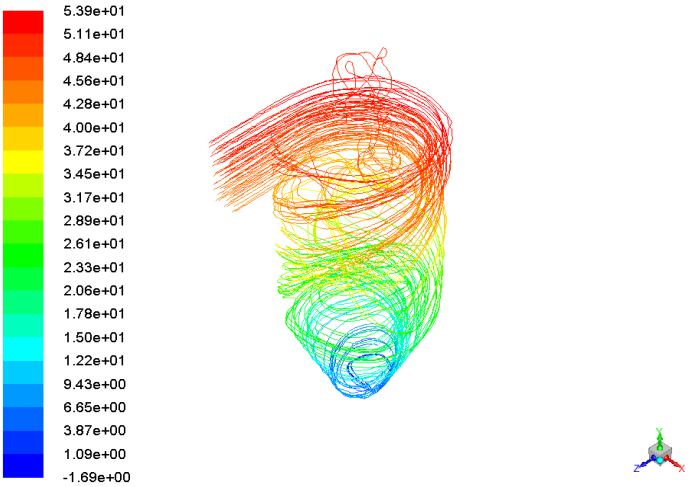

Figure 4-43 - Pressure contour of the particle streamline path

(Case Study One) Observation table:

Cases	Particle Diameter	Particle Velocity (m/s)	Particles Escaped	Particles Trapped	Incomplete Particles	Efficiency (η_i)	Pressure drop (Pa)
Case 1a	0,7114	3	5	33	0	86.2	28.578
Case 1b	0.7735	3	3	31	17	91.17	37.257
Case 1c	0.871	3	2	49	13	96.07	38.522

Table 4-12- Observation table of particle scenario on the cyclone

The separation efficiency is given as

$$\eta_i = \text{Trapped particles} / \text{Total number of particles}$$

Note: The above calculated efficiency is calculated by neglecting the number of incomplete particles.

In this discussion, it will be focused on the particle diameters of 0.7114, 0.7735, and 0.871 mm with an entrance velocity of 3 m/s. The observation table shown above tabulates the results. The smaller particles are initially less affected and have a lower density than the larger ones. At a

specific height from the bottom, the smaller diameter particles recirculate with zero decreasing angles. As a result, they barely make any contact with the partition walls. They tend to swirl with flue gases in the maximum axial velocity zone because of their lower density (generally at zero radiuses or at the vertical mid-section of the separator). The smaller diameter sized particles have a significantly shorter particle residence time. The centrifugal effects of these particles are less than the gas drag force. As a result, they often leave with flue gases and are less affected by the cyclonic effect. Larger particles have a higher inertia than smaller ones because they are denser. The bigger particles swirl and interact with the separator walls because the tangential velocity component and centrifugal impacts dominate them greatly. As a result, the particles gradually sink down the separator walls at a specific downward angle. The middle of the separator does not spin because of a stronger centrifugal force. However, compared to smaller particles, these particles spend a lot more time in the cyclone zone. The larger particles' size changes over time. The larger particles lose momentum and inertial energy over time and, as a result of gravitational attraction, sink to the bottom (where they are confined). Compared to smaller particles, the separation efficiency tends to rise with particle size. Nearly one-third of these smaller dimension particles are gathered at the bottom since they tend to escape with the gas flow. Larger particles, in contrast, exhibit good trapping separation efficiency because they can quickly separate from the mixed flow when subjected to cyclonic conditions. As a consequence of this study evaluating the case on varying particle size with the same inlet velocity, the pressure drop that results is consistent for all cases.

Chapter 5 Conclusion and Recommendation

5.1 Conclusion

The purpose of this research paper is to improve, analyze, and simulate a teff thresher machine with a cyclone separator as a cleaning mechanism. AUTODESK and ANSYS were used for modeling and analysis, respectively. We increased the capacity of the teff thresher and assessed the machine's effectiveness in terms of cleaning efficiency using three different particle sizes and speeds on the cyclone separator.

Threshing capacity is primarily determined by key variables such as feed rate, grain to straw ratio, and separation efficiency. Among these three fundamental variables, the feed rate is determined by the capacity of the labor feeding the threshing drum. An experiment was conducted on Debrezeit and Awash Melkassa Wakotiyo to determine how much a man can deliver at a continuous feed rate and the grain to straw ratio of teff. The average grain to straw ratio, threshing drum rotational speed (rpm), and feed rate (kg/hr.) were *0.4875, 1044.5*, and *820.6*, respectively, according to the demonstration results. These measurements were used to create the newly improved teff thresher. The static analysis results of the horizontal axial flow cylinder were presented, including the cylinder's deformation distribution cloud diagram and stress distribution cloud diagram. The maximum deformation of the horizontal axial flow cylinder under extreme conditions was *0.073* mm, which is less than the practical application requirement of not exceeding *3* mm. The horizontal axial flow cylinder's maximum stress was *19.3* mpa, which is within the yield strength range of the AISI 1018 Carbon Steel material. For the cleaning mechanism, three cases with constant inlet velocity were chosen. Because teff grain particle diameter varies with moisture content, three different moisture contents were used, with particle sizes of *0.7114, 0.7735*, and *0.871* mm, respectively. The properties of the grains in the cyclone have been investigated and presented. The cleaning efficiency was found to be *86.2%, 91.7%*, and *96%*, with pressure drops of *28.578, 37.257*, and *38.522* Pa. The cleaning efficiency of the cyclone increases as particle size increases, and as particle size decreases, so does the cleaning mechanism.

Finally, this research paper explained the design and analysis of improved teff thresher with a cyclone separator and a capacity of *3.5* quintal/hr. taking the best, developed threshers have a

capacity of up to *2* quintal/hr. So we increased the thresher's capacity by *175%*. In addition, a new type of cleaning mechanism is introduced, which has a good cleaning performance and it have machine components that need small maintenance because it don't possess any moving parts.

5.2 Recommendation

- From the result it is highly recommended to use the newly improved teff thresher with cyclone separator having improved capacity, cleaning mechanism and simple to operate.
- To achieve the required capacity, the recommended feed rate is 0.3472 kg/sec, so the labor responsible for feeding teff to the threshing drum should keep the feed rate constant and the required amount as much as possible keep the uniformity of feed rate.
- Before beginning the threshing process, the machine operator should inspect the entire machine and maintain a rotational speed of 1200 rpm under no load conditions. But more than 1200rpm not recommended threshing *teff* crop.
- 12% moisture content is best and helps to achieve the required threshing capacity.
- Adoption of teff, mechanization technologies will benefit small households by reducing grain losses and increasing income from better handling methods and market prices. The research will provide an opportunity to generate a wide range of benefits in terms of research knowledge and capacity. The research knowledge also benefits policymakers, local manufacturers, researchers, and agricultural extension workers.

5.2.1 Future work

- To the future in order to further increase the capacity of the teff threshers a PTO power source will be a major option of power since the farmers are using a small –medium sized tractors.
- For better increase of the threshing capacity developing a feeding mechanism that can deliver constant feeding rate to the threshing cylinder is necessary.
- Experimental analysis on cyclone separator on different moisture content and varieties of teff.

References

[1] A. A. Nadew, “Design and Development of Tef Grain and Chaff,” , 2015.

[2] Merga Workesa Dula, “Development and Evaluation of Teff Threshing Machine,” *Int. J. Eng. Res.*, vol. V5, no. 11, pp. 420–429, 2016, doi: 10.17577/ijertv5is110250.

[3] G. K. Gelaw, “Theoretical and Experimental Investigation of Threshing Mechanism for Tef (Eragrostistef (Zucc .) Trotter) on the Basis of its Engineering (Physical and Mechanical) Properties,” no. June, 2020.

[4] G. Kidanemariam, “Theoretical and Experimental Investigation of Threshing Mechanism for Tef,” no. June, 2020.

[5] J. Fu, Z. Chen, L. J. Han, and L. Q. Ren, “Review of grain threshing theory and technology,” *Int. J. Agric. Biol. Eng.*, vol. 11, no. 3, pp. 12–20, 2018, doi: 10.25165/j.ijabe.20181103.3432.

[6] M. Govindaraj, P. Masilamani, and V. Alex Albert, “Influence of Harvesting and Threshing Methods on Storability of Rice Varieties,” *Madras Agric. J.*, vol. 104, no. 10–12, p. 395, 2017, doi: 10.29321/maj.2017.000086.

[7] A. E. P. Feb, “ASAE EP 496.2 FEB03 Agricultural Machinery Management American Society of Agricultural Engineers”.

[8] M. H. Saeidirad, M. Esaghzade, A. Arabhosseini, and S. Zarifneshat, “Influence of machine-crop parameters on the threshability of sorghum,” *Agric. Eng. Int. CIGR J.*, vol. 15, no. 3, pp. 55–59, 2013.

[9] Olugboji OA, “Development of a Rice Threshing Machine,” *Au J.T*, vol. 8, no. 2, Available: http://www.journal.au.edu/au_techno/2004/oct04/vol8num2_art04.pdf

[10] P. Dhananchezhiyan, S. Parveen, and K. Rangasamy, “Development And Performance Evaluation Of Low Cost Portable Paddy Thresher For Small Farmers,” *Int. J. Eng. Res. Technol.*, vol. 2, no. 7, pp. 571–585, 2013, [Online]. Available: www.ijert.org

[11] J. M. Gregory, “Combine model for grain threshing,” *Math. Comput. Model.*, vol. 11, no. C, pp. 506–509, 1988, doi: 10.1016/0895-7177(88)90544-4.

[12] R. Singh and M. Sreedhar, “Bio-Tribology and Its Applications in Medical Sciences - a Review,” *Int. J. Mech. Eng. Robot. Res.*, vol. 3, no. 3, pp. 141–144, 2014.

[13] O. SAMUEL, ABICH and A, “Optimization of Threshing Performance of a Spike Tooth,” 2018.

[14] G. Bekele, D. Woyessa, and W. Tafa, “Improvement of Asella Wheat and Barley Thresher,” *Int. J. Sci. Res. Publ.*, vol. 10, no. 10, pp. 487–495, 2020, doi: 10.29322/ijsrp.10.10.2020.p10666.

[15] P. I. Miu and H. D. Kutzbach, “Modeling and simulation of grain threshing and separation in threshing units-Part I,” *Comput. Electron. Agric.*, vol. 60, no. 1, pp. 96–104, 2008, doi: 10.1016/j.compag.2007.07.003.

[16] K. S. Shekhar, “Design of the Components of A Stationary Power Thresher for Paddy Crop,”p.27,[Online].Available:http://courseware.cutm.ac.in/wp-content/uploads/2020/06/PPT_Design-of-threhsher.pdf

[17] F. Kargbo, J. Xing, and Y. Zhang, “Property analysis and pretreatment of rice straw for energy use in grain drying: A review,” *Agric. Biol. J. North Am.*, vol. 1, no. 3, pp. 195–200, 2010, doi: 10.5251/abjna.2010.1.3.195.200.

[18] K. J. Simonyan, “14 . Simonyan , K . J ., Y . D . Yiljep and O . J . Mudiare (2006). Modelling the Cleaning Process of a Stationary Sorghum Thresher . Agricultural Engineering International : the CIGR Ejournal :... Modeling the Grain Cleaning Process of a Stationary Sor,” no. January, 2015.

[19] E. Sehsah, A. Elhameed, and H. Bahnasy, “Faculty of Agriculture Equipment By Abd El-Hameed Hamada Bahnasy El-Hanafy,” no. February 2018, 2019.

[20] M. J. Aarabi and R. Ebrahimi, “Pneumatic separation of Mami cultivar almond (Prunus amygdalus) kernel from cracked shell,” *J. Exp. Biol. Agric. Sci.*, vol. 5, no. Spl-1-SAFSAW, pp. 573–577, 2017, doi: 10.18006/2017.5(4).573.577.

[21] V. I. O. Ndirika, “a Mathematical Model for Predicting Output Capacity of Selected Stationary Spike-Tooth Grain Threshers,” *Appl. Eng. Agric.*, vol. 22, no. 2, pp. 195–200, 2006, doi: 10.13031/2013.20281.

[22] A. Of, T. H. E. Separation, O. F. Straw, C. F. Wheat, B. Y. An, and A. I. R. Blast, “Analysis Of The Separation Of Straw And Chaff From Wheat function of particle ” vol. 26, no. 2, pp. 181–187, 1984.

[23] A. K. Srivastava, C. E. Goering, R. P. Rohrbach, and D. R. Buckmaster, “Grain Harvesting,” *Eng. Princ. Ag*, pp. 403–435, 2012.

[24] A. Abewa *et al.*, “Teff grain physical and chemical quality responses to soil physicochemical properties and the environment,” *Agronomy*, vol. 9, no. 6, pp. 1–19, 2019, doi: 10.3390/agronomy9060283.

[25] A. D. Zewdu and W. K. Solomon, “Moisture-Dependent Physical Properties of Tef Seed,” *Biosyst. Eng.*, vol. 96, no. 1, pp. 57–63, 2007, doi: 10.1016/j.biosystemseng.2006.09.008.

[26] G. Sitkey, *Developments in Agricultural Engineering 8*. 1986.

[27] A. Awgichew, “Aerodynamic Properties of Tef for Separation from Chaff,” *Civ. Environ. Res.*, vol. 11, no. 3, pp. 39–43, 2019, doi: 10.7176/cer/11-3-05.

[28] I. Technologies, “School Of Engineering And Information Technologies Title : Study On Aeration And Pneumatic Conveying Of Teff Seeds,” no. April, 2010.

[29] “Misener and Lee 1973.pdf.”

[30] H. H. Shalaby, “on the Potential of Large Eddy Simulation To Simulate Cyclone Separators,” *Thesis*, no. February 2007, p. 137, 2007.

[31] M. K. Afify, M. M. A. El-Sharabasy, and M. M. A. Ali, “Development of a local threshing machine suits for threshing black seed (Nigella sativa),” *Misr J. Ag. Eng., Farm*

Mach. Power, vol. 24, no. 4, pp. 699–724, 2007.

[32] A. Kumar, D. Mohan, R. Patel, and M. Varghese, "Development of grain threshers based on ergonomic design criteria," *Appl. Ergon.*, vol. 33, no. 5, pp. 503–508, 2002, doi: 10.1016/S0003-6870(02)00029-7.

[33] R. L. Mott, *Machine elements in mechanical design*. 1985. doi: 10.1016/0301-679x(87)90097-1.

[34] R. G.budynas, *shigleys mechanical engineering design*, 9th ed. [Online]. Available: https://www.ptonline.com/articles/how-to-get-better-mfi-results

[35] R. K. SINNOT, *Coulson and Richardson's Chemical Engineering, Volume 6, Design, 3rd edition*, vol. 4, no. 1. 2557.

Appendix

1. Cost estimation of the threshing machine

It. No.	Description	Material	Size(L x W) (mm x mm)	Qty	Unit Price (birr)	Total Price (birr)
1.	Feeding Table	Mild steel Sheet Metal(SM) 1.5mm	1.38mx0.95m	1	2,164	2,164
2.	Feeding table reinforcement	MS sheet 1.5 mm(thickness)	0.3mx0.4m	1	198	198
3.	Drum Shaft	MS rod	Diameter 43 mm x1.2m	1	1000	1,000
4.	Drum Assembly	MS rod 8 mm diameter and flat bar 4x40 mm	40mmx4mmx5.4m flat bar	1	800	800
			Diameter 8mm x5.4mm length	1	450	450
5.	Drum Upper Cover	Sheet metal 1.5 mm thickness	1.4mx1.5m	1	3460	3,460
6.	Chaff Outlet	Sheet metal 1.5 mm thickness	0.3mx0.4m	1	198	198
7.	Drum Shaft Bearing	Standard purchased with bore diameter 30 mm	Outer diameter=72mm Bore diameter=35mm Width=17mm	2	3,000	6,000
8.	Bolts to the bearings	M12	M12x80 mm	8	25	200
9.	Pulley	Aluminum	48cmx20mm	1	2100	2,100
			12cm x20mm	1	1300	1,300
10.	Pulley Belts	3V belt cross section	100 inch.	2	800	1,600
11.	Concave	SM 2 mm thick	0.945mx0.896m	1	1778	1,778

12.	Auger Screw Shaft	Rod 50 mm diameter	1.356 m	1	1500	1,500
13.	Screw shaft bearing	Standard purchased with bore diameter 30 mm	Outer diameter=72mm Bore diameter=35mm Width=17mm	2	3,000	6,000
14.	Screw shaft holding cover	Sm 1.5 mm thickness	2.7mx1.525m	1	6700	6,700
15.	Fan blade	Sm 1.5 mm thickness	100mmx60mm	6	150	900
16.	Fan Housing	Sm 1.5 mm thickness	0.3mx0.3m	1	100	100
17.	Cyclone Separator	Sm 1 mm thickness	1mx2m	1	2800	2,800
18.	Pipe from the fan to cyclone	Sm 1 mm thickness	0.5mx1.8m	1	1100	1,100
19.	blower	Sm 1.5 mm thick mm	0.5mx0.5m	1	300	300
20.	Hose from the blower to Cyclone	Plastic hose of diameter 500 mm.	2m.	1	700	700
21.	Frame	Angle Iron 40x40x2mm	13m	1	4800	4,800
22.	Engine Seat Frame	Angle Iron 40x40x2mm	6 m.	1	2400	2,400
23.	8hp Diesel Engine			1	50,000	50,000

- Material Cost -98,548 Birr
- Labor cost –15 x 450=6,750Birr
- Machining cost=5,000Birr
- Subtotal = 98,548+6,750+5,000=110,298 birr
- Manufacturing cost for threshing unit = 10,300 Birr
- Grand total cost =120,598 Birr

2. Data collected

During the evaluation of *teff* thresher is we have select spilt plot design with biomass was As treatment 40, 50, 60 kg, feed rate 700,800,900 and 1000, 1100, 1200 rpm (speed) with all are three replication with 27 times data was recorded .

(a) Field performance of teff thresher Test at DEBREZEIT

(b) Field performance test of *teff* thresher awash Melkassa Waketiyo

Test result of grain to straw ratio, rpm and feed rate

No. of trail	*Grain to Straw ratio (g / s)*	*Rotational Speed of the threshing drum (rpm)*	*Feed rate(Kg / hr.)*
1	0.51	950	592.6
2	0.49	958	695.6
3	0.51	988	676
4	0.49	1057	685.7
5	0.5	1055	672.3
6	0.47	1160	695.7
7	0.51	1180	738.4
8	0.49	1175	786.9
9	0.48	950	655
10	0.47	958	694
11	0.47	988	698
12	0.48	1055	750
13	0.49	1068	857
14	0.47	1160	867

15	0.47	1180	705
16	0.48	950	692
17	0.48	958	661
18	0.51	988	679
19	0.5	1057	809
20	0.48	1055	791
Average	0.4875	1044.5	720.06

3. Tables

Table 3.1 Screw conveyor –capacity in Cu.Ft.per Hr. (Cubic feet per Hour)

Trough Loading	Screw Dia.	Pipe Size (Nom. Dia.) Used for Capacity Tables	Maximum RPM	Capacity in Cu. Ft. Per Hr.*	
				At Maximum RPM	At 1 RPM
45%	6	2	165	368	2.23
	9	2 ½	155	1240	8.00
	12	3	145	2813	19.40
	14	3 ½	140	4330	30.93
	16	3 ½	130	6126	47.12
	18	4	120	8052	67.10
	20	4	110	10253	93.21
	24	4	100	16368	163.68
	30	4	90	29150	323.89

Table 3.2 Typical Maximum Rnages for Slopes and transverse Deflections

Table 7–2

Typical Maximum Ranges for Slopes and Transverse Deflections

Slopes	
Tapered roller	0.0005–0.0012 rad
Cylindrical roller	0.0008–0.0012 rad
Deep-groove ball	0.001–0.003 rad
Spherical ball	0.026–0.052 rad
Self-align ball	0.026–0.052 rad
Uncrowned spur gear	< 0.0005 rad
Transverse Deflections	
Spur gears with $P < 10$ teeth/in	0.010 in
Spur gears with $11 < P < 19$	0.005 in
Spur gears with $20 < P < 50$	0.003 in

4. Drawing of the thresher

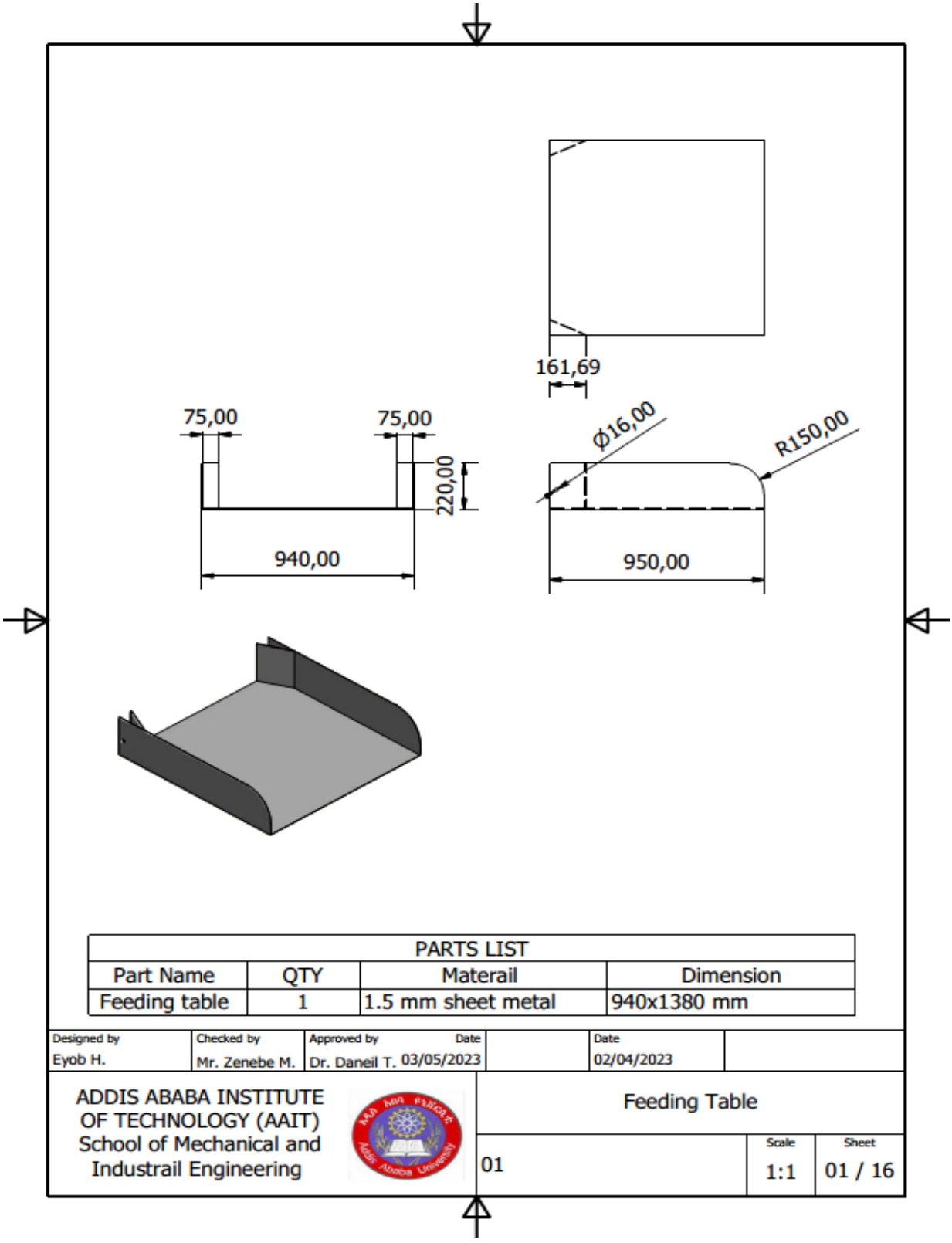

PARTS LIST			
Part Name	QTY	Materail	Dimension
Feeding table	1	1.5 mm sheet metal	940x1380 mm

Designed by	Checked by	Approved by	Date		Date	
Eyob H.	Mr. Zenebe M.	Dr. Daneil T.	03/05/2023		02/04/2023	

ADDIS ABABA INSTITUTE OF TECHNOLOGY (AAIT)
School of Mechanical and Industrail Engineering

Feeding Table

	Scale	Sheet
01	1:1	01 / 16

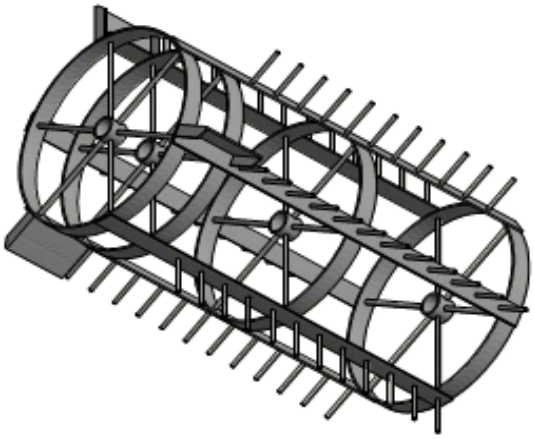

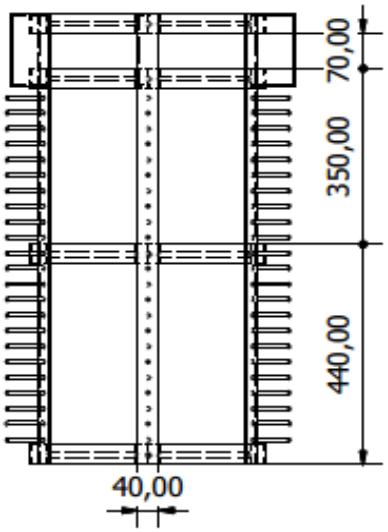

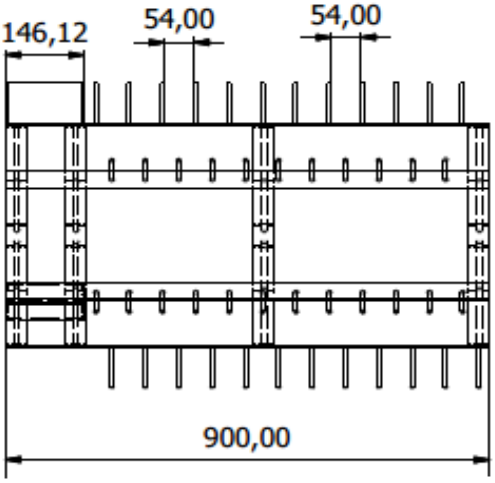

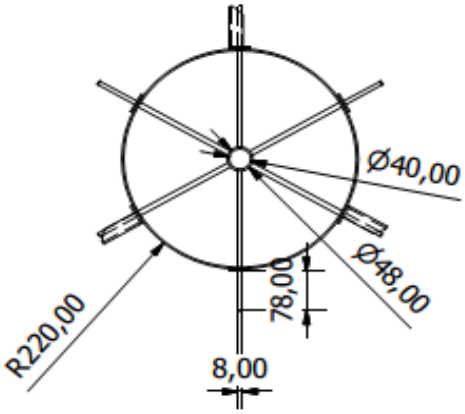

PARTS LIST			
Part Name	QTY	Materail	Dimension
Threshing Drum	1	40x40x3 Flat bar 8mm rod	600x900 mm

Designed by	Checked by	Approved by	Date	Date	
Eyob H.	Mr. Zenebe M.	Dr. Daneil T.	03/05/2023	02/04/2023	

ADDIS ABABA INSTITUTE OF TECHNOLOGY (AAIT) School of Mechanical and Industrail Engineering	Threshing Drum		
	02	Scale 1:1	Sheet 02 / 16

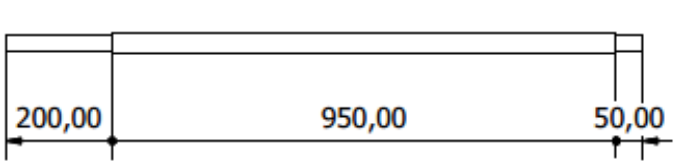

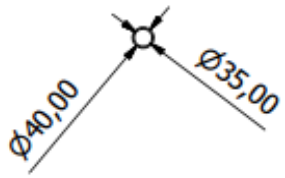

PARTS LIST			
Part Name	QTY	Materail	Dimension
Threshing Drum Shaft	1	40 mm rod	40x1200 mm

Designed by	Checked by	Approved by	Date	Date	
Eyob H.	Mr. Zenebe M.	Dr. Daneil T.	03/05/2023	02/04/2023	

ADDIS ABABA INSTITUTE OF TECHNOLOGY (AAIT) School of Mechanical and Industrail Engineering		Threshing Drum Shaft	
	03	Scale 1:1	Sheet 03 / 16

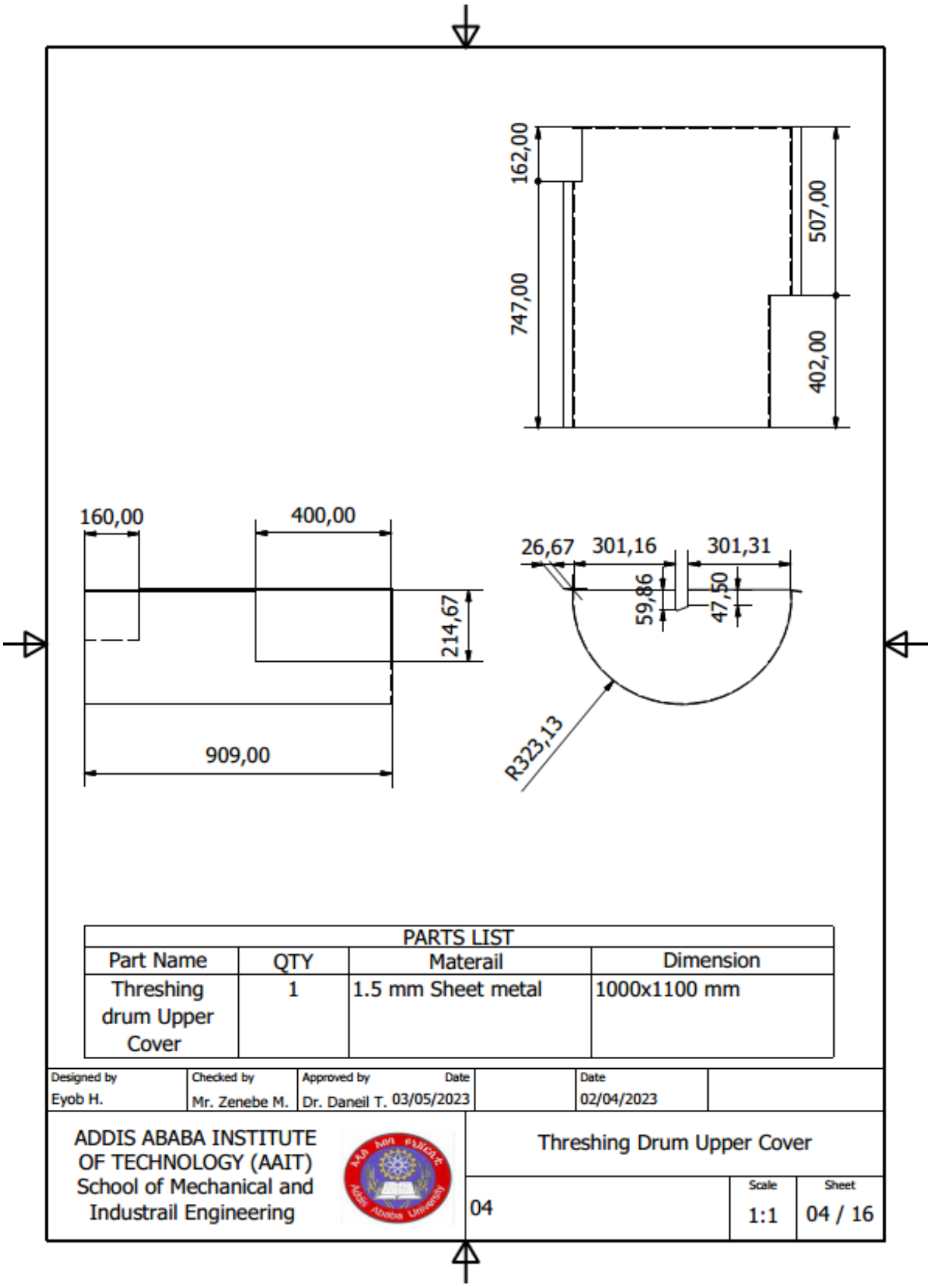

PARTS LIST			
Part Name	QTY	Materail	Dimension
Threshing drum Upper Cover	1	1.5 mm Sheet metal	1000x1100 mm

Designed by	Checked by	Approved by	Date		Date	
Eyob H.	Mr. Zenebe M.	Dr. Daneil T.	03/05/2023		02/04/2023	

ADDIS ABABA INSTITUTE OF TECHNOLOGY (AAIT) School of Mechanical and Industrail Engineering	Threshing Drum Upper Cover		
	04	Scale 1:1	Sheet 04 / 16

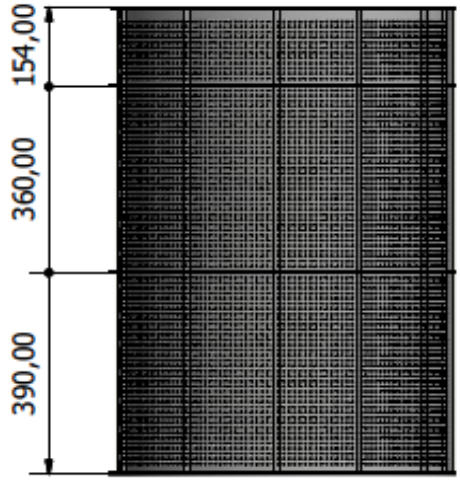

3 mm Diameter Hole

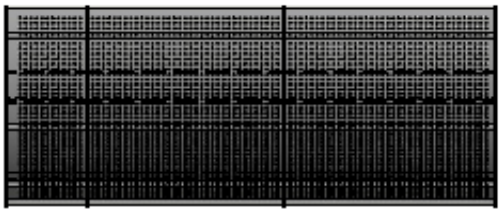

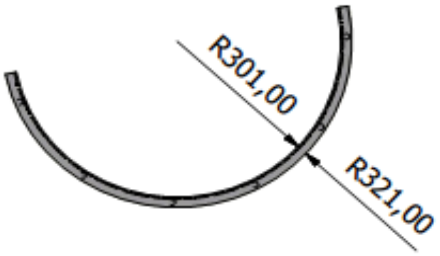

PARTS LIST			
Part Name	QTY	Materail	Dimension
Concave	1	1.5 mm Sheet metal 40x40x2 flat bar	700x1200 mm

Designed by	Checked by	Approved by	Date		Date	
Eyob H.	Mr. Zenebe M.	Dr. Daneil T.	03/05/2023		02/04/2023	

ADDIS ABABA INSTITUTE OF TECHNOLOGY (AAIT)
School of Mechanical and Industrail Engineering

Concave

	Scale	Sheet
05	1:1	05 / 16

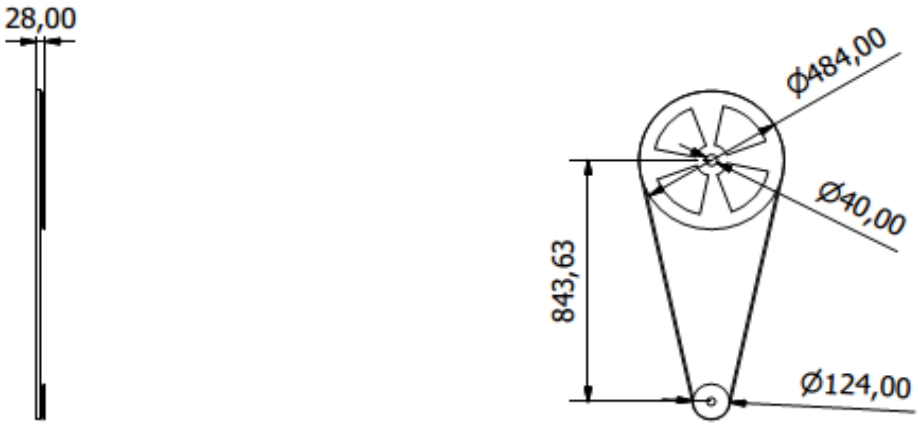

PARTS LIST			
Part Name	QTY	Materail	Dimension
PULLEY	1	Aluminuim	484 x 35 mm

Designed by	Checked by	Approved by	Date		Date	
Eyob H.	Mr. Zenebe M.	Dr. Daneil T.	03/05/2023		02/04/2023	

ADDIS ABABA INSTITUTE OF TECHNOLOGY (AAIT)
School of Mechanical and Industrail Engineering

Pulley

	Scale	Sheet
05	1:1	05 / 16

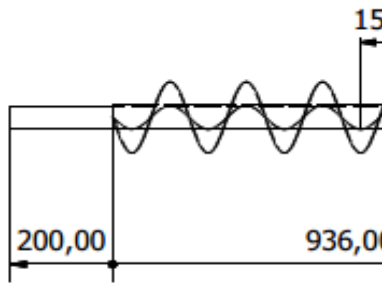

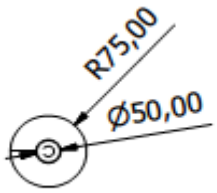

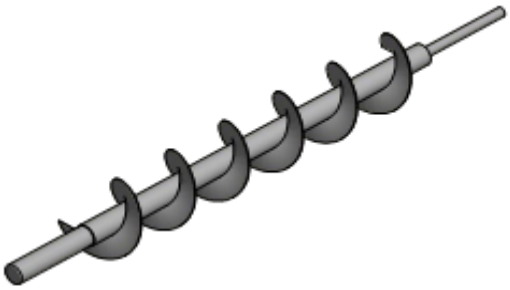

PARTS LIST			
Part Name	QTY	Materail	Dimension
Screw Conveyor	1	CHS 50 mm 1.5 mm sheet metal	50x1200 mm 1000x1300 mm

Designed by	Checked by	Approved by	Date		Date	
Eyob H.	Mr. Zenebe M.	Dr. Daneil T.	03/05/2023		02/04/2023	

ADDIS ABABA INSTITUTE OF TECHNOLOGY (AAIT)
School of Mechanical and Industrail Engineering

Screw Conveyor

	Scale	Sheet
06	1:1	06 / 16

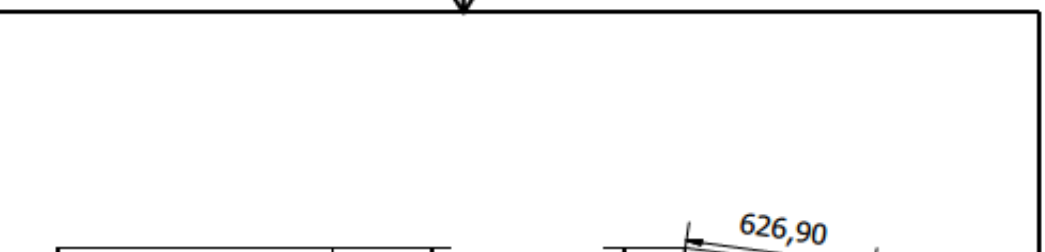

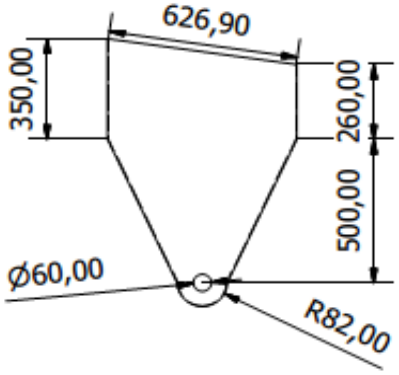

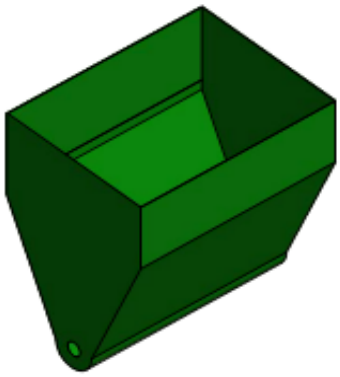

PARTS LIST			
Part Name	QTY	Materail	Dimension
Screw Conveyor cover	1	1.5 mm sheet metal	1000x2000 mm

Designed by	Checked by	Approved by	Date		Date
Eyob H.	Mr. Zenebe M.	Dr. Daneil T.	03/05/2023		02/04/2023

ADDIS ABABA INSTITUTE OF TECHNOLOGY (AAIT)
School of Mechanical and Industrail Engineering

Screw Conveyor Cover

	Scale	Sheet
07	1:1	07 / 16

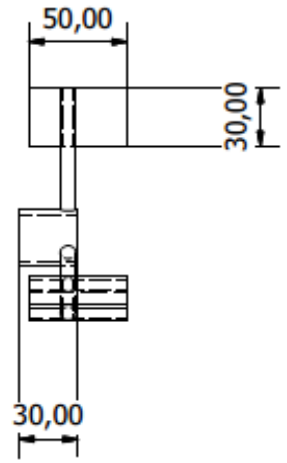

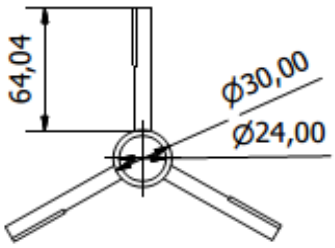

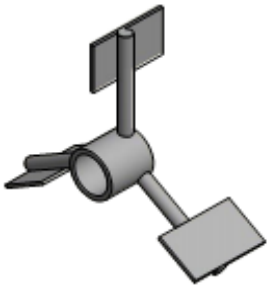

PARTS LIST			
Part Name	QTY	Materail	Dimension
Fan	1	3 mm sheet metal 8 mm rod	30x60 mm 1200mm

Designed by	Checked by	Approved by	Date		Date	
Eyob H.	Mr. Zenebe M.	Dr. Daneil T.	03/05/2023		02/04/2023	

ADDIS ABABA INSTITUTE OF TECHNOLOGY (AAIT) School of Mechanical and Industrail Engineering	Fan Blade		
	08	Scale 1:1	Sheet 08 / 16

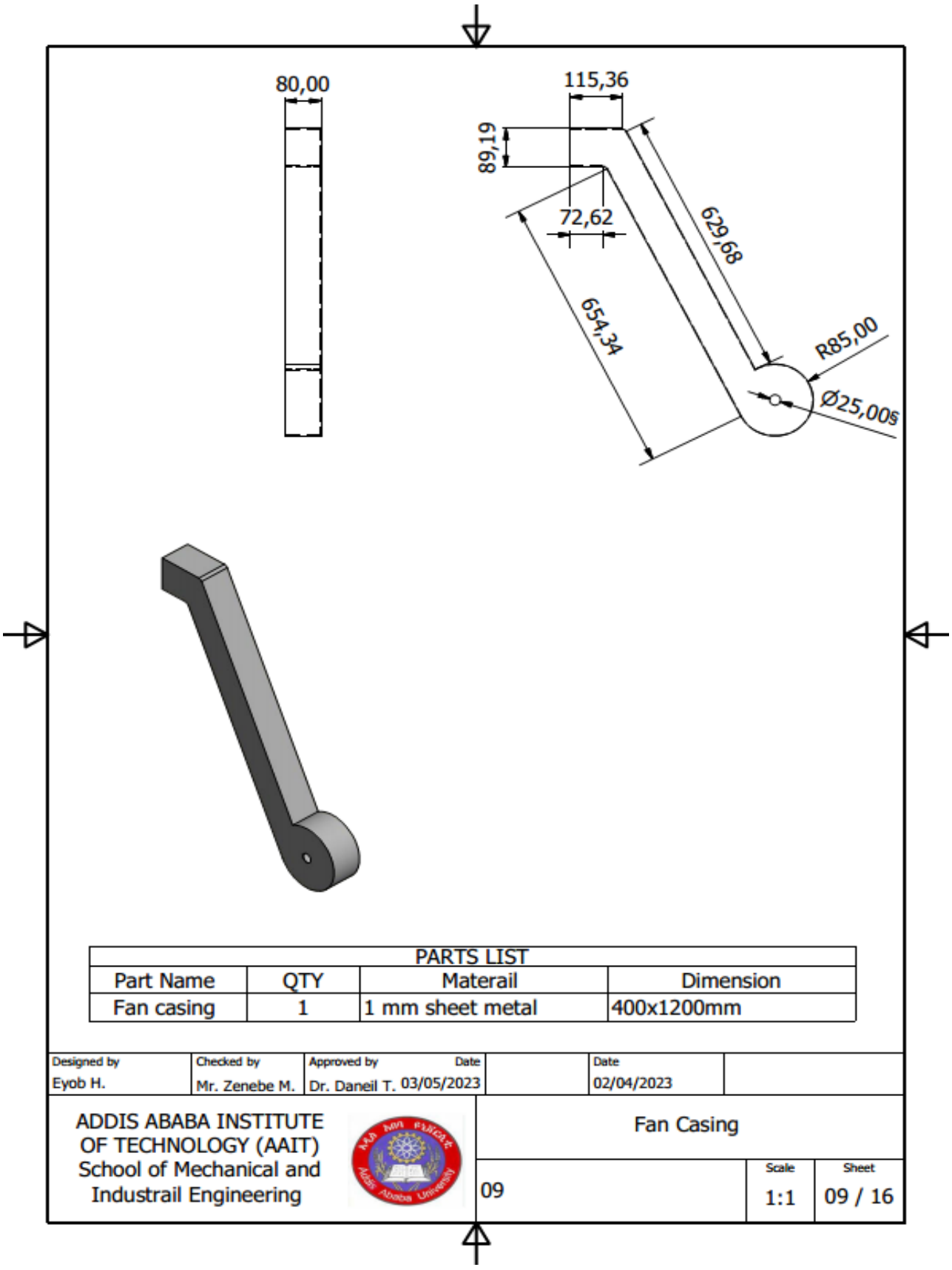

PARTS LIST			
Part Name	QTY	Materail	Dimension
Fan casing	1	1 mm sheet metal	400x1200mm

Designed by	Checked by	Approved by	Date		Date	
Eyob H.	Mr. Zenebe M.	Dr. Daneil T.	03/05/2023		02/04/2023	

ADDIS ABABA INSTITUTE OF TECHNOLOGY (AAIT) School of Mechanical and Industrail Engineering	Fan Casing		
	09	Scale 1:1	Sheet 09 / 16

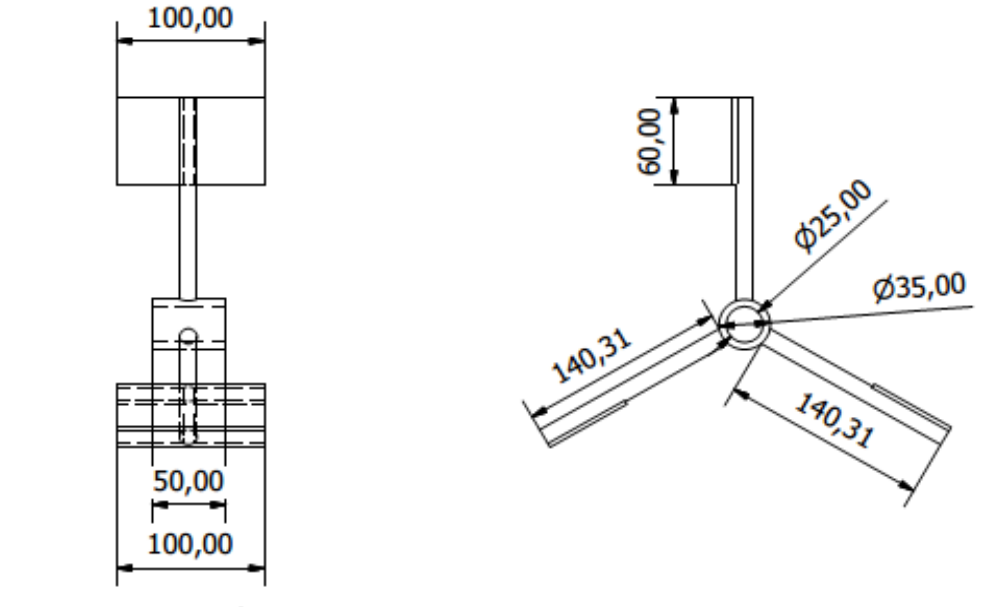

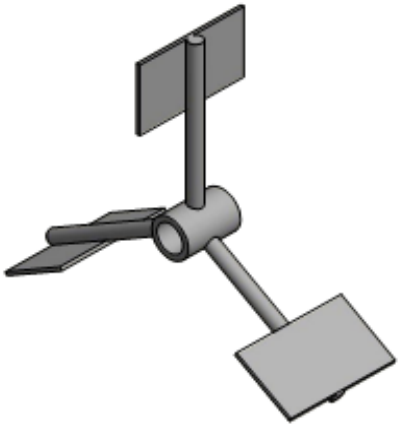

PARTS LIST			
Part Name	QTY	Materail	Dimension
Blower	1	3 mm sheet metal 8 mm rod	400x1200mm

Designed by	Checked by	Approved by	Date	Date	
Eyob H.	Mr. Zenebe M.	Dr. Daneil T.	03/05/2023	02/04/2023	

ADDIS ABABA INSTITUTE OF TECHNOLOGY (AAIT)
School of Mechanical and Industrail Engineering

Blower

	Scale	Sheet
10	1:1	10 / 16

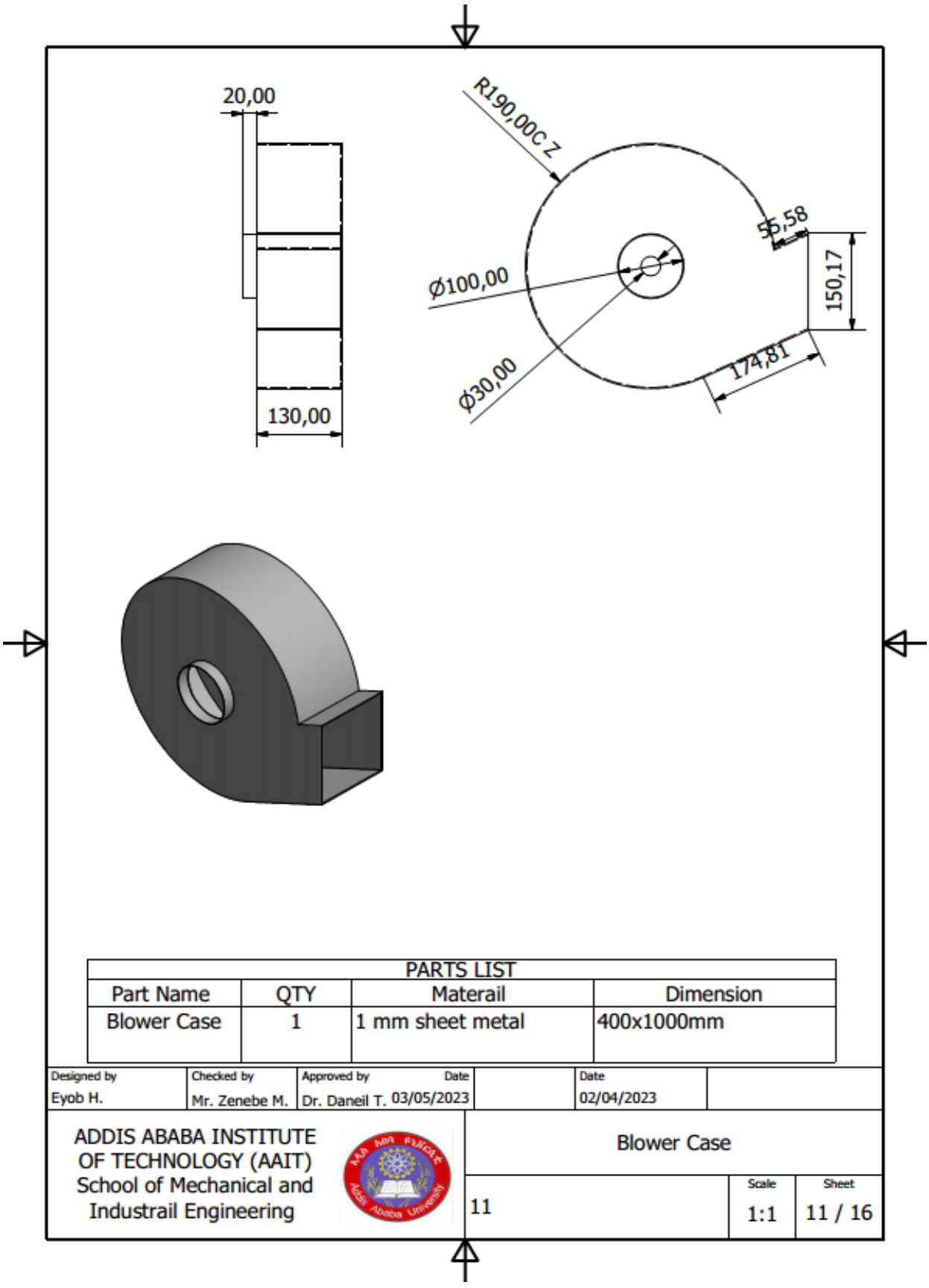

PARTS LIST			
Part Name	QTY	Materail	Dimension
Blower Case	1	1 mm sheet metal	400x1000mm

Designed by	Checked by	Approved by	Date		Date
Eyob H.	Mr. Zenebe M.	Dr. Daneil T.	03/05/2023		02/04/2023

ADDIS ABABA INSTITUTE OF TECHNOLOGY (AAIT)
School of Mechanical and Industrail Engineering

Blower Case

11

Scale 1:1

Sheet 11 / 16

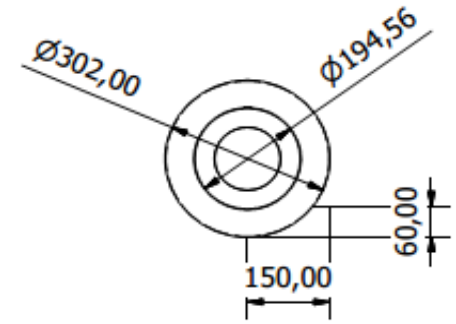

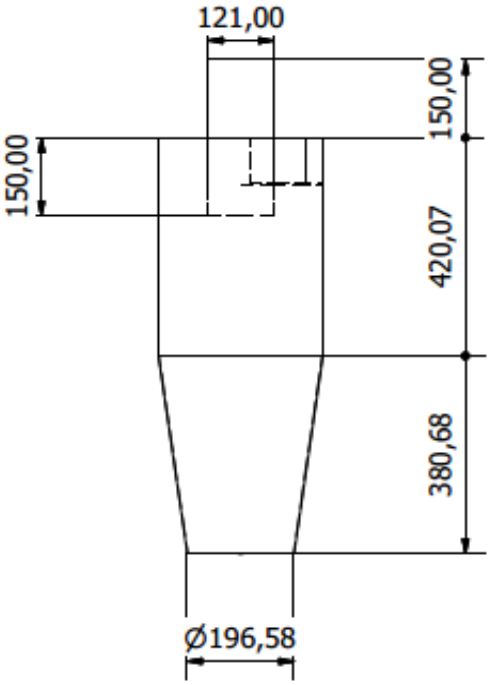

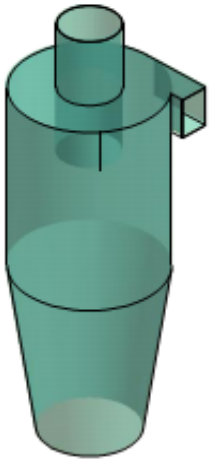

PARTS LIST			
Part Name	QTY	Materail	Dimension
Cyclone Separator	1	1 mm sheet metal	800x1000mm

Designed by	Checked by	Approved by	Date	Date	
Eyob H.	Mr. Zenebe M.	Dr. Daneil T.	03/05/2023	02/04/2023	

ADDIS ABABA INSTITUTE OF TECHNOLOGY (AAIT)
School of Mechanical and Industrail Engineering

Cyclone

12

Scale 1:1

Sheet 12 / 16

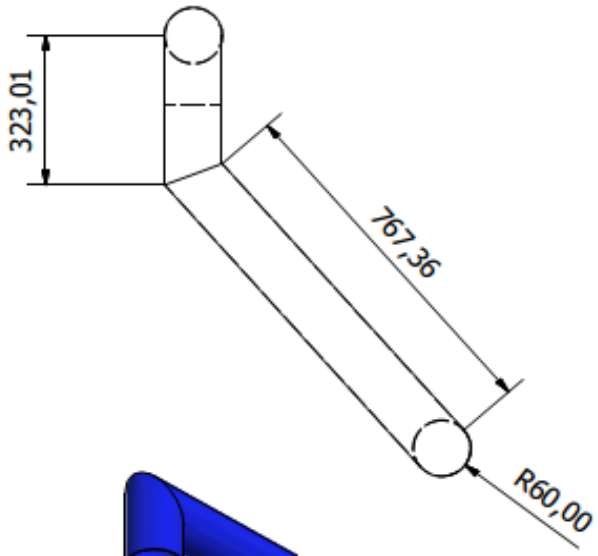

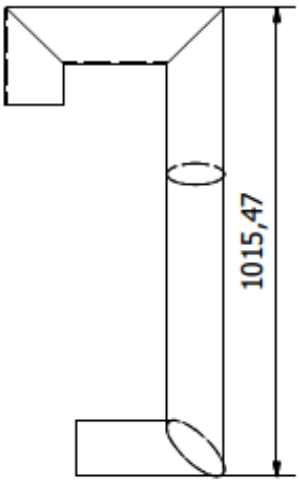

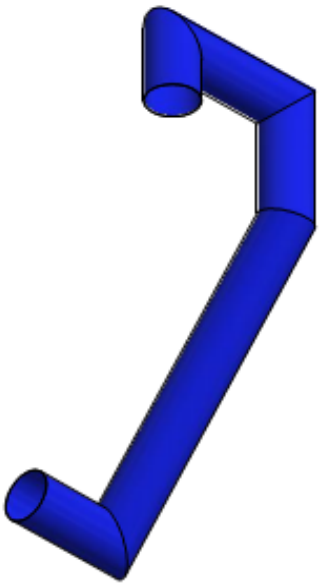

PARTS LIST			
Part Name	QTY	Materail	Dimension
Hose	1	Plastic	diameter 60mm x2 m

Designed by	Checked by	Approved by	Date	Date	
Eyob H.	Mr. Zenebe M.	Dr. Daneil T.	03/05/2023	02/04/2023	

ADDIS ABABA INSTITUTE OF TECHNOLOGY (AAIT)
School of Mechanical and Industrail Engineering

Hose

	Scale	Sheet
13	1:1	13 / 16

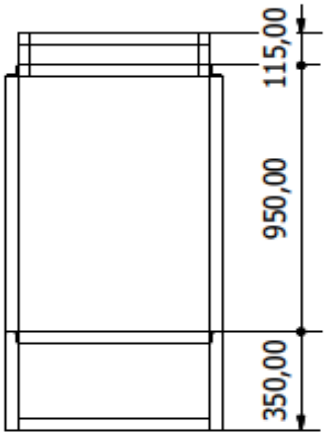

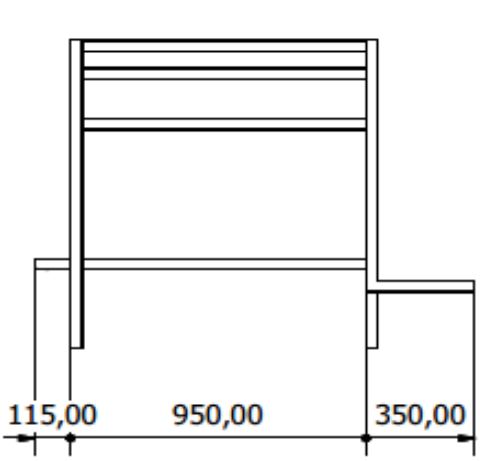

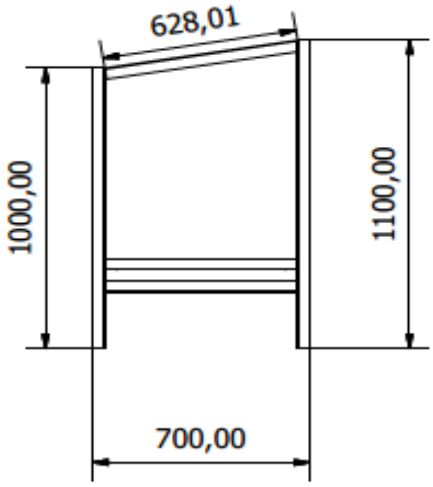

PARTS LIST			
Part Name	QTY	Materail	Dimension
Frame	1	Angle Iron 40X40X3 mm	700 x x1100 x1500 mm

Designed by	Checked by	Approved by	Date		Date	
Eyob H.	Mr. Zenebe M.	Dr. Daneil T.	03/05/2023		02/04/2023	

ADDIS ABABA INSTITUTE OF TECHNOLOGY (AAIT)
School of Mechanical and Industrail Engineering

Frame

	Scale	Sheet
14	1:1	14 / 16

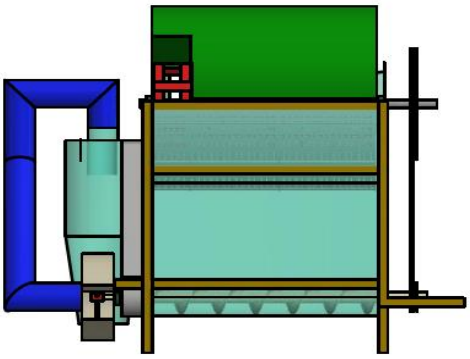

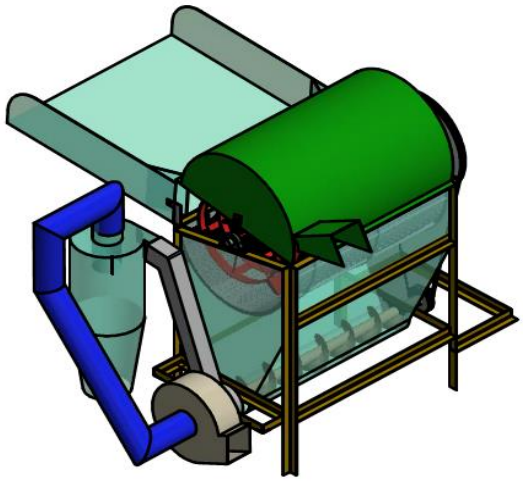

Part Name	Dimension
3D Model of Teff Thresher	1800 x1520 x1950 mm

Designed by	Checked by	Approved by	Date		Date	
Eyob H.	Mr. Zenebe M.	Dr. Daneil T.	03/05/2023		02/04/2023	

ADDIS ABABA INSTITUTE OF TECHNOLOGY (AAIT)
School of Mechanical and Industrail Engineering

3D MODEL OF TEFF THRESHER

	Scale	Sheet
15	1:1	15 / 16